NATÁLIA ARGENE LOVATE PEREIRA FLEISCHFRESSER

CORRELATIONS FOR THE PREDICTION OF THE HEAD CURVE OF CENTRIFUGAL PUMPS BASED ON EXPERIMENTAL DATA

CORRELAÇÕES PARA A PREDIÇÃO DA CURVA DE ALTURA DE BOMBAS CENTRÍFUGAS BASEADAS EM DADOS EXPERIMENTAIS

CAMPINAS
2015

UNIVERSIDADE ESTADUAL DE CAMPINAS

FACULDADE DE ENGENHARIA MECÂNICA

E INSTITUTO DE GEOCIÊNCIAS

NATÁLIA ARGENE LOVATE PEREIRA FLEISCHFRESSER

CORRELATIONS FOR THE PREDICTION OF THE HEAD CURVE OF CENTRIFUGAL PUMPS BASED ON EXPERIMENTAL DATA

CORRELAÇÕES PARA A PREDIÇÃO DA CURVA DE ALTURA DE BOMBAS CENTRÍFUGAS BASEADAS EM DADOS EXPERIMENTAIS

Dissertation presented to the Mechanical Engineering Faculty and Geosciences Institute of the University of Campinas in partial fulfillment of the requirements for the degree of Master in Petroleum Sciences and Engineering in the area of Exploitation.

Dissertação apresentada à Faculdade de Engenharia Mecânica e Instituto de Geociências da Universidade Estadual de Campinas como parte dos requisitos exigidos para a obtenção do título de Mestra em Ciências e Engenharia de Petróleo na área de Explotação.

Orientador: Prof. Dr. Antonio Carlos Bannwart

Este exemplar corresponde à versão final da dissertação defendida pela aluna Natália Argene Lovate Pereira Fleischfresser, e orientada pelo Prof. Dr. Antonio Carlos Bannwart.

CAMPINAS

2015

Ficha catalográfica
Universidade Estadual de Campinas
Biblioteca da Área de Engenharia e Arquitetura
Rose Meire da Silva - CRB 8/5974

F628c

Fleischfresser, Natália Argene Lovate Pereira, 1985-
Correlations for the prediction of the head curve of centrifugal pumps based on experimental data / Natália Argene Lovate Pereira Fleischfresser. – Campinas, SP : [s.n.], 2015.

Orientador: Antonio Carlos Bannwart.
Dissertação (mestrado) – Universidade Estadual de Campinas, Faculdade de Engenharia Mecânica e Instituto de Geociências.

1. Bombas centrífugas. 2. Fluidodinâmica. I. Bannwart, Antonio Carlos,1955-. II. Universidade Estadual de Campinas. Faculdade de Engenharia Mecânica. III. Título.

Informações para Biblioteca Digital

Título em outro idioma: Correlações para a predição da curva de altura de bombas centrífugas baseadas em dados experimentais
Palavras-chave em inglês:
Centrifugal pumps
Fluid dynamics
Área de concentração: Explotação
Titulação: Mestra em Ciências e Engenharia de Petróleo
Banca examinadora:
Antonio Carlos Bannwart [Orientador]
Ricardo Augusto Mazza
Jorge Luis Baliño
Data de defesa: 06-07-2015
Programa de Pós-Graduação: Ciências e Engenharia de Petróleo

UNIVERSIDADE ESTADUAL DE CAMPINAS

FACULDADE DE ENGENHARIA MECÂNICA

E INSTITUTO DE GEOCIÊNCIAS

DISSERTAÇÃO DE MESTRADO ACADÊMICO

CORRELATIONS FOR THE PREDICTION OF THE HEAD CURVE OF CENTRIFUGAL PUMPS BASED ON EXPERIMENTAL DATA

Autor: Natália Argene Lovate Pereira Fleischfresser
Orientador: Prof. Dr. Antonio Carlos Bannwart

A banca examinadora composta pelos membros abaixo aprovou esta dissertação:

Prof. Dr. Antonio Carlos Bannwart
Departamento de Energia – Faculdade de Engenharia Mecânica – Unicamp

Prof. Dr. Ricardo Augusto Mazza
Departamento de Energia – Faculdade de Engenharia Mecânica – Unicamp

Prof. Dr. Jorge Luis Baliño
Departamento de Engenharia Mecânica, Escola Politécnica, Universidade de São Paulo

Campinas, 06 de julho de 2015.

DEDICATION

I dedicate this work to my husband Christian, my mother Sandra, my father Alexandre and my brother Lucas, who have supported me during this journey.

ACKNOWLEDGEMENTS

Reaching the final phase of this journey is very rewarding because it took a lot of effort to arrive here. I had to be persistent to dedicate in order to consolidate my studies with work, but also patient to adapt myself to the university environment after years away of the academic scene. But looking back at the last four and a half years, this process has allowed me to grow and learn a lot. Furthermore, I met several special and valuable people, that I'm sure will succeed in their professional and personal lives.

I would like to thank every person that directly or indirectly helped me during this process.

First of all, I thank Prof. Dr. Antonio Carlos Bannwart for giving me the opportunity to learn and work with him and for giving me space to develop this work with a lot of autonomy. I thank him for trusting and respecting me as a professional.

I thank Dr. Jorge Luiz Biazussi for all of his dedication, for showing me his work and helping me with the development of my own thesis. I also thank him for his care in always answering my questions promptly.

I thank Prof. Dr. Ricardo Augusto Mazza, Prof. Dr. Jorge Luis Baliño and Prof. Dr. Marcelo Souza de Castro for their valuable contributions and suggestions during the review process.

I also thank Sérgio Loeser for revising my work analyzing it from the industry perspective.

I thank Michelle Fulaneto, Fátima Lima, Alice Kiyoka, Diogo Furlan and Vanessa Kojima for helping me with all the materials and logistics. Without them it would be impossible to conciliate studies and work.

I thank my husband Christian for reviewing my work several times and for his patience and incentive.

I thank my mother Sandra, father Alexandre and brother Lucas also for their patience and incentive.

“Everything should be made as simple as possible, but not simpler”

Albert Einstein

ABSTRACT

The hydraulic performance of centrifugal pumps depends on several hydraulic dimensions of the pump, but most of them are not easily accessible. Therefore, the pump's hydraulic performance always has to be informed by the pump manufacturer. Furthermore, in order to protect their intellectual property, manufacturers rarely share more detailed information about the pump hydraulics with the public. As a consequence, pump users and researchers don't have access to all the data they possibly need. In literature, there are several proposed models based on fluid dynamic principles and experimental data that attempt to predict the hydraulic performance of centrifugal pumps. Alternatively, it is also possible to calculate a pump's performance with numerical simulation. However, the accuracy of such models is usually proportional to the number of necessary parameters – those of which may not be easily accessible, as stated before. In this work, a simple approach available in literature, based on fluid dynamic principles, that predicts a pump hydraulic performance with only a few accessible hydraulic dimensions, is validated with several experimental data. Eighty tests of different types of pumps, with a large range of specific speeds are considered. From this analysis, correlations among the coefficients of the model equation and the main hydraulic data of the pumps are proposed. Afterwards, several *shut-off* head prediction methods available in literature are analyzed in order to define the one that best predicts the *shut-off* head of the given tested data. Finally, for each pump type, the best combination of correlations and *shut-off* head prediction method are selected to reduce the error on the whole head curve prediction. Given all the assumptions and simplifications, the objective of this work is to present a method applicable to several pump types that easily provides a prediction of the whole head curve with reasonable error.

Key Word: Centrifugal Pumps, Hydraulic Performance, Experimental Validation, Head Curve Prediction, *Shut-off* Head Prediction

RESUMO

A performance hidráulica de bombas centrífugas depende de várias entre suas dimensões hidráulicas, mas a maioria delas não é facilmente acessível. Por este motivo, a performance hidráulica da bomba deve sempre ser disponibilizada pelo seu fabricante. No entanto, para proteger sua propriedade intelectual, fabricantes raramente compartilham com o público informações mais detalhadas sobre a hidráulica da bomba. Como consequência, os usuários dos equipamentos e pesquisadores não têm acesso a todas as informações de que podem necessitar. Na literatura, há diversos modelos para a predição da performance hidráulica de bombas centrífugas, baseados nos princípios da fluidodinâmica e em dados experimentais. Alternativamente, é possível calcular a performance das bombas através de simulações numéricas. Entretanto, a precisão destes modelos é normalmente proporcional ao número de parâmetros envolvidos, os quais podem não ser de fácil acesso, como mencionado anteriormente. Neste trabalho, uma abordagem simples disponível na literatura, baseada nos princípios de fluidodinâmica, que prediz a performance hidráulica de bombas com poucas e acessíveis dimensões hidráulicas, é validada com uma grande variedade de dados experimentais. Os dados de oitenta testes de diferentes tipos de bomba, cobrindo uma ampla extensão de velocidades específicas, são considerados. A partir desta análise, correlações entre os coeficientes da equação do modelo e os principais dados hidráulicos das bombas são propostas. Em seguida, diversos métodos de predição da altura no *shut-off* disponíveis na literatura são analisados para que seja possível definir o que melhor prediz a altura no *shut-off* considerando os dados de teste. Finalmente, para cada tipo de bomba, a melhor combinação entre correlações e método de predição de altura no *shut-off* é selecionada para reduzir o erro na predição das curvas de altura completas. Dadas todas as premissas e simplificações, o objetivo deste trabalho é apresentar um método aplicável para diversos tipos de bomba que facilmente prediz a curva de altura com erro razoável.

Palavras Chave: Bombas Centrífugas, Performance Hidráulica, Validação Experimental, Predição da Curva de Altura, Predição da Altura no *Shut-off*

TABLE OF CONTENTS

LIST OF FIGURES

LIST OF TABLES

LIST OF ACRONYMS

API	American Petroleum Institute
ASME	American Society of Mechanical Engineers
BB1, BB2, BB3, BB4, BB5	Between bearing pumps types 1, 2, 3, 4, 5
BEP	Best efficiency point
CFD	Computational Fluid Dynamics
ESP	Electrical submersible pump
HIS	Hydraulic Institute Standards
INMETRO	Instituto Nacional de Metrologia, Qualidade e Tecnologia
ISO	International Organization for Standardization
NPSH	Net positive suction head
OH2	Overhung pumps type 2
PS	Pressure side
SI units	International system units
SRU	Sulphate removal units
SS	Suction side
VS2	Vertically suspended pumps type 2

LIST SYMBOLS

Roman letters

A_3	Minimum distance between vanes at diffuser inlet	m
A_8	Volute inlet height	m
A_n	Normal area	m^2
B_1	Impeller inlet width	m
B_2	Impeller outlet width	m
B_3	Diffuser inlet width	m
B_8	Volute inlet width	m
C_H	Head coefficient	-
C_P	Power coefficient	-
C_Q	Flow coefficient	-
D_0	Impeller inlet inner diameter	m
D_1	Impeller inlet outer diameter	m
D_2	Impeller vanes outlet diameter	m
D_3	Diffuser inlet diameter	m
f	Friction factor	-
g	Acceleration due to gravity	m/s^2
H	Head of elevation	m
H_0	Head at *shut-off*	m
$H_{0.FN.\ mod}$	Modified Frost and Nilsen's *shut-off* head	m

$H_{0.FN.imp}$	Impeller contribution of Frost and Nilsen's *shut-off* head	m
$H_{0.FN.vol}$	Volute contribution of Frost and Nilsen's *shut-off* head	m
$H_{0.Pk}$	Peck's *shut-off* head	m
$H_{0.Pt}$	Patel's *shut-off* head	m
$H_{0.Pt.mod}$	Modified Patel's *shut-off* head	m
$H_{0.S}$	Stepanoff's *shut-off* head	m
$H_{0.St.\ imp}$	Impeller contribution of Stirling's *shut-off* head	m
$H_{0.St.\ mod}$	Modified Stirling's *shut-off* head	m
$H_{0.St.\ vol}$	Volute contribution of Stirling's *shut-off* head	m
$H_{0.T}$	Thorne's *shut-off* head	m
$k_1, k_2, k_3, k_4, k_5, k_6$	Head curve model equation coefficients	-
L_i	Hydraulic dimensions	m
n	Viscous effect in high flow rate	-
n_q	Specific speed	1/s
$n_{q.Ref}$	Gülich's reference specific speed	1/s
N_S	Dimensionless specific speed	-
$P_{discharge}$	Discharge pressure	Pa
$P_{suction}$	Suction pressure	Pa
Q	Flow rate	m^3/s
r_1	Impeller vanes inlet radius	m
r_2	Impeller vanes outlet radius	m
Re_ω	Rotational Reynolds number	-

R_o	Rossby number	-
T_e	Torque	N.m
u	Peripheral velocity	m/s
u_1	Inlet peripheral velocity	m/s
u_2	Outlet peripheral velocity	m/s
u_{C_Q}	Flow coefficient error	%
u_{C_H}	Head coefficient error	%
u_{D_2}	Impeller vanes outlet diameter error	%
$u_{\Delta P}$	Differential pressure error	%
$u_{P.discharge}$	Discharge pressure error	%
$u_{P.suction}$	Suction pressure error	%
u_ρ	Density error	%
u_Q	Flow error	%
u_ω	Speed error	%
V_{t1}	Inlet fluid tangential velocity	m/s
V_{t2}	Outlet fluid tangential velocity	m/s
w	Velocity tangent to the impeller vane	m/s
$\dot{W}$	Shaft power	W
X	Inverse of rotational Reynolds number	-

Greek letters

β_1	Impeller vanes inlet angle	rad

β_2	Impeller vanes outlet angle	rad
ΔP	Differential pressure	Pa
$\Delta P_{distortion}$	Distortion pressure losses	Pa
ΔP_{Euler}	Euler differential pressure	Pa
$\Delta P_{friction}$	Friction pressure losses	Pa
ΔP_i	Ideal differential presure	Pa
ΔP_{loc}	Localized pressure losses	Pa
ΔP_{losses}	Hydraulic pressure losses	Pa
$\Delta P_{recirculation}$	Recirculation pressure losses	Pa
$\Delta P_{sec.flow}$	Pressure losses due to secondary flow	Pa
ΔP_{shock}	Shock pressure losses	Pa
ΔP_{tourb}	Tourbillion pressure losses	Pa
ϵ	Roughness	m
η	Efficiency	-
μ	Viscosity	Pa.s
ρ	Density	kg/m³
Ψ	Gülich's pressure coefficient	-
Ψ_0	Gülich's *shut-off* pressure coefficient	-
Ψ_{Pk}	Peck's correction factor for Euler's equation	-
Ψ_{Pt}	Patel's correction factor for Euler's equation	-
Ψ_S	Stepanoff's correction factor for Euler's equation	-
ω	Rotational speed	1/s

1 INTRODUCTION

Centrifugal pumps are turbo machines that provide energy increase to the fluid. They have a stationary casing, which can be a volute or diffusers, with one or more impellers inside, one or two bearing housings and a shaft, as shown in Figure 1. The impeller mounted on the shaft is driven via a coupling by a motor or turbine. The centrifugal force generated at the impellers is transformed into a static pressure increase to the flow. The fluid exiting the impeller is decelerated in the volute or diffuser in order to utilize the greatest possible part of the kinetic energy at the impeller outlet for increasing the static pressure.

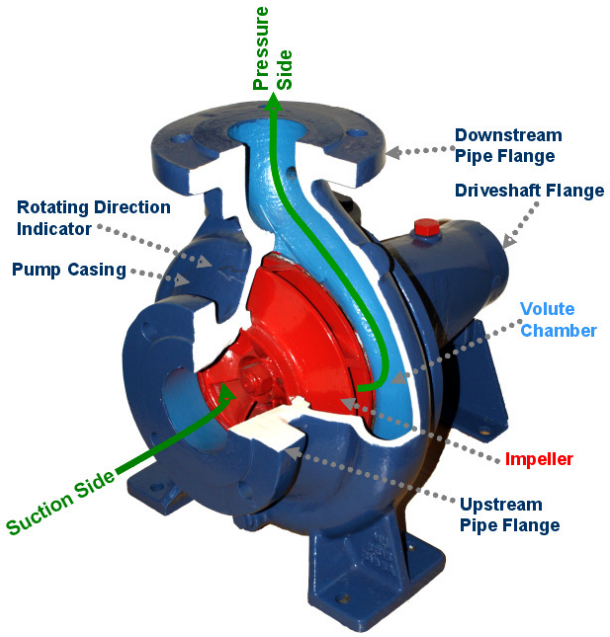

Figure 1 - Centrifugal pump.

The flow energy is composed of kinetic energy, pressure and potential energy. In order to transport fluid from one place to another, pumps are used to provide a static pressure increase to the flow, which could be useful overcoming a height difference and long distances (pressure losses in the line).

As already mentioned, the stationary part around the impeller can be a diffuser or a volute. These are two different pump concepts, which have their applicability, advantages and disadvantages. In both cases, the pumps can have one or multiple stages.

Centrifugal pumps are widely used in the industry. Some examples of segments that use centrifugal pumps are Oil & Gas (off-shore, distribution, refineries), power, water and wastewater, pulp and paper and general industry.

The differential pressure provided by the pump (ΔP) is usually represented by its related head of elevation (H), where ρ is the fluid density and g is the acceleration due to gravity.

$$H = \frac{\Delta P}{\rho g} \tag{1}$$

This representation makes it possible to show the performance of a pump for fluids with different densities in just one curve.

The pump hydraulic performance is defined by the head, shaft power, efficiency and NPSH curves versus flow rate. In Figure 2, the performance curves of a centrifugal pump are shown.

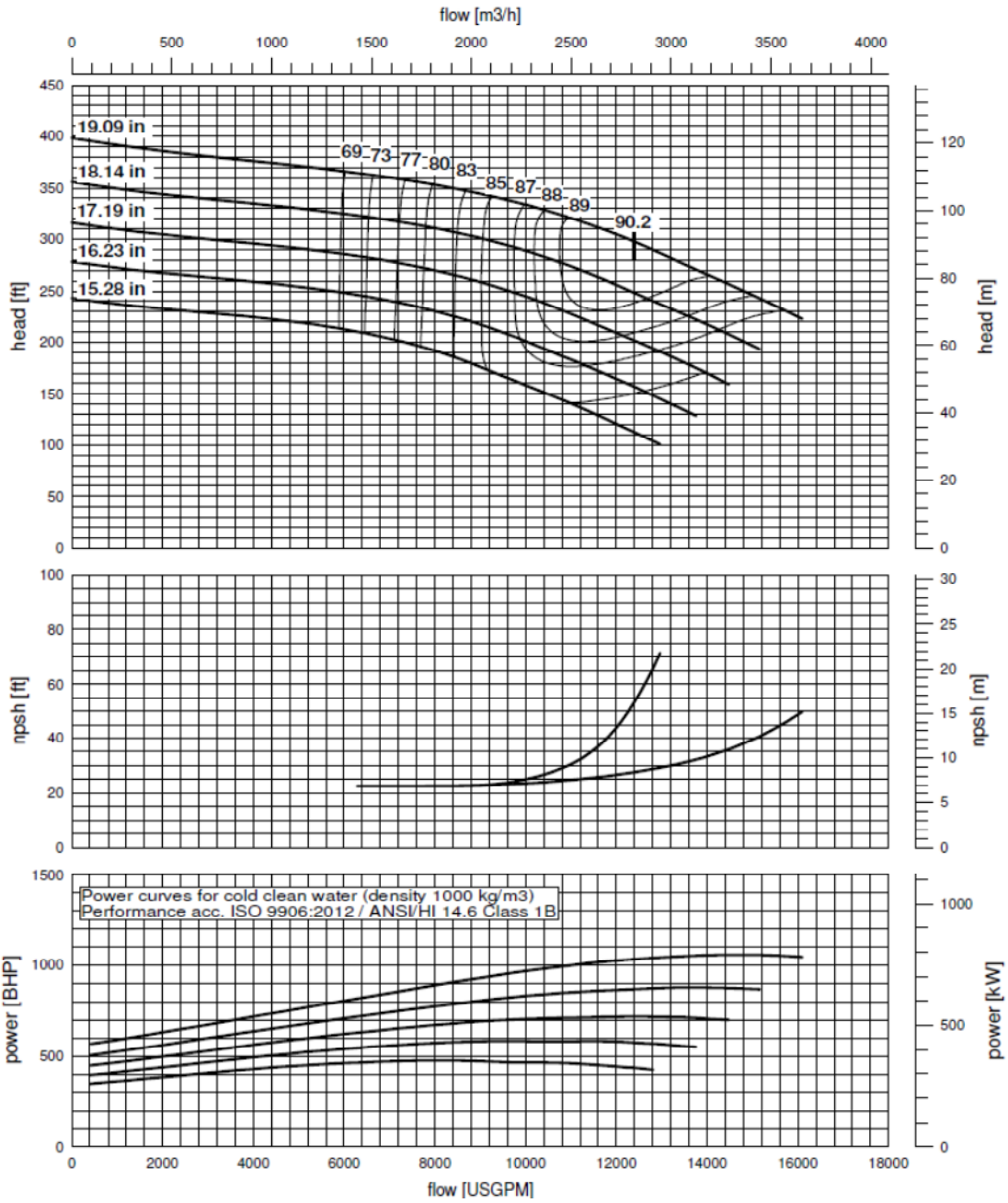

Figure 2 - Performance curves of a centrifugal pump.

These curves are associated to just one pump model and represent the pump performance while pumping a liquid with low viscosity (similar to the water viscosity). Furthermore, these curves are related to just one impeller outlet diameter and rotation speed.

The range of operation of a pump defines the maximum and minimum impeller outlet diameter and maximum and minimum flow rates for that model.

Usually, pumps are grouped in families. Each family represents a group of pumps with the same design concept, but in different sizes. When all the pump ranges are put together, a wide area of operation (flow versus head) is covered, as shown in Figure 3.

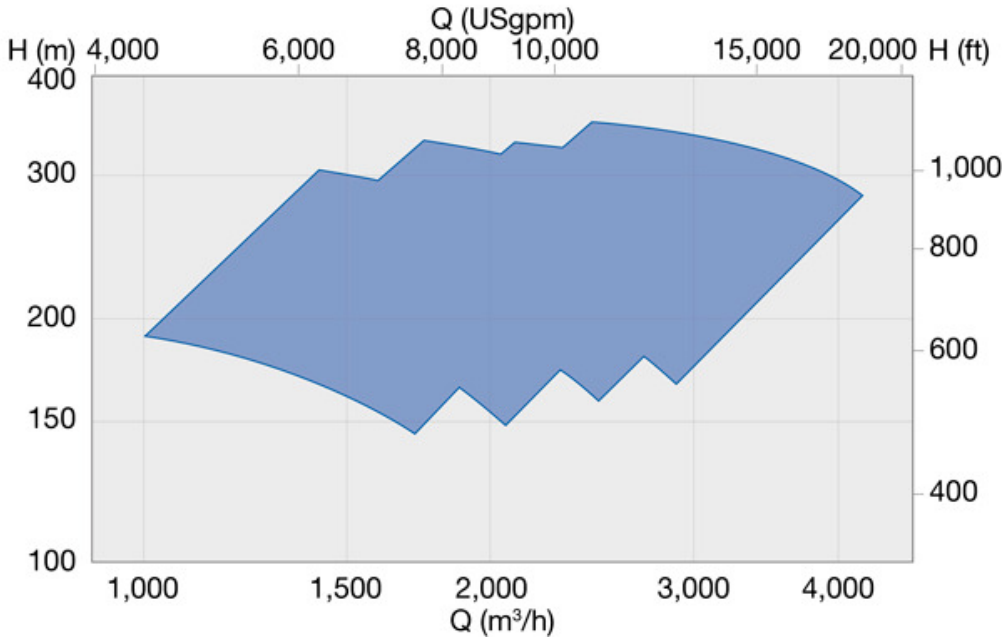

Figure 3 – Operating range.

The head and shaft power ($\dot{W}$) are measureable parameters and the efficiency (η) is calculated according to the Equation (2), where Q is the flow rate:

$$\eta = \frac{QH\rho}{P} \tag{2}$$

The operating point that provides the best efficiency at the maximum impeller outlet diameter is called BEP (best efficiency point). This is the operating condition for which the hydraulics have been developed.

The specific speed is a characteristic number that represents the hydraulics and it is calculated based on the conditions of the BEP, according to the Equation (3), where ω is the rotational speed:

$$n_q = \frac{\omega\sqrt{Q}}{H^{3/4}} \tag{3}$$

The hydraulic performance depends on several hydraulic dimensions of the pump. The main ones are listed below and presented in Figure 4:

Impeller: D_2, B_2, β_2, D_1 and D_0

Diffuser/volute: A_3, B_3, D_3, A_8 and B_8

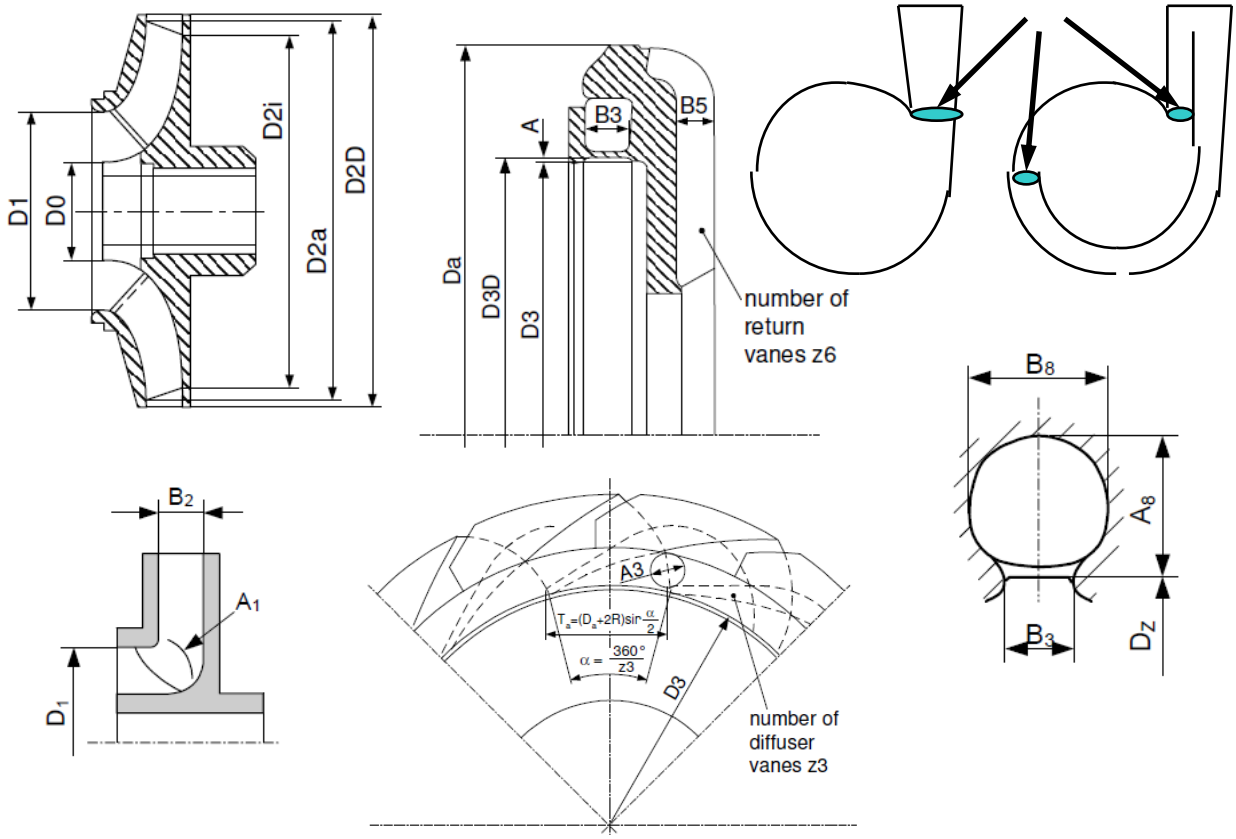

Figure 4 – Main pump hydraulic dimensions.

Usually the dimensions identified by the subscript "1" are related to the impeller leading edge, "2" to the impeller trailing edge, "3" to the diffuser or volute leading edge and "4" to the diffuser or volute trailing edge. The subscript "8" also indicates important dimensions in the volute throat.

1.1 Motivation

During the conception phase of a project, it may be necessary to estimate the performance of some of the equipment in order to assess the project cost and its viability. However, most pump hydraulic dimensions are not easily accessible. As a result, the pump hydraulic

performance always has to be informed by the pump manufacturer, who has designed the pump hydraulics.

Furthermore, in order to protect their intellectual property, manufacturers rarely share more detailed information about the pump hydraulics with the public. As a consequence, pump users and researchers don't have access to all the data they possibly need.

In literature, there are several proposed models based on fluid dynamic principles and experimental data that attempt to predict the hydraulic performance of centrifugal pumps. Alternatively, it is also possible to calculate a pump's performance with numerical simulation. However, the accuracy of such models is usually proportional to the number of necessary parameters – those of which may not be easily accessible, as stated before.

Based on this scenario, it would be very useful to predict a pump's hydraulic performance with only a few accessible hydraulic dimensions, so that the dependency on the manufacturer's information would be reduced. Furthermore anyone would be able to predict the hydraulic performance of a pump with acceptable accuracy.

1.2 Objectives

Biazussi (2014) presented a simple single-phase approach (model), based on fluid dynamic principles, that defines the head versus flow rate curve. It is presented in Chapter 3. According to this approach, for fluids with low viscosity, the head curve is a quadratic function of the flow rate, as expected. Some assumptions and simplifications were considered, so that the model would only depend on a few accessible hydraulic dimensions and the performance would be predicted with reasonable error.

One of the equation coefficients, k_1, is defined by accessible hydraulic dimensions of the pump. The other coefficients are adjusted by the model in order to reproduce the given tested data. Some tests were held in order to validate this model and also propose correlations among these coefficients and basic hydraulic data of the pumps.

The results of the work were presented and were considered reliable for these few cases studied. However more experimental data was necessary to fully validate the model.

The current work uses Biazussi (2014)'s work as a starting point. The data from eighty tests was collected so that the aforementioned model could be validated and that its coverage could be defined. Several different types of centrifugal pumps with a large range of specific speeds were considered and are described in Chapter 4.

In Chapter 5, the tested hydraulic performances were compared to the results provided by the model. Furthermore, the mentioned equation coefficients were plotted against the pump specific speed in order to analyze if there was a correlation among them. It was possible to find clear tendencies, even considering all the different types of pumps.

Considering these tendencies, equations were proposed in order to make it possible to define the head curve against flow based only on the specific speed and main hydraulic dimensions of the pump, such as D_2, B_2, β_2 and D_1. The correlation based curves were compared to the tested curves and the difference between them was analyzed.

Afterwards, since an offset of the prediction of the head curve was observed in some cases, several *shut-off* head prediction methods available in literature were analyzed in order to define the one that best predicts the *shut-off* head of the given tested data.

Finally, for each pump type, the best combination of correlations and *shut-off* head prediction method was selected to reduce the error on the whole head curve prediction.

Given all the assumptions and simplifications, the objective of the current work is to present correlations applicable to several pump types that easily provides a prediction of the pump head curve with reasonable error.

2 LITERATURE REVIEW

2.1 Dimensional analysis

Dimensional analysis is used to represent all the parameters in a dimensionless way, so that it is possible to compare different scenarios. With regard to the pump performance, using dimensional analysis it is possible to compare performances considering different speeds or impeller outlet diameter, for instance. Gülich (2007) presents a detailed explanation of the dimensional analysis.

The independent variables related to the pump performance are differential pressure (ΔP) and shaft power ($\dot{W}$). These variables depend on the flow rate (Q), speed (ω), impeller outlet diameter (D_2), roughness (ϵ), viscosity (μ) and density (ρ). Therefore:

$$\Delta P = f_1(Q, D_2, \omega, \rho, \mu, \epsilon) \qquad \dot{W} = f_2(Q, D_2, \omega, \rho, \mu, \epsilon) \tag{4}$$

Based on the dimensional analysis, the following dimensionless coefficients are defined:

Flow coefficient: $C_Q = \frac{Q}{\omega {D_2}^3}$ (5)

Head coefficient: $C_H = \frac{\Delta P}{\rho \omega^2 {D_2}^2}$; $C_H = f_3\left(C_Q, X, \epsilon/D_2\right)$ (6)

Power coefficient: $C_P = \frac{\dot{W}}{\rho \omega^3 {D_2}^5}$; $C_P = f_4\left(C_Q, X, \epsilon/D_2\right)$ (7)

where $X = \frac{1}{Re_\omega} = \frac{\mu}{\rho \omega {D_2}^2}$. (8)

The parameter ϵ/D_2 is the relative roughness, which affects the pump efficiency. The efficiency η is related to these dimensionless coefficients in the following way:

$$\eta = \frac{\rho Q \Delta P}{\dot{W}} = \frac{C_Q C_H}{C_P} = f_5\left(C_Q, X, \epsilon/D_2\right) \tag{9}$$

The dimensionless specific speed is represented as:

$$N_s = \frac{\sqrt{C_Q}}{{C_H}^{3/4}} \tag{10}$$

2.2 One-dimensional calculation with velocity triangles

The velocity of the fluid within the diffuser and the impeller can be understood with the help of the velocity triangle, which breaks down the fluid's main velocity components in certain positions, as shown in Figure 5.

In this analysis, some considerations need to be made:

- The flow is permanent and one-dimensional;
- The flow is uniform through the impeller;
- Secondary flow is disregarded.

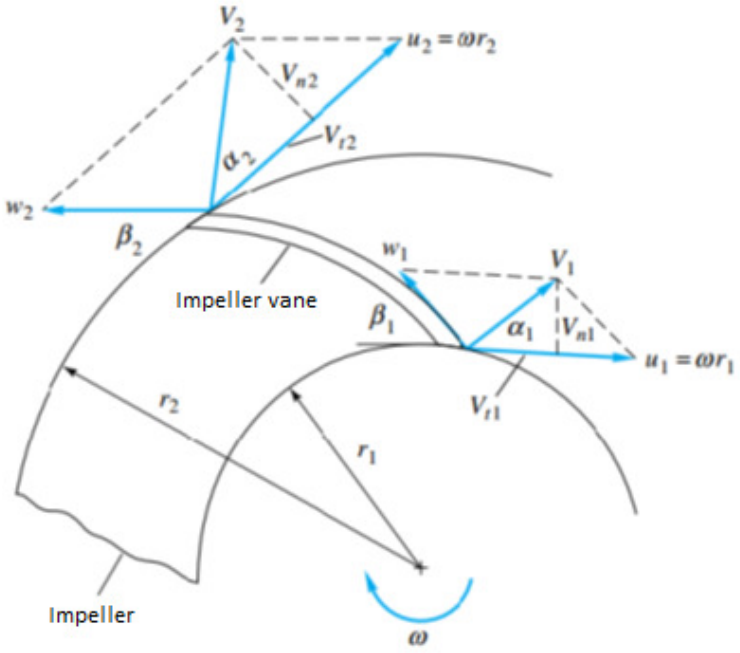

Figure 5 – Impeller inlet and outlet velocity triangles (Biazussi, 2014).

Similar to the hydraulic dimensions, the parameters related to the impeller leading edge are identified by the subscript "1" and the ones related to the impeller trailing edge by the subscript "2".

The flow velocity is defined by two components. The first one is the velocity tangent to the impeller vane w. The second one is the peripheral velocity, $u = \omega r$. Then the absolute flow velocity V is the vector sum of these two components.

$$\vec{V} = \vec{w} + \vec{u} \quad (11)$$

By balancing the moment of inertia, while admitting permanent flow and disregarding the effect of gravity, the power that the impeller exerts on the fluid can be formulated as:

$$\dot{W} = \rho Q(\omega r_2 V_{t2} - \omega r_1 V_{t1}) \quad (12)$$

Given that $\dot{W}_s = T_e \omega$, the torque (T_e) can be written as:

$$T_e = \rho Q(r_2 V_{t2} - r_1 V_{t1}) \quad (13)$$

In an ideal system where no losses are considered, $\dot{W}_s = \rho g Q H$. Thus, the ideal differential pressure provided by the impeller is represented by:

$$\Delta P_i = \rho(u_2 V_{t2} - u_1 V_{t1}) \quad (14)$$

The equation above is called the Euler equation for turbo machines. It can be seen that the power, torque and differential head depend only on the peripheral velocities and the tangential component of the absolute velocities on the impeller inlet and outlet.

If we consider that the flow has no tangential velocity on entering the impeller ($V_{t1} = 0$), and apply some geometric correlations based on the triangle velocities, the Euler equation can be written as:

$$\Delta P_i = \rho u_2^2 \left(1 - \frac{Q \cot \beta_2}{2\pi r_2 B_2 u_2}\right) \quad (15)$$

where, according to Figure 5, β_2 is the outlet angle of the impeller vane and B_2 is the width of the impeller outlet.

2.3 Pressure losses

According to Gülich (2007), losses arise whenever a fluid flows through (or components move in) a machine. The useful power is therefore always smaller than the power supplied at the pump shaft, where the losses are dissipated into heat. The sources of loss are classified in the following groups:

- Mechanical losses in bearings and shaft seals. Since these losses don't cause fluid heat, they are considered external losses;

- Volumetric losses due to all leakages which are pumped by the impeller, including leakage through the annular seals, device for axial thrust balancing, balance holes and central balance devices;
- Disk friction losses generated on rear and front shrouds of the impellers which rotate in the fluid;
- Similar friction losses created by the components of axial thrust balance devices;
- Leakage through the interstage seals in multistage pumps. These leakages do not flow through the impeller. Consequently, they do not influence the power transferred from the impeller vanes to the fluid;
- Hydraulic losses due to friction and vortex dissipation in all components between suction and discharge nozzle;
- Fluid recirculation at partload creates high losses due to an exchange of momentum between stalled and non-separated fluid zones.

The real head curve can be obtained by subtracting the hydraulic losses caused by friction and vortex dissipation from the theoretical head.

2.3.1 Friction losses

The shear stresses created by the velocity gradient in the non-separated boundary layers are responsible for the friction losses. According to Gülich (2007), experience shows that roughness increases the flow resistance in turbulent flow. However, this is only the case if the roughness elements protrude beyond the laminar sub-layer. In laminar flow the roughness has no influence on the resistance since there is no exchange of momentum across the flow. With growing Reynolds number, the boundary layer thickness decreases and the permissible roughness drops as well. Vortex shedding from the roughness peaks creates energy dissipation due to the exchange of momentum with the main flow. In the fully rough domain the losses become independent of the Reynolds number and increase with the square of the flow velocity.

2.3.2 Vortex dissipation (form drag)

In this work, all of the following were considered as vortex dissipation losses: localized losses, shock losses, losses due to secondary flow and recirculation. Since recirculation causes vortex dissipation, the losses due to this effect will be also considered as hydraulic losses.

While static pressure can be converted into kinetic energy without a major loss (accelerated flow), the reverse process of converting kinetic energy into static pressure involves far greater losses, because the velocity distributions are actually mostly non-uniform and subject to further distortion upon deceleration. Non-uniform flow generates losses caused by turbulent dissipation, known as "form" losses, and this is considered to be the main source of energy loss in pumps, especially at high specific speeds. Flow separations and secondary flows also increase the non-uniformity of a velocity distribution and, consequently, the losses.

2.3.2.1 Localized losses

The localized losses occur at the inlet and outlet of the impeller and casing/diffuser. This is due to the sudden change of section area and also because of the shift from a rotating component to a stationary one, or vice-versa. Fluid viscosity does not influence these losses, as they are purely inertial.

2.3.2.2 Shock losses

When the flow approaches the impeller or diffuser vanes at an incorrect angle, shock losses occur, as shown in Figure 6. These losses, which are also considered as vortex dissipation losses, are normally low at the design point and increase at off-design conditions with $(Q/Q_{BEP} - 1)^x$, where $x = 2$ is usually assumed.

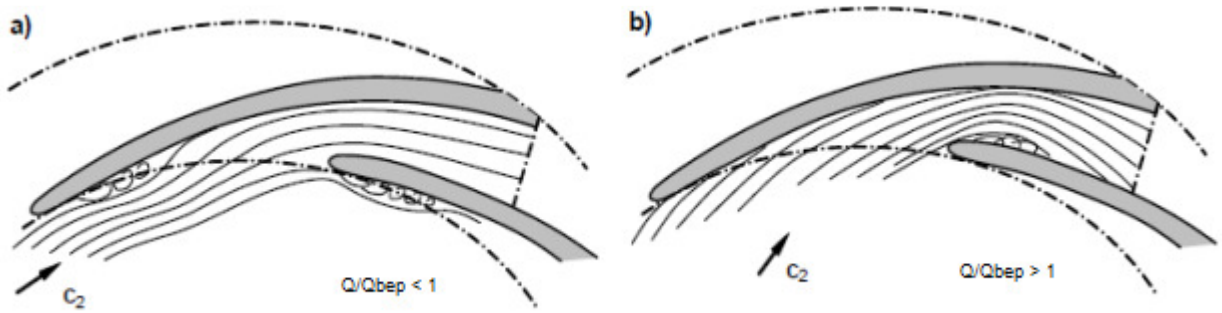

Figure 6 - Effect of local flow separation at impeller or diffuser inlet (Gülich, 2007).

Because of the complicated three-dimensional flow patterns, these losses cannot be predicted theoretically. Either empirical pressure loss coefficients are used for estimation or numerical methods are employed.

2.3.2.3 Losses due to secondary flow - Flow deflection caused by the vanes

According to Gülich (2007), the moment acting on the vanes can be considered a result of the integral of the pressure and shear stress distributions across the vane surface (vane forces). It can be determined that different flow conditions are found between vane pressure and suction surfaces, since the pressure distributions result from the velocity distributions around the vanes.

According to Stepanoff (1957), this pressure distribution profile makes the relative velocity at the suction side (SS) of the impeller vane be greater than the one at the pressure side (PS). As a result, a smaller real differential pressure is generated at the impeller than if there were a uniform velocity profile.

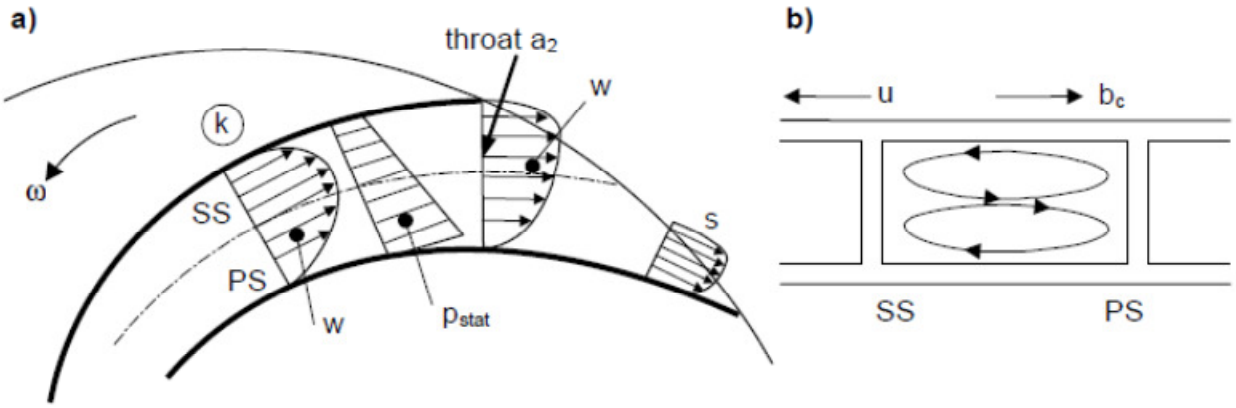

Figure 7 - Slip phenomenon. a) Flow between the vanes; b) Secondary flow (Gülich, 2007).

Furthermore, the flow is not able to follow the exact contour of the vanes. It is the deviation between the vane and flow angles that makes the work transfer possible. The described phenomenon is quantified by the "slip factor" or by the "deviation angle" and is shown in Figure 7.

Generally, secondary flows are induced when the fluid is subjected to forces acting perpendicular to the main flow direction. These forces generate corresponding pressure gradients which are determined by the resultant of the centrifugal and Coriolis accelerations. Consequently, the ratio of these accelerations, known as "Rossby number" R_O, determines the direction into which the flow will be deflected (Gülich, 2007).

In theory, if R_O is near 1, no relevant secondary flow would be expected. If R_O<1, the Coriolis forces are dominant and the flow direction is towards the pressure side of the vane. On the other hand, if R_O>1, the flow direction is towards the suction side of the vane.

2.3.2.4 Recirculation

When a pump works significantly below the best efficiency point, it is said to be operating at partload. Since vane inlet angles and channel cross sections are too large for the reduced flow rate, flow patterns during partload are significantly different from those at the design point. The flow becomes highly tridimensional since it separates in the impeller and the collector. At sufficiently lower flow, recirculation is observed at impeller inlet and outlet.

According to Fraser (1981), the total head produced is the sum of the centrifugal head and the dynamic head. The centrifugal head is independent of the flow rate, but the dynamic head is a function of the absolute velocity and therefore is a function of the flow rate. At some capacity, the dynamic head might exceed the centrifugal head, causing the pressure gradient to revert. The direction of the flow reverses, which causes flow recirculation.

Recirculation is a reversal of the flow at the inlet or at the discharge tips of the impeller vanes. All impellers display a start point of suction recirculation and a start point of discharge recirculation at some specific capacity, and the effects of recirculation can be very damaging depending on the size and speed of the pump. Therefore, the starting point of suction recirculation has to be considered when defining the pump's minimum flow. Furthermore, the starting point of discharge recirculation has to be analyzed due to its influence on the pump efficiency, especially in large specific speed pumps.

2.3.3 Secondary losses

Secondary losses also cause fluid heat and they have to be taken into account as power losses. However they are not considered as pressure (head) losses.

2.3.3.1 Disk friction losses

When a circular disk or a cylinder rotates in a fluid, shear stresses corresponding to the local friction coefficient occur on its surface. The friction coefficient depends on the Reynolds number and the surface roughness.

If the body rotates in a casing (as is the case in a pump) the velocity distribution between casing and rotating body depends on the distance between the impeller shroud and the casing wall as well as on the boundary layers which form on the stationary and rotating surfaces. In other words, $u = \omega r$ can no longer be assumed.

The disk friction losses in a pump depend on the following parameters: Reynolds number, roughness of the rotating disk and casing wall, axial sidewall gap, shape of the casing and size of

the impeller sidewall gap, influencing the boundary layer and leakage flow through the impeller sidewall gap, partload recirculation and exchange of momentum.

The last three parameters can severely influence the disk friction loss and render its calculation quite uncertain, especially with large leakage flows and at partload. Even at the best efficiency point, the tolerance of the calculated disk friction loss is estimated to be about 25%.

The share of disk friction losses in the power consumption of a pump drops exponentially with increasing specific speed and increasing head coefficient. With low specific speeds disk friction is the main source of loss and can achieve up to 30% of the useful power of the impeller.

2.3.3.2 Leakage losses

Close running clearances between impeller and casing/diffuser or on axial thrust balance devices limit the leakage from the impeller outlet to the inlet. Any leakage reduces the pump efficiency. Since the entire mechanical energy transferred by the impeller to the leakage flow (i.e. the increase of the static head and the kinetic energy) is throttled in the seal and converted into heat, one percent of leakage flow also means an efficiency loss of one percent (Gülich, 2007).

2.3.3.3 Mechanical losses

The mechanical losses are generated by the radial and axial bearings and by the shaft seals. Occasionally these losses include auxiliary equipment driven by the pump shaft.

The mechanical efficiency of large pumps is around 99.5% or even above. In contrast, the mechanical losses of small pumps (say below 5 kW) can use up a considerable portion of the coupling power. Examples are process pumps which are often equipped with dual mechanical seals.

2.4 Head curve prediction methods

As already mentioned, in literature, there are several proposed models based on fluid dynamic principles and experimental data that attempt to predict the hydraulic performance of centrifugal pumps. There are also various methods to calculate a pump's performance with numerical simulation. Some of these methods are presented below.

Patel et al. (1981) presents a theoretical model to predict the whole head curve of centrifugal pumps based on fluid dynamic principles, over a wide range of specific speeds, considering various sizes and types of pumps. The head curve is presented as being the Euler head minus friction and shock losses. The results are found to be in good agreement with the experimental data of more than 50 pumps, with an error of ± 3%.

Sun & Tsukamoto (2001) presents a CFD model to predict off-design performance of diffuser pumps, a condition in which the effects of rotor/stator interaction and the pump system characteristics become significant. The predicted head curve is validated by experimental data. The model produces a good prediction of pump off-design performance.

Li et al. (2002) affirms that most published guidelines for the selection and design of centrifugal pumps are based on performance data collected before 1960, on pump designs of the 1920's and 1950's. It analyzes the performance of a modern pump in an attempt to update the information. According to this work, calculating the performance of a modern pump from the available published guidelines may lead to discrepancies of up to 10% from the real performance.

Sun & Prado (2003) presents a single-phase model based on fluid dynamic principles, for different ESP pump types, liquid properties and motor speeds. Friction and shock losses are taken into account. A comparison between the predicted performance and the pump performances based on the Affinity Law is presented.

Asuaje et al. (2005) presents a 3D-CFD simulation of the impeller and volute of a centrifugal pump. This flow simulation is carried out for several impeller vane numbers and the relate volute tongue positions. According to this work, the volute tongue causes an unsymmetrical flow distribution in the impeller, which is confirmed by experimental data. Finally, velocity and pressure fields are calculated for different flow rates.

Cheah et al. (2007) presents a numerical simulation of the internal flow in a centrifugal pump impeller by using a three-dimensional Navier-Stokes code. Both design and off-design

conditions are analyzed. The results show that the impeller passage flow at the design point is smooth and follows the curvature of the vane. However, flow separation is observed at the leading edge due to non-tangential inflow conditions. When the centrifugal pump is operating under off-design conditions, unsteady flow develops in the impeller passage. The results are compared to experimental data over a wide range of flow and show good agreement.

Thin et al (2008) presents a method to predict the performance curves of a centrifugal pumps based on fluid dynamic principles. The theoretical head, slip factor, shock losses, recirculation and friction losses are taken into account. The pump considered in this work is a single-stage end suction centrifugal pump, with low specific speed.

Das et al. (2010) presents a performance prediction method for centrifugal submersible slurry pumps, based on fluid dynamic principles. Initially, the head curve for clean water is considered as the theoretical head deducted by the head losses. Then, the effects of solid particle size, specific gravity and concentration on pump slurry flow are shown. Finally, additional head losses due to solid particles in the slurry are predicted and deducted from the clean water head to establish the performance of centrifugal slurry pump. The performance prediction using this method is more accurate around the design flow rate and gives a more accurate prediction of centrifugal slurry pump performance for mostly homogenous slurry than it does for heterogeneous slurry.

Jafarzadeh et al. (2011) presents a general three-dimensional numerical simulation of turbulent fluid flow in order to predict the velocity and pressure fields of a centrifugal pump. A low specific speed, high speed pump is considered. A commercial CFD code is used. The comparison between the resultant performance curves and experimental data shows acceptable agreement. Furthermore, the effect of the number of impeller vanes on the hydraulic efficiency and the effect of the position of the vanes with respect to the tongue of the volute on the start of the separation are analyzed.

El-Naggar (2013) presents a one-dimensional flow procedure for the prediction of centrifugal pump performance, based on principle theories of turbomachines, such as the Euler equation and the energy equation. The loss at the impeller exit associated to the slip factor and the volute loss are estimated. The predicted curves are consistent with experimental characteristics of centrifugal pumps.

Shah et al. (2013) presents a critical review of the CFD analysis of centrifugal pumps along with the future scopes for further improvements, since in recent years it has been observed a growing availability of computational resources and progress in the accuracy of numerical methods. According to this work, the most active areas of research and development are the analysis of two-phase flow, pumps handling non-Newtonian fluids and fluid-structure interaction. The CFD approach provides many advantages compared to other approaches, but due to its theoretical nature, validation with experimental results is highly recommended.

Biazussi (2014) presents a simple single-phase approach, based on fluid dynamic principles, that defines the head versus flow rate curve. According to this approach, for fluids with low viscosity, the head curve is a quadratic function of the flow rate, as expected. Some assumptions and simplifications were considered, so that the model would only depend on a few accessible hydraulic dimensions and the performance would be predicted with reasonable error.

Considering the aim of this work, the model presented by Biazussi (2014) is chosen as the starting point, due to its simplicity and dependency on few and accessible data of the pumps.

2.5 *Shut-off* head prediction

According to Dyson (2002), for many years, much of the pump community's focus has concentrated on improving prediction methods for best efficiency point conditions. But this is not true for the prediction methods available to estimate off-design performance. Investigations at partload operation are difficult. The area of off-design behavior that has received least attention is the prediction of the level of head a pump produces when its discharge valve is closed and the flow through the pump approaches zero, the *shut-off* condition.

Dyson (2002) and Newton (1998) compared some *shut-off* head prediction methods available in literature. These methods are either based on empirical data or developed from an analytical approach, they are presented below.

2.5.1 Stepanoff's method

The Euler equation simplified for the *shut-off* condition is presented as:

$$H_0 = \left(\frac{u_2^2}{g}\right) \quad (16)$$

On this basis, many statistical investigations have attempted to modify this theoretical maximum head by the application of a universal correction factor.

Stepanoff (1957) proposes the use of the factor Ψ_S, a constant, independent of the pump geometry and equal to 0.585.

$$H_{0.S} = \Psi_S \left(\frac{u_2^2}{g}\right) \quad (17)$$

This factor was derived from a review of a number of centrifugal pumps. The spread of error is over 20 per cent.

2.5.2 Peck's method

A similar correction factor for the Euler equation is proposed by Peck (1968), who also based his work on statistical analysis of pump geometry.

$$H_{0.Pk} = \Psi_{Pk} \left(\frac{u_2^2}{g}\right) \quad (18)$$

He suggested that the pump configuration affected this constant. In this way:

- For single suction volute pumps, Ψ_{Pk} = 0.575;
- For double suction volute pumps, Ψ_{Pk} = 0.625;
- For multistage volute pumps, Ψ_{Pk} = 0.6.

The available data has shown that the spread of the results is still wide.

2.5.3 Patel's method

According to Patel (1981), the specific speed of the pump has an influence on the *shut-off* head. Typically, a low specific speed pump may have a flat performance curve, while a high

specific speed one may have a higher head rise to *shut-off*. Patel (1981) proposes the following correction factor to the Euler equation:

$$H_{0.Pt} = \Psi_{Pt}\left(\frac{u_2^2}{g}\right) \tag{19}$$

$$\Psi_{Pt} = 0.65 - 0.00344 n_q \tag{20}$$

The specific speed n_q is calculated with metric units. The range of specific speed of the pumps analyzed by Patel is from 12 to 50.

Using the database to separate out pump configuration, the difference between each pump type becomes apparent. The data suggests that this method can be further modified to also take into account the pump configuration. The Patel's modified correction factor would then be:

- For single suction pumps:

$$H_{0.Pt.mod} = \frac{H_{0.Pt}}{0.9165+0.0001 n_q} \tag{21}$$

- For double suction pumps:

$$H_{0.Pt.mod} = \frac{H_{0.Pt}}{0.9923+0.0001 n_q} \tag{22}$$

- For multistage pumps:

$$H_{0.Pt.mod} = \frac{H_{0.Pt}}{0.8559+0.0002 n_q} \tag{23}$$

According to Dyson (2002), this method presents an increased accuracy compared to the previous ones.

2.5.4 Thorne's method

Thorne (1988) proposes a correction factor for the Euler equation based on empirical constants for the impeller and casing:

$$H_{0.T} = \left(\frac{u_2^2}{g}\right)\left[\left(\frac{1}{slip}\right) - \left(\frac{C_{1m}}{2u_1}\right)\left(A^2 + \frac{B^2}{slip^2}\right)\right] \tag{24}$$

$$slip = 1 + \left(\frac{a}{z}\right)\left(\frac{1+\beta_2}{60}\right)\left(\frac{2}{1-(D_1/D_2)^2}\right) \tag{25}$$

The casing factor in the slip equation $a = 0.77$, z is the number of impeller vanes, C_{1m} is the inlet meridional velocity. A is the ratio of the impeller inlet and outlet radius and B is the ratio of the inlet radius and the cutwater radius.

This method attempts to consider the impeller inlet and outlet diameters, which have influence on recirculation, causing negative effects on the *shut-off* head. The slip represents the effect of the impeller vane geometry. The casing is taken into account by the use of an empirically derived coefficient. The pump configuration is not taken into account.

According to Dyson (2002), this method consistently overpredicts the value of the *shut-off* head, with errors of over 20 per cent.

As proposed by Dyson (2002), the accuracy of Thorne's method could be increased by the use of the following correction factors, according to the pump configuration:

- For single suction pumps 1/1.31;
- For double suction pumps 1/1.1;
- For multistage pumps 1/1.36.

2.5.5 Stirling's method

Stirling (1982) proposes that the *shut-off* head be composed of three components: impeller contribution (as if the impeller were a solid body), volute contribution and inlet backflow (when liquid exits from the impeller eye and flows into the inlet channel).

$$H_{0.St.imp} = \frac{1}{2g}\left(u_2^2 - \frac{u_1^2}{2}\right) \tag{26}$$

$$H_{0.St.vol} = \frac{u_2^2}{2g}\left(h_0 - \left\{\frac{\phi_R}{tan(\beta_2 - \delta A)}\right\}\phi_R AR\right) \tag{27}$$

$$\delta A = 1.17E - 3\left(\frac{P_2\beta_2}{C_d}\right) \tag{28}$$

$$\phi_R = -0.2331\left(\frac{r_1}{r_2}\right) + 0.1952 \tag{29}$$

where *AR* is the ratio of rotor outlet area to the volute throat area, h_0 is the slip factor, P_2 is the impeller vane pitch at r_2 and C_d is a coefficient which takes into account the thickness of a rotating disk when calculating its disk friction.

This prediction method attempts to consider the contribution of important geometric features such as suction diameter, impeller diameter and volute. However it still relies on empirically derived constants. The pump configuration does not have a marked statistical effect on the predicted head, but the method consistently underpredicts the *shut-off* head.

Therefore, a modifying factor can be applied to the Stirling equation.

$$H_{0.St.mod} = \frac{H_{0.St}}{0.9339 - 0.00006 n_q} \quad (30)$$

2.5.6 Frost and Nilsen's method

Frost and Nilsen (1991) also proposes a method based on the contribution of the impeller and volute. However, while Stirling's method uses empirical coefficients, Frost and Nilsen's is purely analytical. The flow in the impeller is assumed to exhibit solid body rotation.

$$H_{0.FN.imp} = \frac{u_2^2}{2g}\left[1 - \left(\frac{r_1}{r_2}\right)^2\right] \quad (31)$$

According to Newton, (1998), they were uncertain of the value of r_1 and identified three possibilities: the impeller vane inlet radius, the radius of the suction pipe or zero, due to the fact that forced vortex rotation will spread to the centerline.

The volute contribution was obtained by assuming that the velocity distribution within the diffuser satisfied the following three flow conditions: the velocity at the exit of the impeller is equal to the vane velocity, there is no net flow in the discharge duct, and there is continuity of the recirculating flow in the volute.

$$H_{0.FN.vol} = \left(\frac{\zeta r_2}{(r_m - r_2)^2}\right)\left[r_m \, ln\left(\frac{r_4}{r_2}\right) - 2r_m(r_4 - r_2) + \left(\frac{r_4^2 - r_2^2}{2}\right)\right]\frac{1}{g} \quad (32)$$

where ζ is the angular velocity of the impeller, r_4 is the height from the impeller centerline to the throat, r_m is (radius at tongue - r_4)/2 and r_2 is the radius at the middle of the throat. According to Dyson (2002), although this method doesn't consider the negative contribution from the backflow, it is more accurate than the previous methods.

Dyson (2002) also presents a modifying factor for the Frost and Nilsen's equation:

$$H_{0.FN.mod} = \frac{H_{0.FN}}{0.9282 - 0.00005 n_q} \quad (33)$$

2.5.7 Gülich's method

Based on numerous measurements in all types of centrifugal pumps, Gülich (2007) presents a graph of the pressure coefficient as a function of the specific speed. He also presents an

estimate of the *shut-off* head. As with all statistics, the figures show mean values and mean errors but do not permit any statement on possible deviation of the individual measurement which, in principle, can be of any magnitude (Gülich, 2007).

$$\Psi = \frac{2gH}{u_2^2} \tag{34}$$

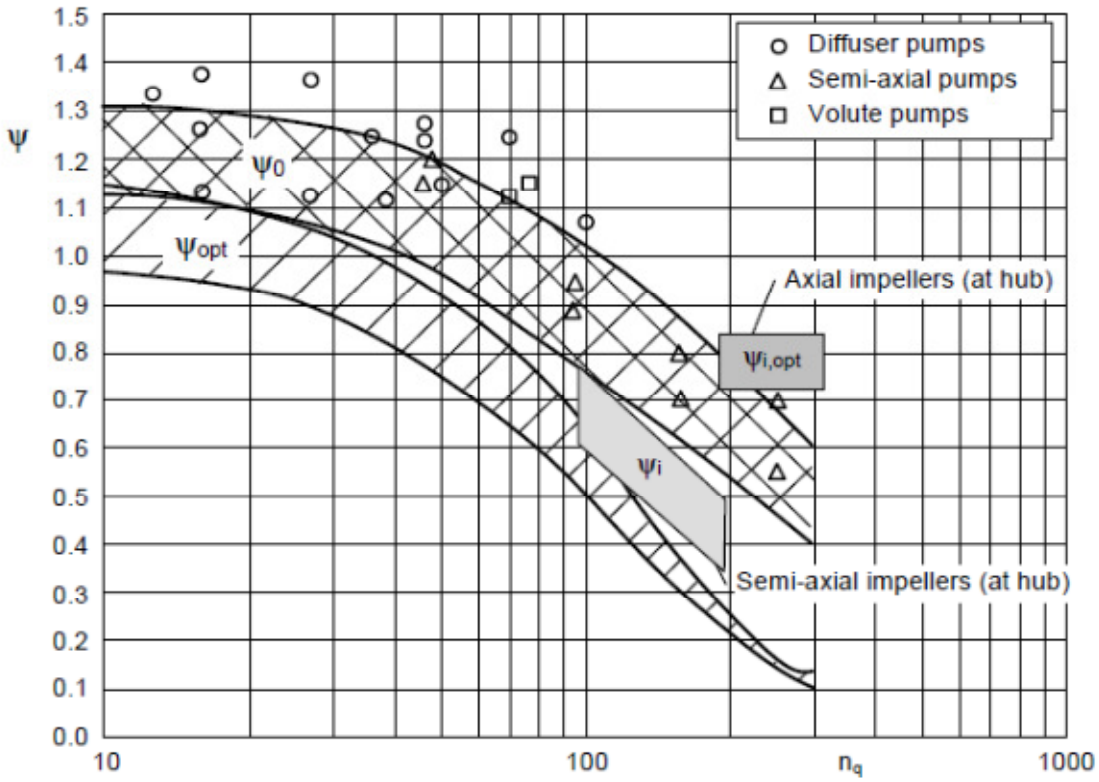

Figure 8 – Pressure coefficients (Gülich, 2007).

Analytical functions for the *shut-off* pressure coefficients are provided by Equations (35) and (36):

For diffuser pumps: $\Psi_0 = 1.31e^{-0.3n_q/n_{q.Ref}}$ (35)

For volute pumps: $\Psi_0 = 1.25e^{-0.3n_q/n_{q.Ref}}$ (36)

where $n_{q.Ref} = 100$.

The previous section clearly demonstrates that the *shut-off* head takes into account numerous phenomena and its prediction is very complex.

3 THEORETICAL MODEL

The theoretical model used in this work is the one developed by Biazussi (2014) and it is presented below. This model establishes a method for the interpretation of the head versus flow rate of a centrifugal pump. The following premises are considered:

- Homogeneous and single-phase flow;
- One-dimensional and permanent flow;
- Uniform flow through the impeller;
- Constant speed;
- Negligible torque due to superficial and field forces.

Dimensional analysis provides a better understanding of the flow and the physical effects involved before starting a theoretical and experimental analysis, allowing for the extraction of data trends that would otherwise remain disorganized and incoherent.

The differential pressure is a function of the head provided by the pump, while the head depends on the volumetric flow rate (Q), speed (ω), density (ρ), viscosity (μ), impeller diameter (D_2) and other hydraulic dimensions (L_i).

$$\Delta P = h_1(Q, \omega, \rho, \mu, D_2, L_i) \tag{37}$$

As previously shown in Chapter 2, through dimensional analysis, we can derive the following equations:

Capacity coefficient: $C_Q = \frac{Q}{\omega {D_2}^3}$

Head coefficient: $C_H = \frac{\Delta P}{\rho \omega^2 {D_2}^2}$

Viscosity coefficient: $X = \frac{\mu}{\rho \omega {D_2}^2} = \frac{1}{Re_\omega}$

Geometric coefficients: $\frac{L_i}{D_2}$ (38)

As a result:

$$C_H = F\left(C_Q, X, \frac{L_i}{D_2}\right) \quad \rightarrow \quad \frac{\Delta P}{\rho \omega^2 {D_2}^2} = H_1\left(\frac{Q}{\omega {D_2}^3}, \frac{\mu}{\rho \omega {D_2}^2}, \frac{L_i}{D_2}\right) \quad \rightarrow \quad C_H = H_1\left(C_Q, X, \frac{L_i}{D_2}\right) \tag{39}$$

A generic expression for H_1 has to be defined based on physical phenomena. The correlations have to be adjusted to the experimental data. The pump geometry is taken into account by the model adjustment coefficients.

The differential pressure provided by the pump can be calculated by subtracting the hydraulic pressure losses from the Euler differential pressure:

$$\Delta P = \Delta P_{Euler} - \Delta P_{losses} \tag{40}$$

where:

$$\Delta P_{Euler} = \rho\omega^2 r_2^2 \left(1 - \frac{Q\ cotg\beta_2}{2\pi B_2 \omega r_2^2}\right) \tag{41}$$

And $r_2 = D_2/2$. (42)

The Euler differential pressure can also be written as:

$$\Delta P_{Euler} = \frac{1}{4}\rho\omega^2 {D_2}^2 - k_1 \frac{\rho\omega Q}{D_2} \tag{43}$$

where $k_1 = \frac{D_2\ cot\,\beta_2}{2\pi B_2}$ (44)

And according to the dimensional analysis, the Euler head curve is written as:

$$C_{H\,Euler} = \frac{1}{4} - k_1 C_Q \tag{45}$$

The hydraulic pressure losses are composed of the friction, localized and distortion losses:

$$\Delta P_{losses} = \Delta P_{friction} + \Delta P_{loc} + \Delta P_{distortion} \tag{46}$$

The friction losses are expressed by an equivalent friction factor, which is composed of a turbulent term and a viscous term:

$$\Delta P_{friction} = f \frac{L_i}{D_2} \frac{\rho}{2} \left(\frac{Q}{A_n}\right)^2 = k_a f \rho\omega^2 {D_2}^2 \left(\frac{Q}{\omega {D_2}^3}\right)^2 \tag{47}$$

$$f = k_2^* \frac{\mu D_2}{\rho Q} + k_3^* \left(\frac{\mu D_2}{\rho Q}\right)^n \tag{48}$$

where $A_n = 2\pi\bar{r}\bar{B}$, $k_2 = k_a {k_2}^*$ and $k_3 = k_a {k_3}^*$. Therefore, it follows that:

$$\Delta P_{friction} = \left[k_2 \left(\frac{\mu D_2}{\rho Q}\right) + k_3 \left(\frac{\mu D_2}{\rho Q}\right)^n\right] \rho\omega^2 {D_2}^2 \left(\frac{Q}{\omega {D_2}^3}\right)^2 \tag{49}$$

where n expresses the viscous effect in high flow rate and is always smaller than 1.

According to the dimensional analysis, the friction head losses are written as:

$$C_{H\,friction} = \left[k_2 \left(\frac{\mu D_2}{\rho Q}\right) + k_3 \left(\frac{\mu D_2}{\rho Q}\right)^n\right] {C_Q}^2 \tag{50}$$

The localized losses are considered purely inertial and independent of the viscosity. They are represented by the sum of the dissipative losses that occur in the inlet and outlet of the impeller and casing/diffuser.

$$\Delta P_{loc} = k_6 \rho \omega^2 {D_2}^2 \left(\frac{Q}{\omega {D_2}^3}\right)^2 \quad (51)$$

The localized head losses are written according to the dimensional analysis as follows:

$$C_{H_{loc}} = k_6 {C_Q}^2 \quad (52)$$

The distortion losses represent the sum of the shock losses, losses due to secondary flow and recirculation losses.

For a one-dimensional simple model, the effects of the recirculation losses, losses due to secondary flow and shock losses overlap themselves, which makes it difficult to separate them. In this model they are represented as just one type of loss, called distortion loss.

$$\Delta P_{distortion} = \Delta P_{shock} + \Delta P_{sec.flow} + \Delta P_{recirculation} \quad (53)$$

The shock losses are inertial losses, caused by the misalignment of the fluid velocity with the vane surface, when the pump operates out of BEP of the maximum diameter.

$$\Delta P_{shock} = \rho \omega^2 {D_2}^2 k_4 \left[1 - k_5^* \frac{Q}{\omega {D_2}^3}\right]^2 \quad (54)$$

where k_5^* is based on pump geometry and is defined as:

$$k_5^* = \frac{{D_2}^3 \cot \beta_1}{2\pi B_1 r_1^2} \quad (55)$$

The losses due to secondary flow also depend on the flow rate and are relevant at partload. Secondary flow can be caused by the difference between the pressure at the suction side and the pressure at the pressure side of the impeller vanes, especially in the region closer to the vane outlet.

The recirculation losses occur inside the impellers and depend on the flow rate. These losses are maximized at zero flow (Gülich, 2007) and are expected to be zero at the best efficiency point.

The distortion losses are represented similarly to the shock losses, with similar equation, but without an explicit definition for k_5^*. Therefore, the distortion losses are defined as follows:

$$\Delta P_{distortion} = \rho \omega^2 {D_2}^2 k_4 \left[1 - k_5 \frac{Q}{\omega {D_2}^3}\right]^2 \quad (56)$$

And the distortion head losses are written as follows:

$$C_{H_{distortion}} = k_4\left[1 - k_5 C_Q\right]^2 \tag{57}$$

Therefore, the differential pressure curve can be understood as follows:

$$\Delta P = \frac{1}{4}{D_2}^2\rho\omega^2 - \frac{Q\rho\omega k_1}{D_2} - \frac{Q^2\rho\left[\frac{D_2\mu k_2}{Q\rho} + \left(\frac{D_2\mu}{Q\rho}\right)^n k_3\right]}{{D_2}^4} - {D_2}^2\rho\omega^2 k_4\left(1 - \frac{Qk_5}{{D_2}^3\omega}\right)^2 - \frac{Q^2\rho k_6}{{D_2}^4} \tag{58}$$

According to the dimensional analysis, it follows that:

$$C_H = \frac{1}{4} - k_4 + (-k_1 - Xk_2 + 2k_4k_5)C_Q + \left[-\left(\frac{X}{C_Q}\right)^n k_3 - k_4k_5^2 - k_6\right]C_Q^2 \tag{59}$$

The interpretation of the head versus flow rate curve of a centrifugal pump requires the explicit definition of the coefficient k_1 from the pump geometry and the simultaneous adjustment of the other six dimensionless parameters ($k_2,\ k_3,\ k_4,\ k_5,\ k_6,\ n$).

When the fluid viscosity is low, the parameter X is very small (less than 10^{-8}) and its influence on the head curve can be neglected. In this case, the pump performance depends only on the flow rate and pump geometry.

$$C_H = F\left(C_Q, \frac{L_i}{D_2}\right) \tag{60}$$

Therefore, the head curve is represented by the following equation:

$$C_H = \frac{1}{4} - k_4 + (-k_1 + 2k_4k_5)C_Q + [-k_4k_5^2 - k_6]C_Q^2 \tag{61}$$

4 TEST PROCEDURE AND PUMP TYPES

Since the tests used in the current work were not part of its scope, the test procedure is presented without many details. In Section 4.1 to 4.3, the test procedure with main followed recommendations and main instruments is presented. They are in accordance with the Standard ANSI/HI 14.6. In section 4.4, the different tested pump types are presented.

All the tests were performed according to the test procedure and test recommendations presented below.

4.1 Test procedure

The preferable layout for pump tests is a loop with the following characteristics:

- Closed loop as applicable;
- Pipe losses including valves shall allow for the full flow range to be measured;
- Cooling and heat exchanger as necessary;
- Possibility for degassing;
- Measuring device for dissolved oxygen concentration.

For performance tests a closed test loop with a separate connected tank according to Figure 9 is recommended. This layout ensures that no air gets into the loop after degassing. However, Figure 10 shows a simplified test loop with the main pipe going through the tank. This approach allows for a reduced cost piping layout with fewer valves and a simpler heat exchanger. The main disadvantage of this set-up is that it is possible for air from the tank to re-saturate and/or reenter the main pumping flow. Additionally the tank water level shall provide adequate submergence over the suction (tank outlet) pipe.

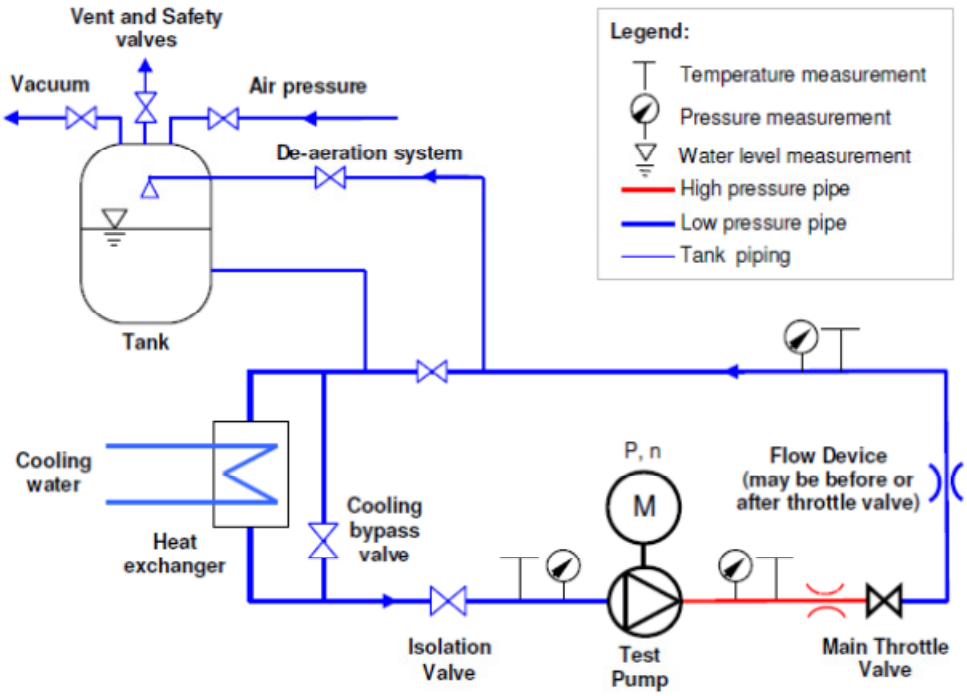

Figure 9 - Closed test loop with connected buffer tank – Horizontal pump.

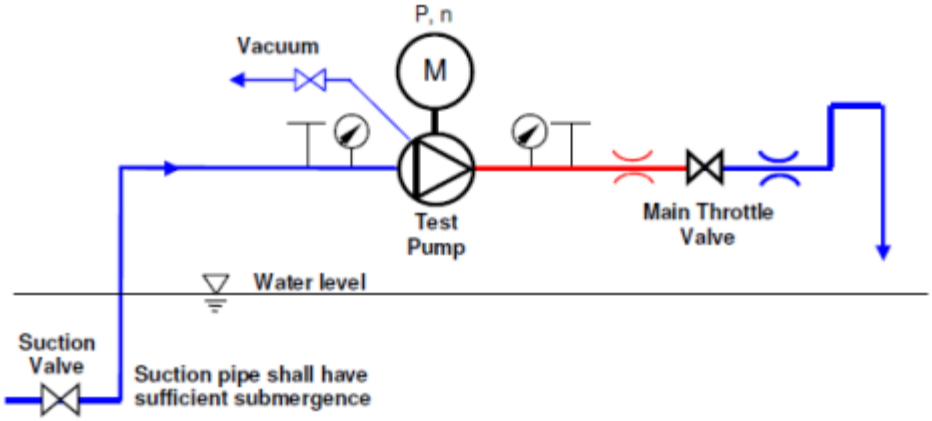

Figure 10 - Open test loop from wet pit – Horizontal pump.

4.2 Recommendations for the tests

Inlet flow disturbances, such as swirl, unbalance in the distribution of velocities and pressures, and sudden variations in velocity can be disruptive to the hydraulic performance of a

pump, its mechanical behavior, and its reliability. The most disturbing flow patterns to a pump are those that result from swirling liquid that has traversed several changes of direction in various planes.

When fittings, such as tees and elbows (especially two elbows at right angles) are located too close to the pump inlet (suction), a spinning action, or swirl, is induced. Higher energy and higher specific speed pumps with lower NPSH margins are more sensitive to suction conditions. Additionally double suction pumps are sensitive to uneven flow caused by an elbow in the plane of the shaft mounted on the suction flange which will direct more flow to one side of the impeller than the other.

For the best performance test results, the fluid flow into the pump should be as smooth and uniform as possible. Therefore a straight section of pipe should be used at the pump inlet. Generally 5 pipe diameters of straight pipe are required to ensure uniform flow. If the minimum recommended pipe lengths cannot be provided, flow-straightening devices should be considered.

Bends, valves, etc. should be limited in the suction line, especially directly upstream of the pump. The last elbow before the suction pipe shall be a long radius elbow.

The suction pipe shall be the same size as the pump suction nozzle. Piping leading to the suction pipe shall be the same size or larger. If a smaller pipe is unavoidable, it shall be at least 10 suction pipe diameters away from the pump suction. Also the fluid velocity and pressures should be checked to ensure that there is a margin over vapor pressure.

Velocities may be increased at the pump suction flange by the use of a gradual reducer (no more than one pipe diameter reduction in a single reducer should be used). A concentric reducer is recommended for vertical inlet (suction) pipes, reducing the possibility of air or vapor accumulation. When piping reducers are required in horizontal suction pipe runs, they shall be of the eccentric design oriented so as to not trap vapor (flat side up).

All inlet (suction) fitting joints shall be tight, especially when the pressure in the piping is below atmospheric, to prevent air leaking into the fluid. Care shall be taken to eliminate high points in the suction piping which may collect vapor. Vents shall be located at all high points of the suction piping.

Long horizontal runs of pipe should be sloped slightly upwards in the direction of flow to allow the fluid flow to sweep air bubbles to a high point which is vented.

The main components used on the performance tests are the following:

- Suction piping: pressured directly from the tank or by means of a booster pump;
- Suction valve: necessary for the NPSH tests;
- Suction pressure gauge;
- Tested pump;
- Driver (electric motor, turbine or diesel engine);
- Discharge pressure gauge: placed after a reasonable straight pipe length in order to provide a constant flow distribution;
- Discharge valve;
- Discharge piping;
- Flowmeter;
- Counter pressure valve.

Before the test, the following items are checked: pump and driver alignments, speed direction, electric parts, suction and discharge pipes, and instrument position and calibration.

During the test, the flow rate is controlled by the discharge valve. For each flow rate, the suction and discharge pressure, the speed and power at shaft end are measured. During the test, the bearings temperature and mechanical seal leakage are monitored.

At least five sets of readings are taken from the zero flow to 120% of the best efficiency flow (BEP). Points are chosen to include the shut off (if allowed), minimum flow, midway between minimum and rated flow, rated flow, BEP (if BEP is not within 5% of rated flow) and 120% of rated flow.

All testing is conducted with water, which is free of contaminants, at temperatures less than 55°C (130°F), or as otherwise specified.

Adequate suction pressure is maintained for safe and smooth operation of the pump during performance testing. Testing shall be performed within 50% to 120% of specified speed.

The instruments used for the test must be able to accurately measure the performance at the rated flow point and ensure that each instrument reading is within 1/3 - 2/3 of the meter range under rated working condition.

- Capacity: flow is measured with either a calibrated venturi meter, dall tube or orifice plate and a differential pressure gauge, transducer, or mercury manometer, or a magnetic, ultrasonic or mass flow meter, with an electronic output;

- Head: discharge pressure, and suction pressure when appropriate, is measured with a transducer, pressure gauge, positive displacement type deadweight tester, or manometer, with a correction added for the water surface or reference plane to gauge measurement. The differential head is calculated, including velocity heads, per the appropriate standard (ISO, HIS, or ASME);
- Power: a digital power meter or a poly-phase wattmeter, in conjunction with current and potential transformers as necessary, is used to measure the input power to the motor. The pump shaft power is computed using the calibration data of the motor (and gear as applicable). Alternatively a torque meter may be used;
- Speed: a photo tachometer, electronic counter and a magnetic pick-up or a hand held photo cell type digital counter is used to measure the pump shaft speed;
- Elevation: gauge elevations are be measured with a measuring stick or tape measure.

Table 1 presents the list of instruments used on the tests considered in this work. The instruments accuracy is such that the accuracy at the measured points is the one presented in this table. The tests were performed with the use of a data acquisition system and other computerized data recording systems that are responsible for the calculation, performance curves plotting and test report generation.

Table 1 - Instruments used during the tests and accuracy at the measured point.

Parameter	Instrument	Accuracy at the measured point
Flow	Magnetic or Ultrasonic Flow Meter, calibrated venturi or Dall tube, or standard orifice plate	± 1.0%
Pressure	Bourdon or pressure gauge, manometer, or pressure transducer	± 0.5%
Speed	Electronic revolution counter	± 0.3%
Impeller diameter	Paquimeter	± 0.05 mm
Power	Three phase watt or power meter with current and potential transformers	± 0.75%
Torque	Torque meter	± 0.5%
Temperature	Resistance or thermocouple type with indicator	± 1.0 ^{o}C

4.3 Vertical pumps

The test procedure and recommendations for vertical pumps are similar to the ones for horizontal pumps. Vertical pumps can be tested in a closed test loop with a suppression tank, according to Figure 11. This layout ensures that no air gets into the loop after degassing. However Figure 12 shows the typical vertical pump testing arrangements in open wet pits. These approaches allow for reduced cost piping layout and testing. The main disadvantage of this set-up is it is impossible to de-aerate the system, therefore fully saturated water must be considered.

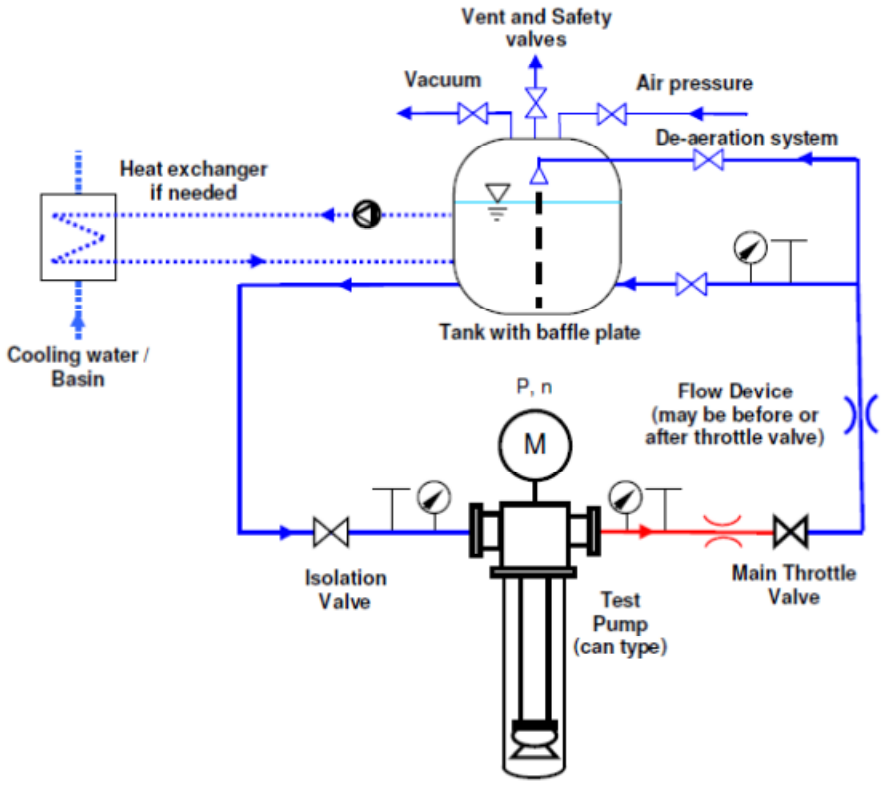

Figure 11 - Closed test loop through a suppression tank – Vertical pump.

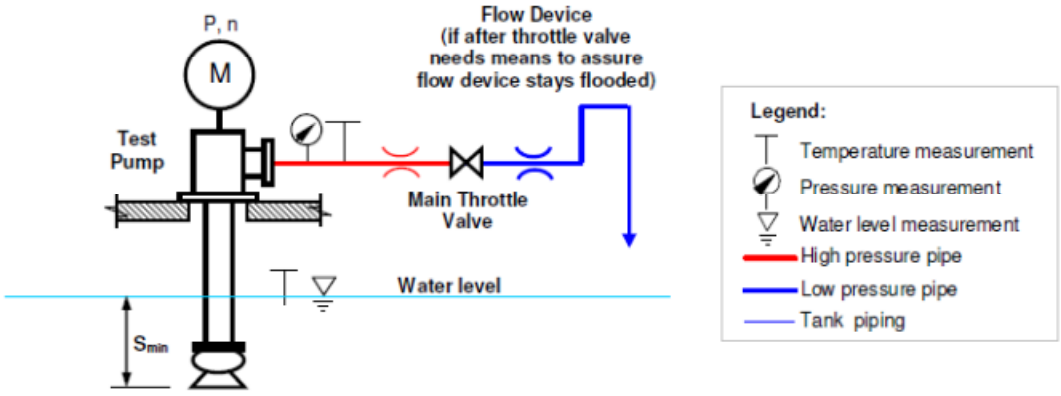

Figure 12 - Open test loop from wet pit – Vertical pump.

When tested in an open loop (wet pit) the pumps suction shall have sufficient submergence to prevent air borne vortexes. For pumps with suction cans or containers the inlet suction pipe shall have a straight section of pipe. Generally 5 pipe diameters of straight pipe are required to

ensure uniform flow at the pressure measurement section. If the minimum recommended pipe lengths cannot be provided, flow-straightening devices should be considered.

The main components used on the performance tests of vertical pumps are the following ones:

- Tested pump;
- Driver (electric motor, turbine or diesel engine);
- Discharge pressure gauge: placed after a reasonable straight pipe length in order to provide a constant flow distribution;
- Discharge valve;
- Discharge piping;
- Flowmeter;
- Counter pressure valve.

4.4 The tested pumps

The tests used in the current work were provided by a global pump manufacturer. Therefore it was possible to collect a big quantity of tests. The test data is shown in APPENDIX B.

In order to ensure the correspondence among the hydraulic dimensions of the pump, only performance tests at the impeller maximum diameter have been considered, so that the impeller outlet angle β_2 and the impeller outlet width B_2, for instance, would in fact correspond to the impeller outlet diameter, D_2.

Furthermore, it was possible to select tests of several types of pumps. These pump types are described here according to the classification presented by the international standard API 610 11th edition, “Centrifugal Pumps for Petroleum, Petrochemical and Natural Gas Industries”. The pump types used in this work are the following ones: OH2, BB1, BB2, BB3, BB4-BB5 and VS2.

4.4.1 Pump type OH2

The OH2 pumps are horizontal, centerline-mounted, single-stage overhung pumps, with single suction. They have a single bearing housing to absorb all forces imposed upon the pump shaft and maintain rotor position during operation. The pumps are mounted on a baseplate and are flexibly coupled to their drivers.

This pump type is widely used in off-shore and on-shore applications and also in the general industry.

Twenty-one tests of OH2 pumps were analyzed in this work, with a range of dimensionless specific speeds from 0.11 to 0.83.

Figure 13 represents a typical OH2 pump.

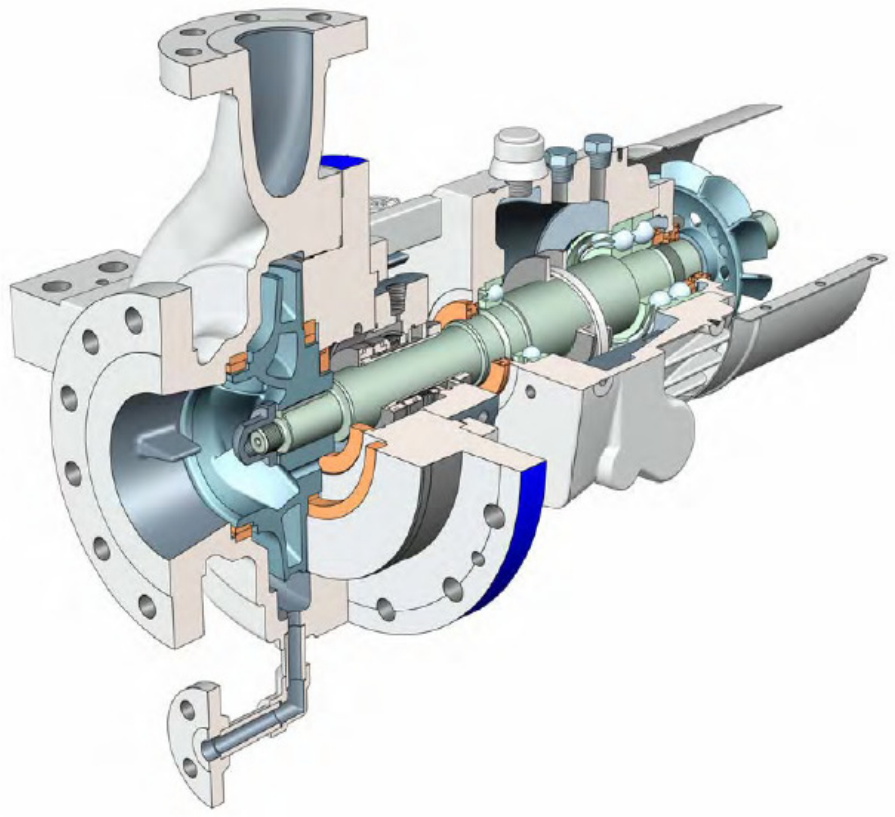

Figure 13 - OH2 pump type.

4.4.2 Pump type BB1

The BB1 pumps are horizontal, between bearings, axial split, volute pumps, with double suction impeller. According to the API 610 11th edition, this type of pump has one or two stages, but in this work just the pumps with one stage are considered in the category.

These pumps are used especially in pipeline applications, refineries and in the water and wastewater markets.

Seventeen tests of BB1 pumps were considered in this work, with a range of dimensionless specific speeds from 0.31 to 1.35. These pumps have a larger impeller outlet width B_2, that corresponds to the two sides of the impeller, which were used in the calculations.

Figure 14 represents a typical BB1 pump.

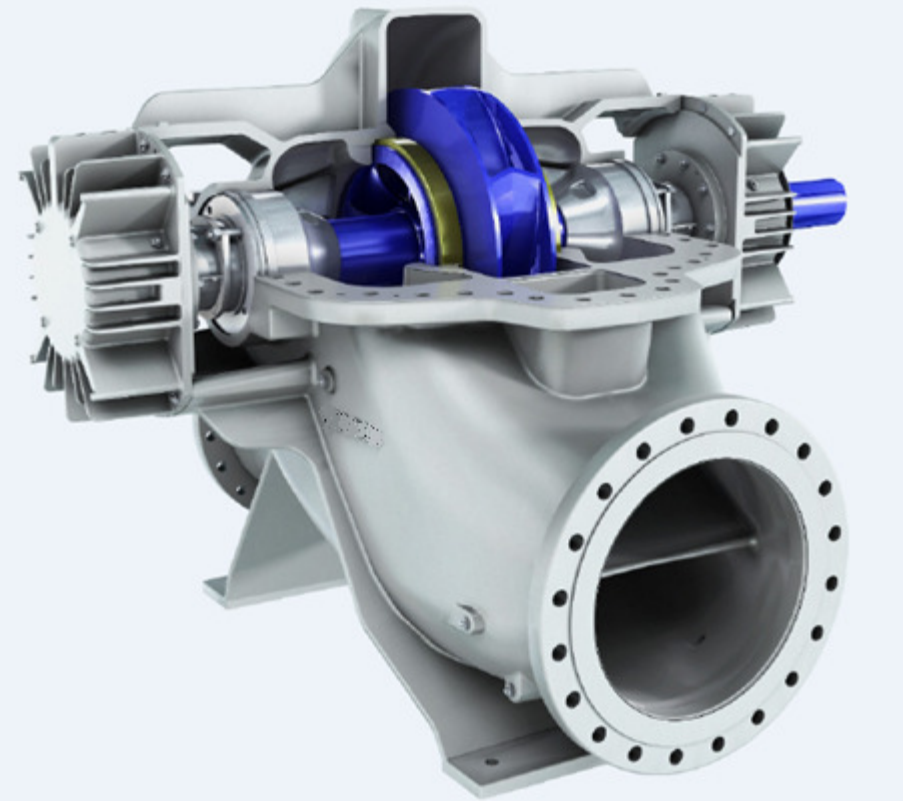

Figure 14 - BB1 pump type.

4.4.3 Pump type BB2

The BB2 pumps are horizontal, between bearings, radial split volute pumps with a double suction impeller. According to the API 610 11th edition, this type of pump has one or two stages, but in this work just the pumps with one stage are considered in the category.

This pump type is used in off-shore applications, such as SRU pumps, and in applications with high temperature.

In this work, two tests of BB2 pumps were considered, with dimensionless specific speeds of 0.32 and 0.47. Like the BB1 pumps, the B_2 used in the calculations corresponds to both sides of the impeller.

Figure 15 represents a typical BB2 pump.

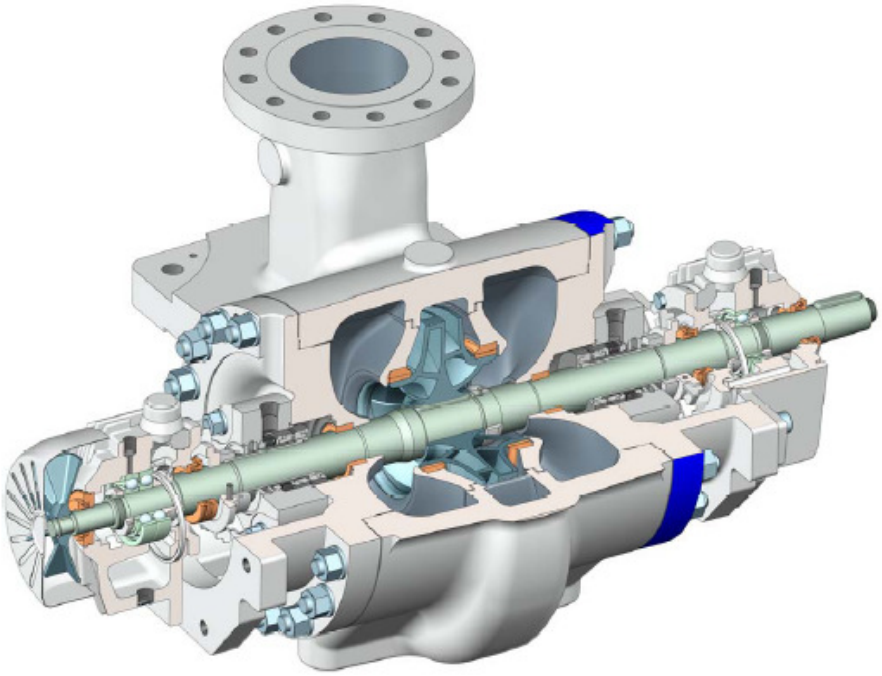

Figure 15 - BB2 pump type.

4.4.4 Pump type BB3

Similar to the BB1 pumps, the BB3 are horizontal, between bearings, axial split volute pumps, but with multiple stages. In this work the pumps with two stages or more are considered in this category.

These pumps are also used in pipeline applications and in the water and wastewater markets, but in applications with more flow rate and pressure than the ones in which the BB1 pumps are used.

In this work, nine tests of BB3 pumps were analyzed, with a range of dimensionless specific speeds from 0.49 to 0.92. Like the BB1 and BB2 pumps, the B_2 used in the calculations corresponds to both sides of the impeller. Furthermore, the hydraulics were analyzed considering just one impeller. The pressure provided by the pump was divided by the number of stages of the pump.

Figure 16 and Figure **17** represent typical BB3 pumps.

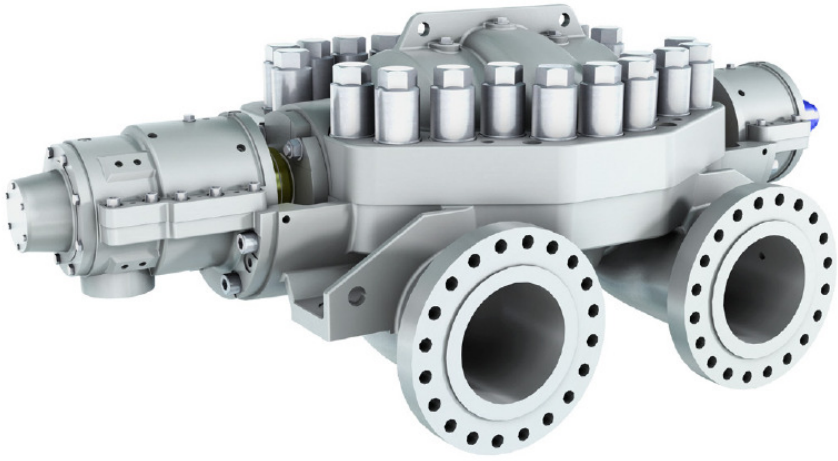

Figure 16 - BB3 pump type.

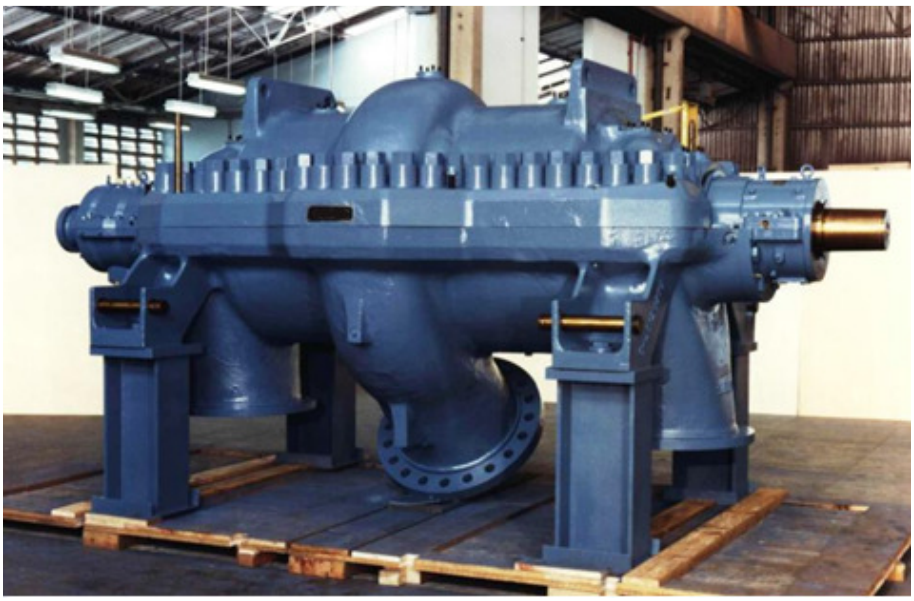

Figure 17 - BB3 pump type.

4.4.5 Pump types BB4 and BB5

The BB4 and BB5 pumps are horizontal, between bearings, radial split pumps, with diffuser and multiple stages. BB4 pumps have a single-casing, while the BB5 ones have a double casing (barrel).

BB4 pumps are mainly used as boiler feed water pumps in the power market. BB5 pumps support the highest pressures and therefore are used in high reliability applications, such as injection pumps on platforms.

Since the hydraulics of BB4 and BB5 pumps are usually the same, they were considered as a single group in this work. Twenty four tests were considered in this category. Like the BB3 pumps, the hydraulics were analyzed considering just one impeller. The pressure provided by the pump was divided by the number of stages of the pump.

In this work, twenty four tests of BB4-BB5 pumps were analyzed, with a range of dimensionless specific speeds from 0.24 to 0.50.

Figure 18 and Figure **19** represent typical BB4 and BB5 pumps.

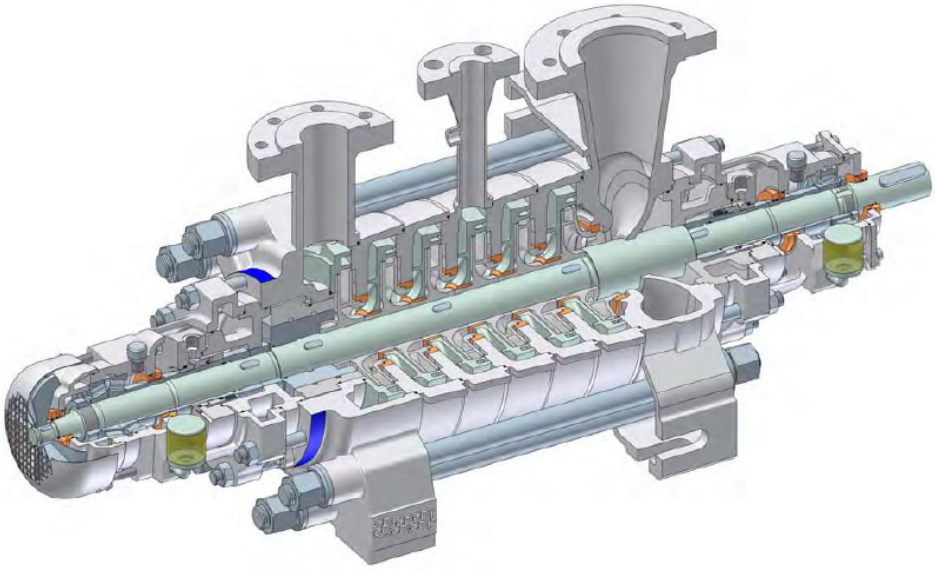

Figure 18 - BB4 pump type.

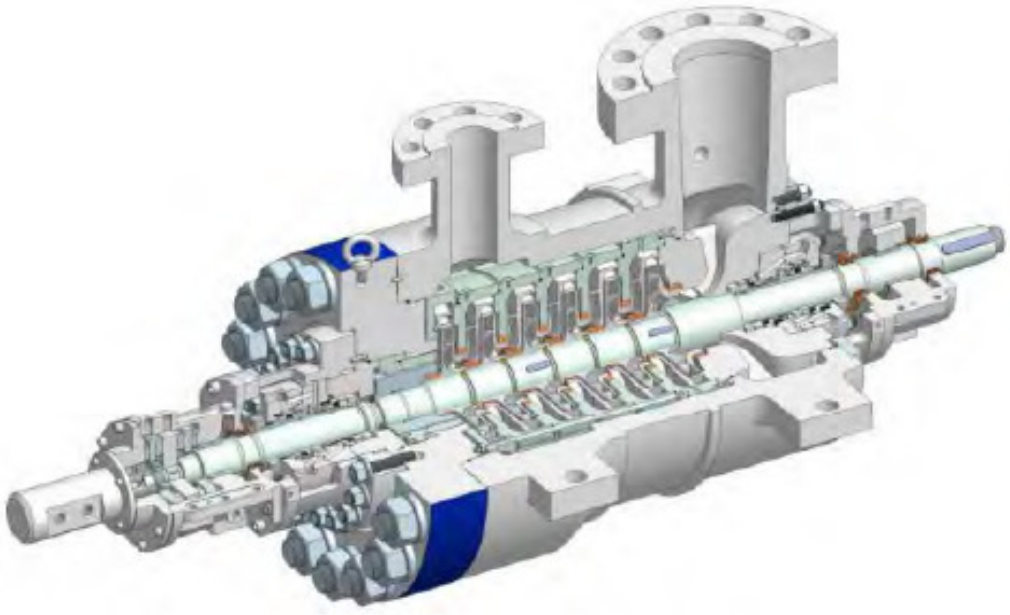

Figure 19 - BB5 pump type.

4.4.6 Pump type VS2

Wet pit, vertically suspended, single-casing volute pumps with discharge through the column are designated as VS2 pumps.

These pumps are widely used in off-shore application, such as fire-fighting system and as seawater lift pumps. They are also used in the water and wastewater market.

Seven tests of VS2 pumps were analyzed in this work, with a range of dimensionless specific speeds from 0.89 to 1.49. It is important to note that, for vertical pumps, at the differential pressure calculation, the level difference between the bowl and the discharge nozzle has to be taken into account, as well as the pressure losses at the column pipe.

Figure 20 represents a typical VS2 pump.

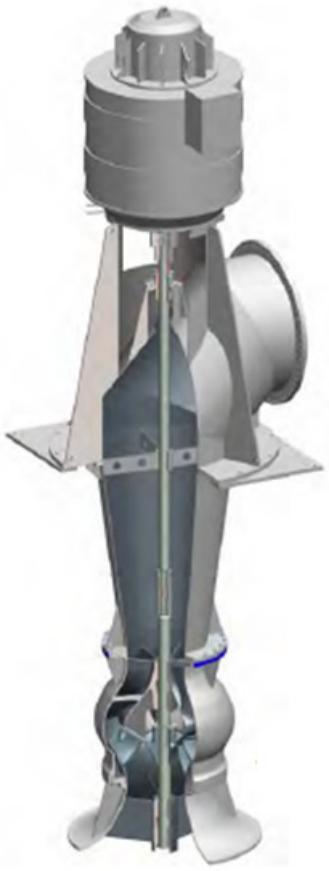

Figure 20 - VS2 pump type.

In total, eighty tests were analyzed in the current work, with a range of dimensionless specific speeds from 0.11 to 1.49. Six different types of pump were considered, including volute and diffuser pumps, single and double suction, horizontal and vertical, single or multistage. This diversity on the tests is essential for the validation of the proposed model.

5 RESULTS AND DISCUSSION

Initially, the tests used in this work are presented. They are compared to the reference curves provided by the pump manufacturer, which are henceforth referred to as theoretical curves. This comparison is not shown for all the eighty tests considered in the current work, just for two tests of each pump type.

Then, the tested curves are compared to the ones adjusted by the model presented by Biazussi (2014). Again, this result is shown just for some tests.

After that, the model equation coefficients are plotted against the pump specific speed in order to analyze the correlation among them. From the analysis of these correlations, equations are proposed, so that the coefficients can be defined from basic characteristics of the pumps, such as specific speed and main dimensions. As a result, the head curve against flow can be defined, only based on these characteristics.

Then, the correlation based curves are compared to the tested curves and the difference between them is discussed.

Afterwards, several shut-off head prediction methods are analyzed, so that the correlations proposed to predict the whole head curve can be improved. Then, the improved head curves are plotted against the correlation based and the tested ones and the difference among them is discussed.

Finally the effectiveness of the proposed method to predict the head curve of centrifugal pumps is evaluated.

5.1 Tested versus theoretical curves

Figure 21 presents a selection of tested flow versus head curves over the related theoretical ones provided by the pump manufacturer.

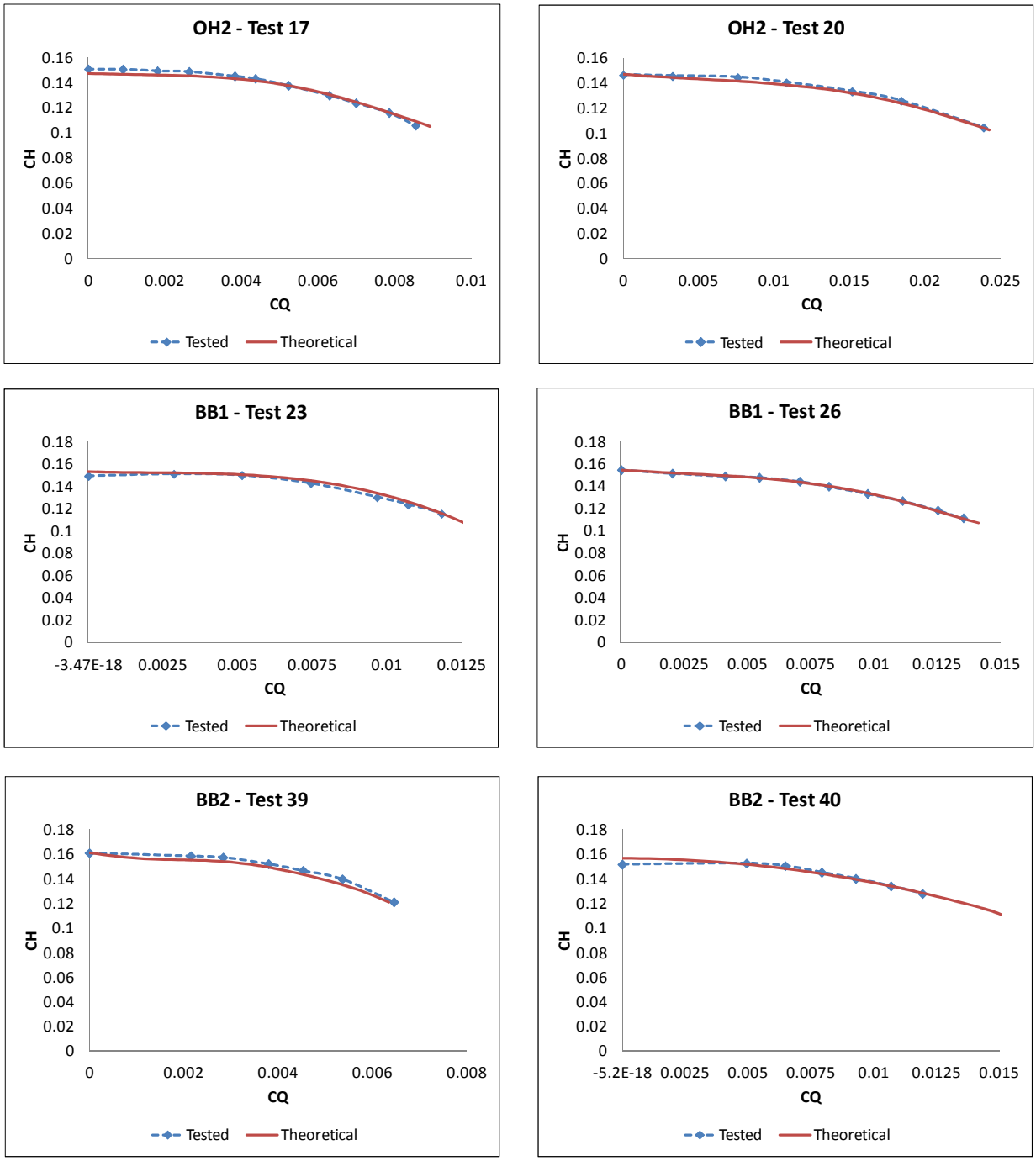

Figure 21 - Theoretical and tested curves.

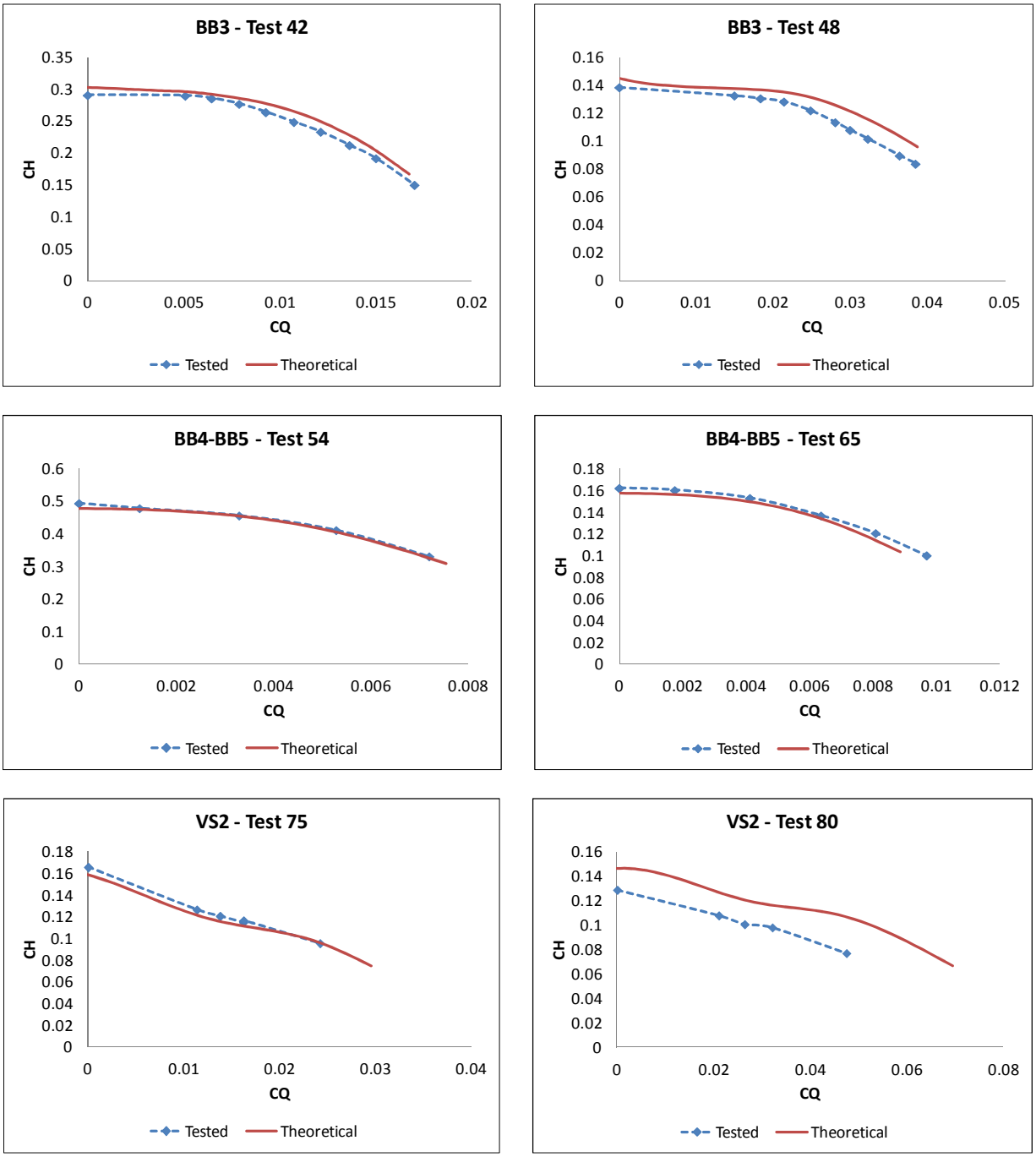

Figure 21 - Theoretical and tested curves (continued).

The calculation method for the flow and head coefficient errors is presented in APPENDIX A. The calculated values presented are associated with the data of test 17. The error associated with the flow coefficient in this case is ± 7.9% and the one associated with the head coefficient is ± 1.4%, as shown in Figure 22.

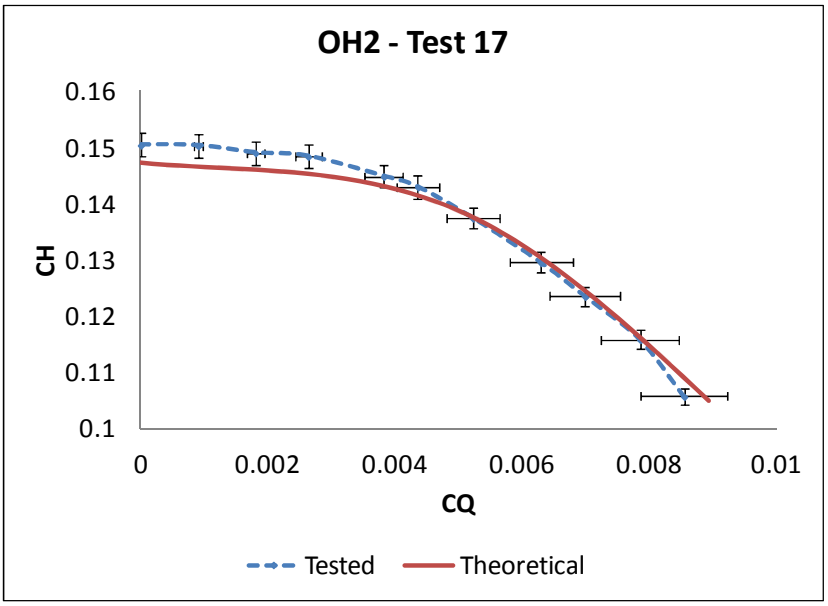

Figure 22 - Tested curve with flow and head coefficient errors.

Besides the experimental data error, the most relevant factors that could result in the differences observed among the curves are variations both in the casting process and during the test procedure. The test standards already allow for certain tolerances in the test results. So there is a margin to accommodate these variations.

The curves considered as reference for the model adjustment and the analysis of the results are the tested ones, since they represent the real performance of the pumps considered in this work.

5.2 Model adjustment for the head curve

The model adjustment proposed in Equation (61) was done by the software Wolfram Mathematica ™ version 9.0.1. The "FindFit" function was used to find the numerical values of the equation coefficients that best fit the input data. The adjustment is based on the minimization of the norm, calculated as follows:

$$Norm = \sqrt{Abs(x)^2 + Abs(y)^2 + Abs(z)^2 + \cdots + Abs(n)^2} \quad (62)$$

where n is the quantity of input data and the variables x, y and z are the deviation between the tested and the calculated values.

The coefficient k_1 is defined based on the pump geometry, according to Equation (44). The coefficients k_4, k_5 and k_6 are adjusted based on the tested data.

In this work, calculated curves are the curves adjusted by the model. Figure 23 presents the calculated curves over a selection of tested curves.

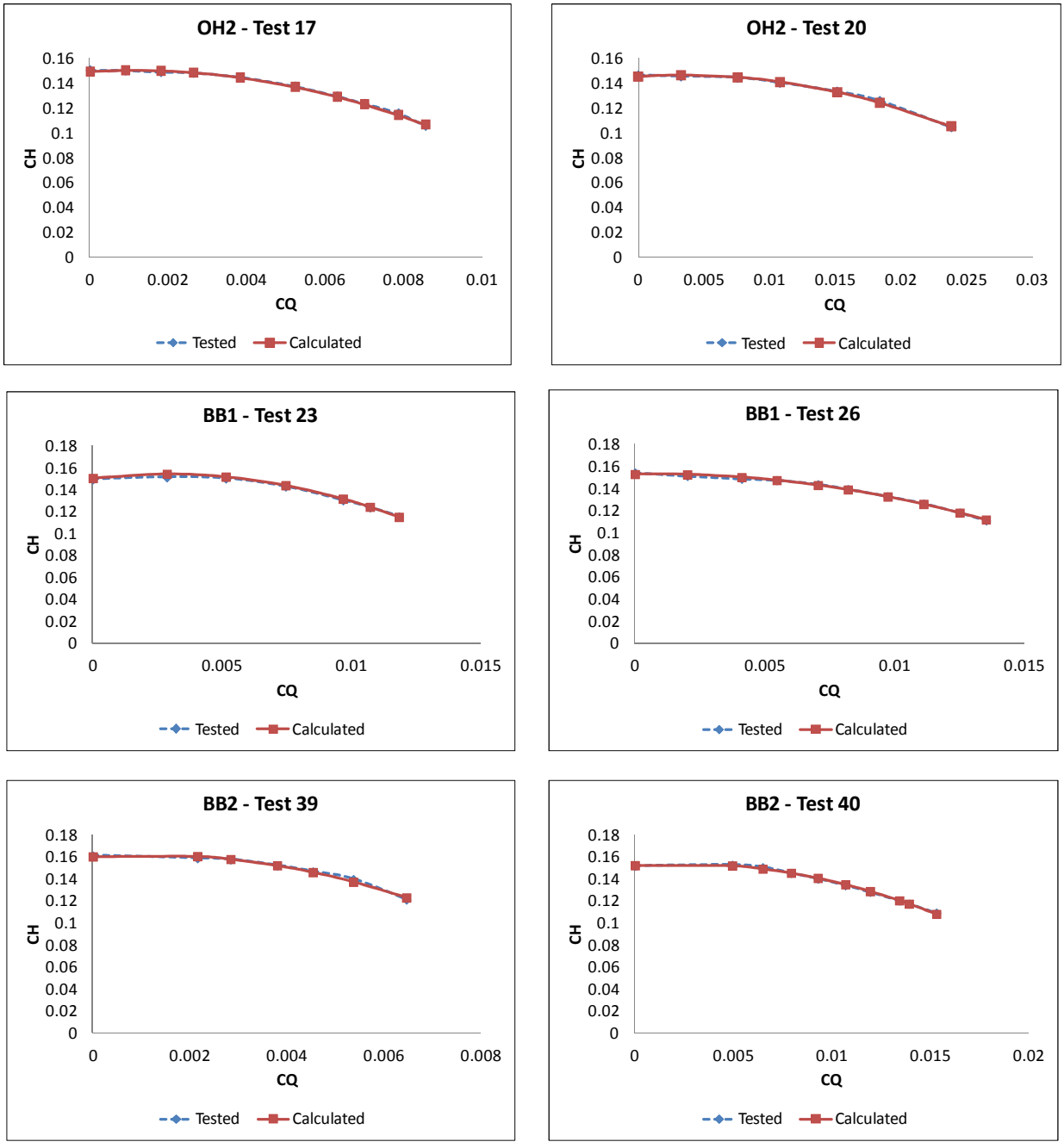

Figure 23 - Calculated and tested curves.

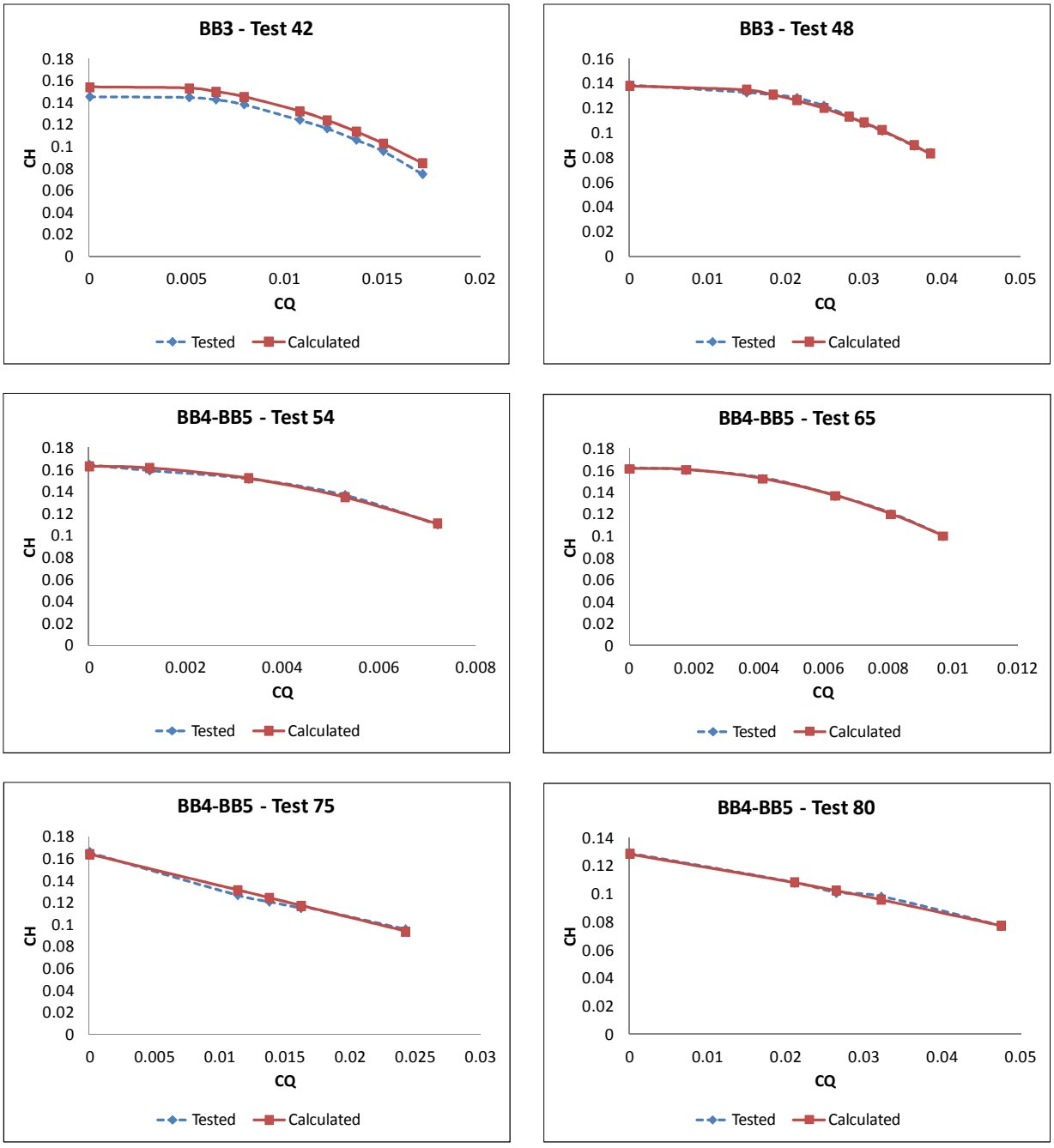

Figure 23 - Calculated and tested curves (continued).

5.2.1 The influence of β_2 on the head curve prediction

In some situations, the outlet angle of the impeller vanes β_2 might be difficult to measure. In these cases, since this hydraulic parameter is essential for the determination of k_1, this coefficient has to be adjusted based on the tested data, as do the other equation coefficients.

In order to evaluate the influence of β_2, several values of β_2 were considered on the head curve prediction by the model. The data of test 40 (BB2 pump) was used on this analysis. The range of β_2 considered was from 15° up to 37.5°. Figure 24 shows the head curve predicted by the model considering all the values of β_2.

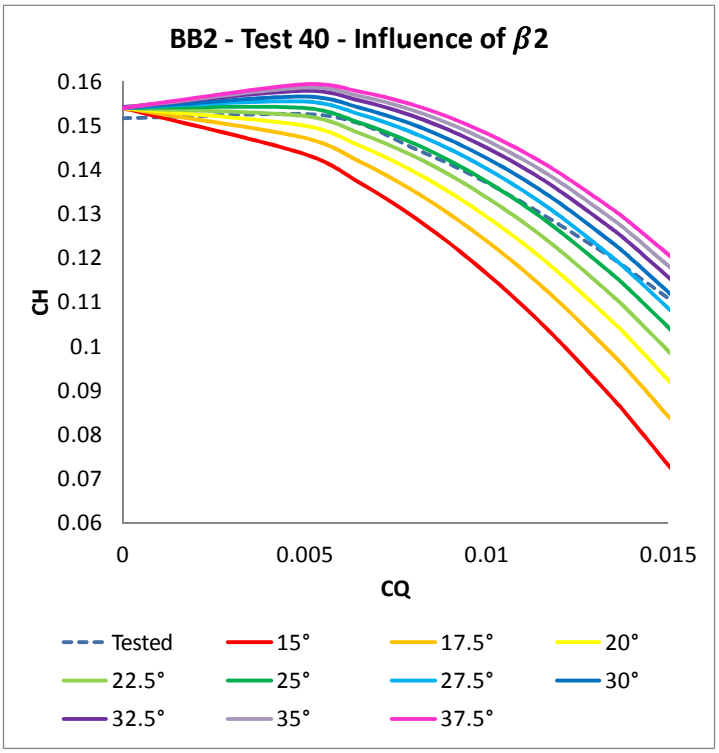

Figure 24 - Influence of $\boldsymbol{\beta_2}$ on the calculated curve.

The bigger β_2 the lower the predicted head losses and, consequently, the flatter the head curve. Based on these results, it is possible to conclude that β_2 in fact influences the shape of the head curve. This conclusion was already expected, since β_2 is one of the hydraulic parameters that define k_1, which multiplies C_Q in the model equation.

The real value of β_2 is 20.8°, but according to Figure 24, the curve that best predicted the shape of the head curve was the one with β_2 = 32.5°, but presenting an off-set that might be related to an error on the *shut-off* head prediction.

Additionally, in order to evaluate the effect of a missing β_2, the model was also run without β_2 and adjusting k_1 based on the tested data. Figure 25 presents a comparison among the tested curve and the head curves predicted with and without β_2.

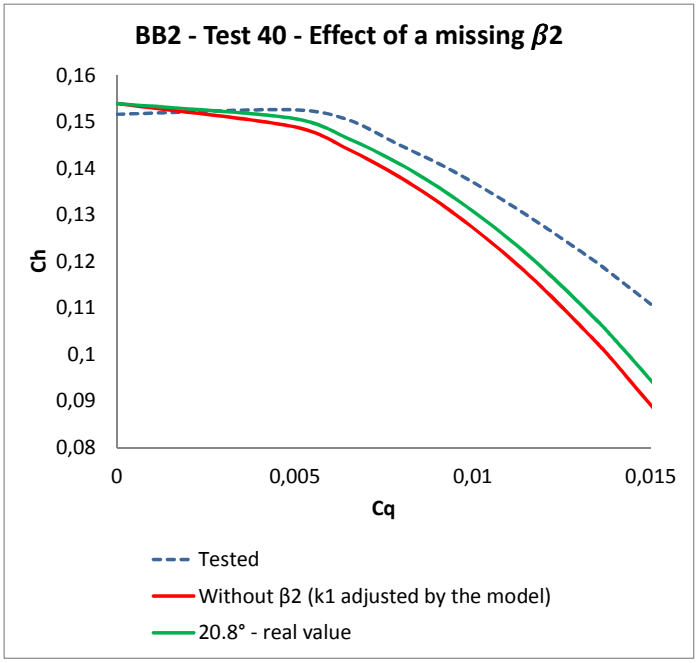

Figure 25 - Effect of a missing $\boldsymbol{\beta_2}$ on the calculated curve.

The head curve predicted without β_2 was not able to reproduce the shape of the tested curve. It over predicted the head losses. However, the curve predicted with the real value of β_2 has also presented a deviation in the shape of the curve. Therefore it is possible to conclude that the absence of a β_2 value in fact influences the head curve prediction, but there are also other influencing factors in play.

5.2.2 The contribution of each head loss on the head curve

As already shown in Chapter 3, the differential pressure provided by the pump can be calculated by subtracting the hydraulic pressure losses (friction, localized and distortion) from the Euler differential pressure.

According to the Equations (45), (50), (52) and (57), and using the data of test 17 (OH2 pump), the Euler head curve, the contribution of each head loss and the head curve with losses are visualized in Figure 26.

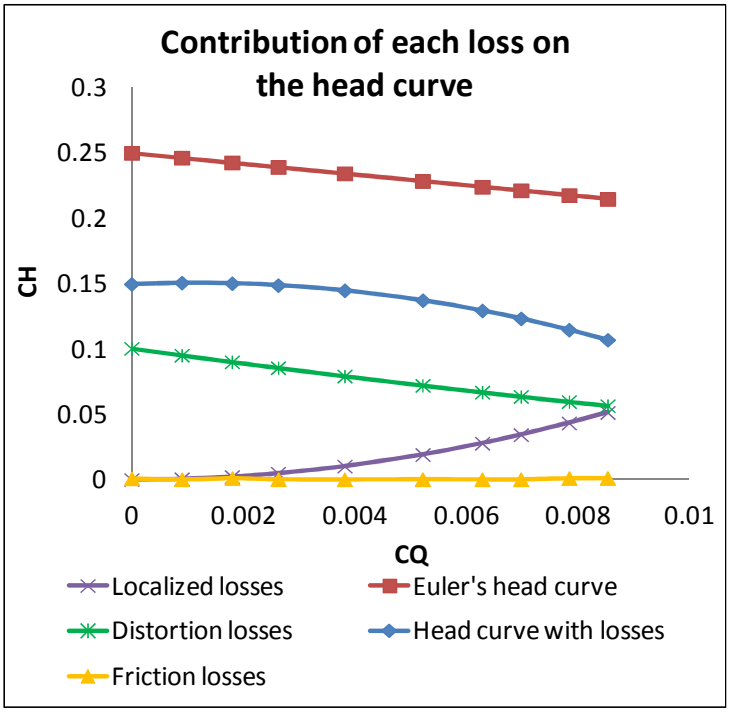

Figure 26 - Contribution of each loss on the head curve.

The friction losses are negligible, since the test was conducted with water, which presents low viscosity.

Figure 27 shows the total head losses curve and the flow at the best efficiency point (BEP). It is clear that the BEP flow does not correspond to the flow in which the losses are minimized.

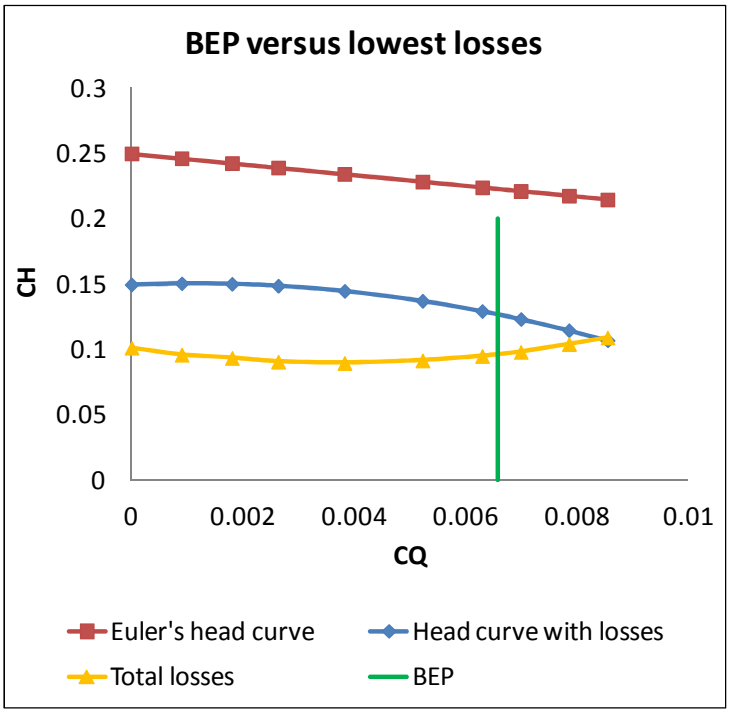

Figure 27 - BEP versus lowest losses.

5.2.3 The influence of the surface finish on the pump performance

According to the theory, the surface finish (roughness) influences the friction factor *f* and, consequently, the friction losses. However, in practice, this affects the pump efficiency more than the head curve. Figure 28 compares the head and efficiency test curves of a certain pump, with and without polishing. The pump material in both cases was chrome steel, A487 CA6NM, and the casting process was done with sand mold.

The tested pump is a BB1 type, with dimensionless specific speed of 0.905 and impeller diameter of 918 mm.

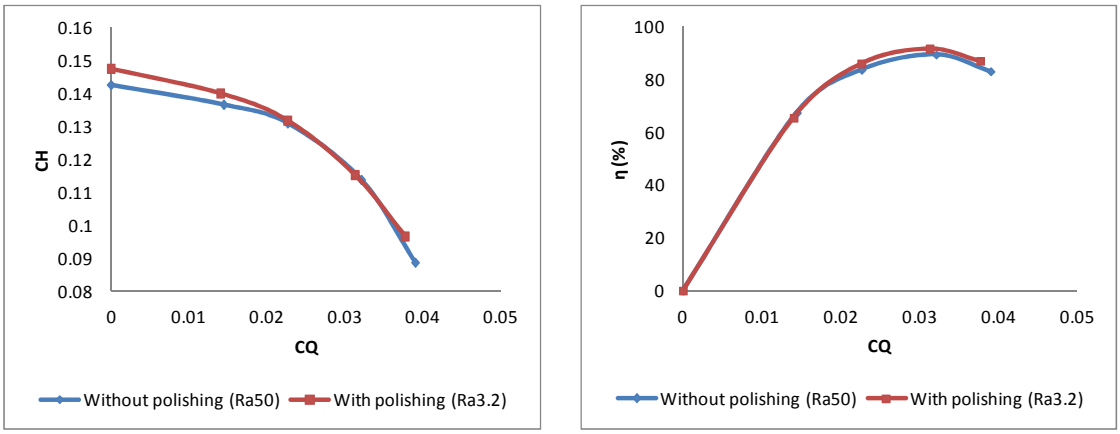

Figure 28 - Head and efficiency curves, with and without polishing

Around the BEP, the head curve almost didn't change, but the polishing from Ra50 to Ra3.2 increased the efficiency by 2.3 percentage points, which is better observed by changing the axis range in Figure 29.

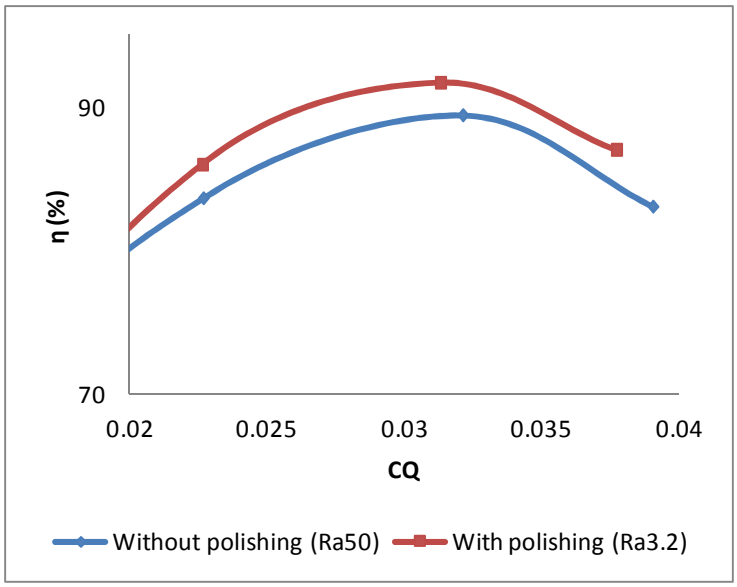

Figure 29 - Efficiency curves, with and without polishing.

These results are in line with the ones shown in Figure 26, in which the friction losses were considered negligible for the head curve.

5.3 Model equation coefficients versus pump geometry

The coefficients k_4, k_5 and k_6 are also dependent on the pump geometry and can be represented as a function of the dimensionless specific speed. This analysis was done by Biazussi (2014), but only with a few test results, and the correlations found among the coefficients and the specific speed were linear, as shown in Figure 30.

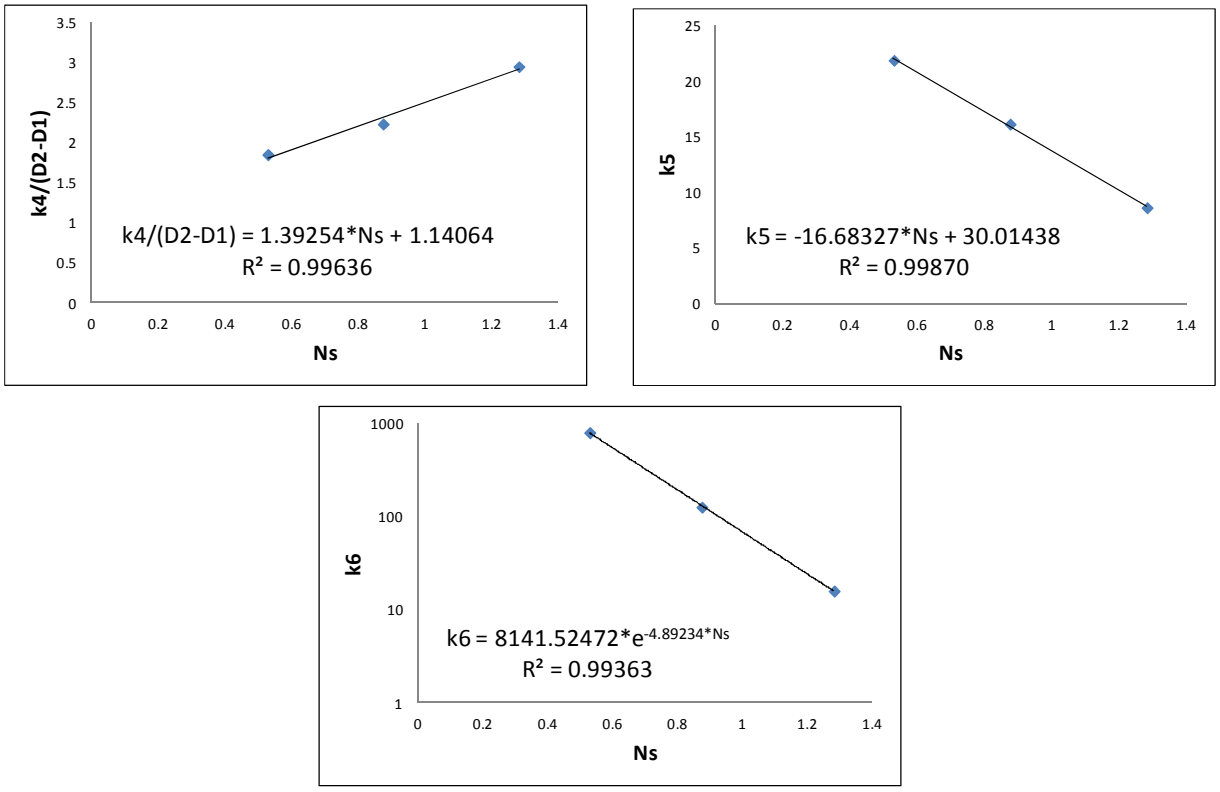

Figure 30 - Equation coefficients vs. specific speed for the tests analyzed by Biazussi (2014).

Biazussi (2014) has even suggested that more tested data should be used in order to better understand these correlations. And this is the biggest contribution of the current work. With the data from eighty tests, it was possible to evaluate these correlations and, in fact, they proved not to follow straight lines.

In Figure 31 to 34, the equation coefficients k_1, k_4, k_5 and k_6 adjusted by the model for all the tests are plotted as functions of the dimensionless specific speed. The points are grouped according to the pump type, but it is possible to notice tendencies when analyzing the results of all the pump types together.

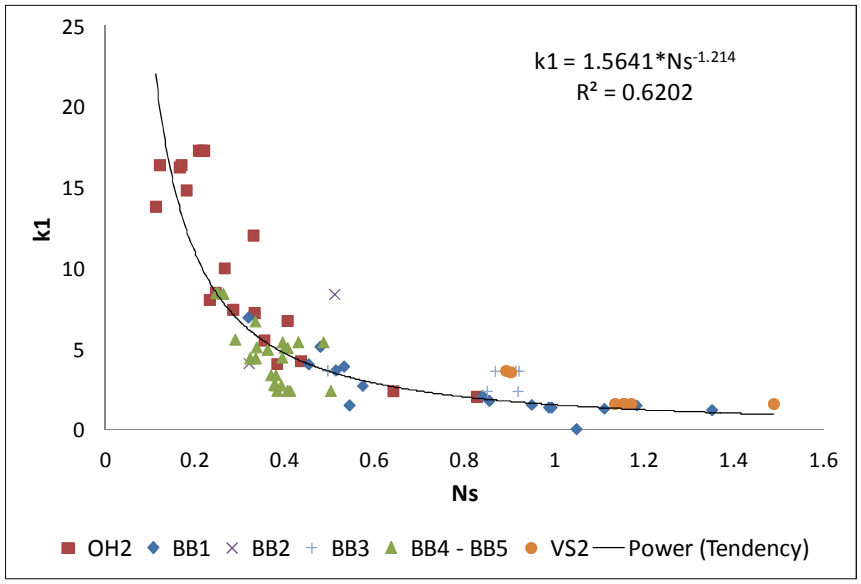

Figure 31 - Equation coefficient $\boldsymbol{k_1}$ vs. specific speed.

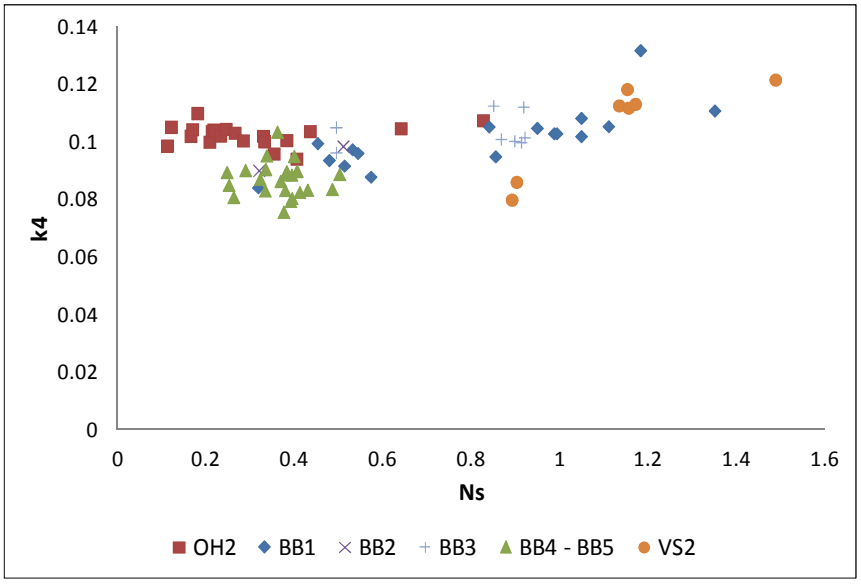

Figure 32 - Equation coefficient $\boldsymbol{k_4}$ *vs.* specific speed.

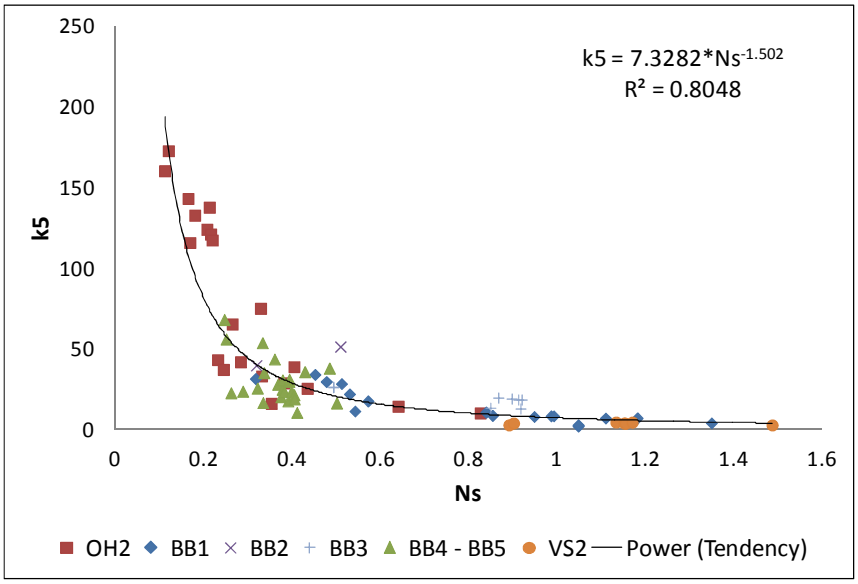

Figure 33 - Equation coefficient $\boldsymbol{k_5}$ vs. specific speed.

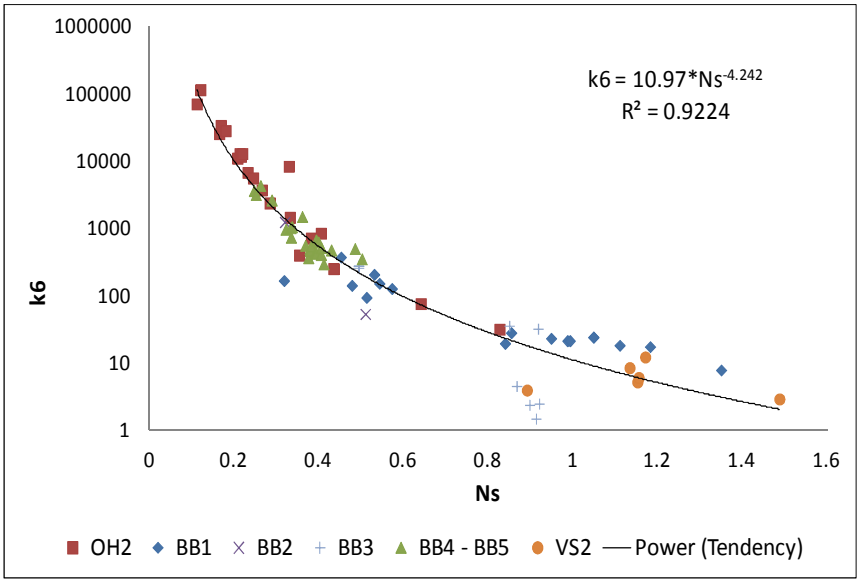

Figure 34 - Equation coefficient $\boldsymbol{k_6}$ vs. specific speed.

The coefficients k_1, k_5 and k_6 could be represented as functions of the dimensionless specific speed directly. The value of the coefficient k_4 is around 0.1 for most tests. However, in order to define a refined correlation for this coefficient, the ratio between the impeller inlet and outlet diameters, D_1 and D_2, has to be also taken into account. A reasonable correlation has been found between $k_4 \frac{D_1}{D_2}$ and the specific speed. Figure 35 shows this correlation.

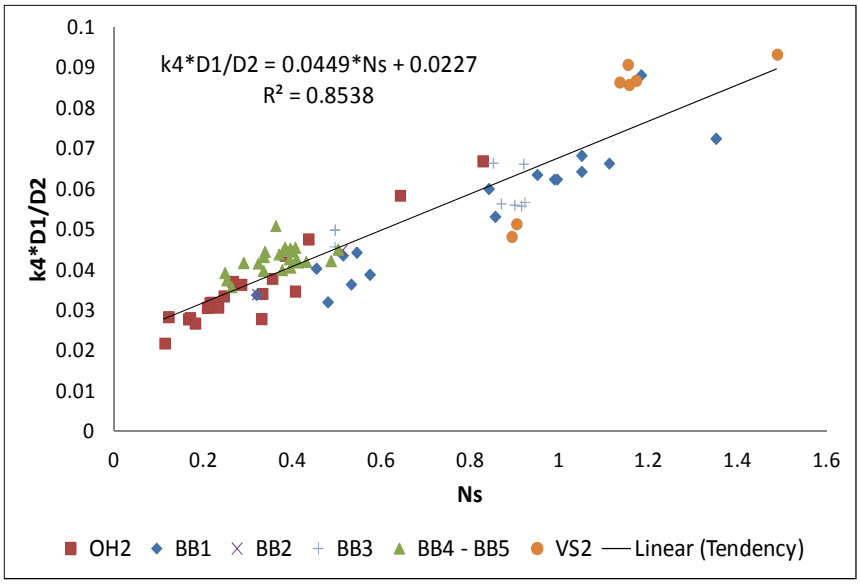

Figure 35 - Equation coefficient $\boldsymbol{k_4 \frac{D_1}{D_2}}$ vs. specific speed.

The ratio $\frac{D_1}{D_2}$ is purely geometric and represents the effect of the impeller vane length on the differential pressure. If the impeller inlet and outlet diameter were the same, no differential pressure would be observed.

The correlations between the coefficients and the dimensionless specific speed can also be represented as equations that are the best fit for each group of points. They are shown as the tendency lines in Figure 31, 33, 34 and 35 above.

With these correlations and Equations (44) and (61), the head curve against flow can be defined only based on basic characteristics of the pump, namely D_2, β_2, B_2, D_1 and N_s, as shown in Table 2:

Table 2 - Correlations among the equation coefficients and basic information of the pump.

$$C_H = \frac{1}{4} - k_4 + (-k_1 + 2k_4k_5)C_Q + [-k_4k_5^2 - k_6]C_Q^2$$

where:

$$k_1 = \frac{D_2 \cot \beta_2}{2\pi B_2}$$

$$k_4 = (0.0449N_s + 0.0227)\frac{D_2}{D_1} \quad (63)$$

$$k_5 = 7.3282{N_s}^{-1,502} \quad (64)$$

$$k_6 = 10.97N_s^{-4,242} \quad (65)$$

It is recommended that the value of the coefficient k_1 is calculated based on the pump geometry, according to Equation (44). The correlation presented in Figure 31 should be used only in case one of the hydraulic parameters that define k_1 is not available, for instance β_2, as discussed in section 5.2.1.

With regard to the coefficient k_4, it is also recommended that its value be obtained based on the correlations presented in Table 2. However, if the hydraulic parameter D_1 is not available, it is possible to approximate k_4 to 0.1, according to Figure 32.

This simplification is in line with Stepanoff's method for the shut-off head prediction, as shown below:

According to the Euler head equation, Equation (45), the head at shut-off is:

$$C_{H_{0.Euler}} = 0.25 \quad (66)$$

As shown in Chapter 2, Stepanoff (1957) proposes the use of the correction factor Ψ_S for the Euler head, having a constant value of 0.585. Therefore:

$$C_{H_{0.Stepanoff}} = 0.25 * 0.585 = 0.14625 \quad (67)$$

According to Equation (61), the head at shut-off is:

$$C_{H_0} = \frac{1}{4} - k_4 \quad (68)$$

Therefore, considering the Equations (67) and (68), the coefficient k_4 would be:

$$k_4 = \frac{1}{4} - 0.14625 = 0.10375 \quad (69)$$

5.4 Correlation based head curves

In this work, correlation based curves are the head versus flow curves based on equations presented in Table 2. Figure 36 compares the correlation based curves (Table 2) to the tested ones.

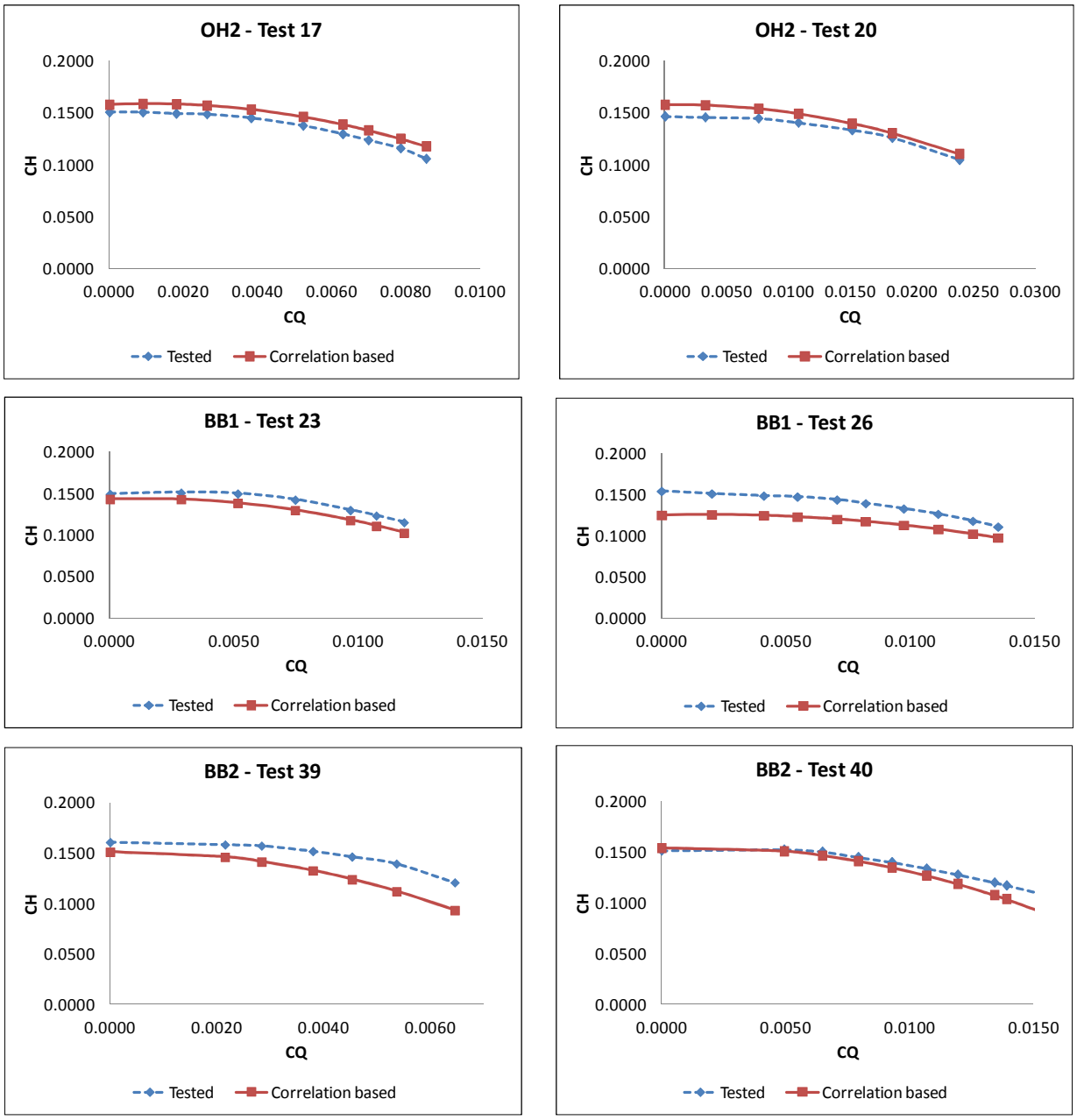

Figure 36 Correlation based and tested curves.

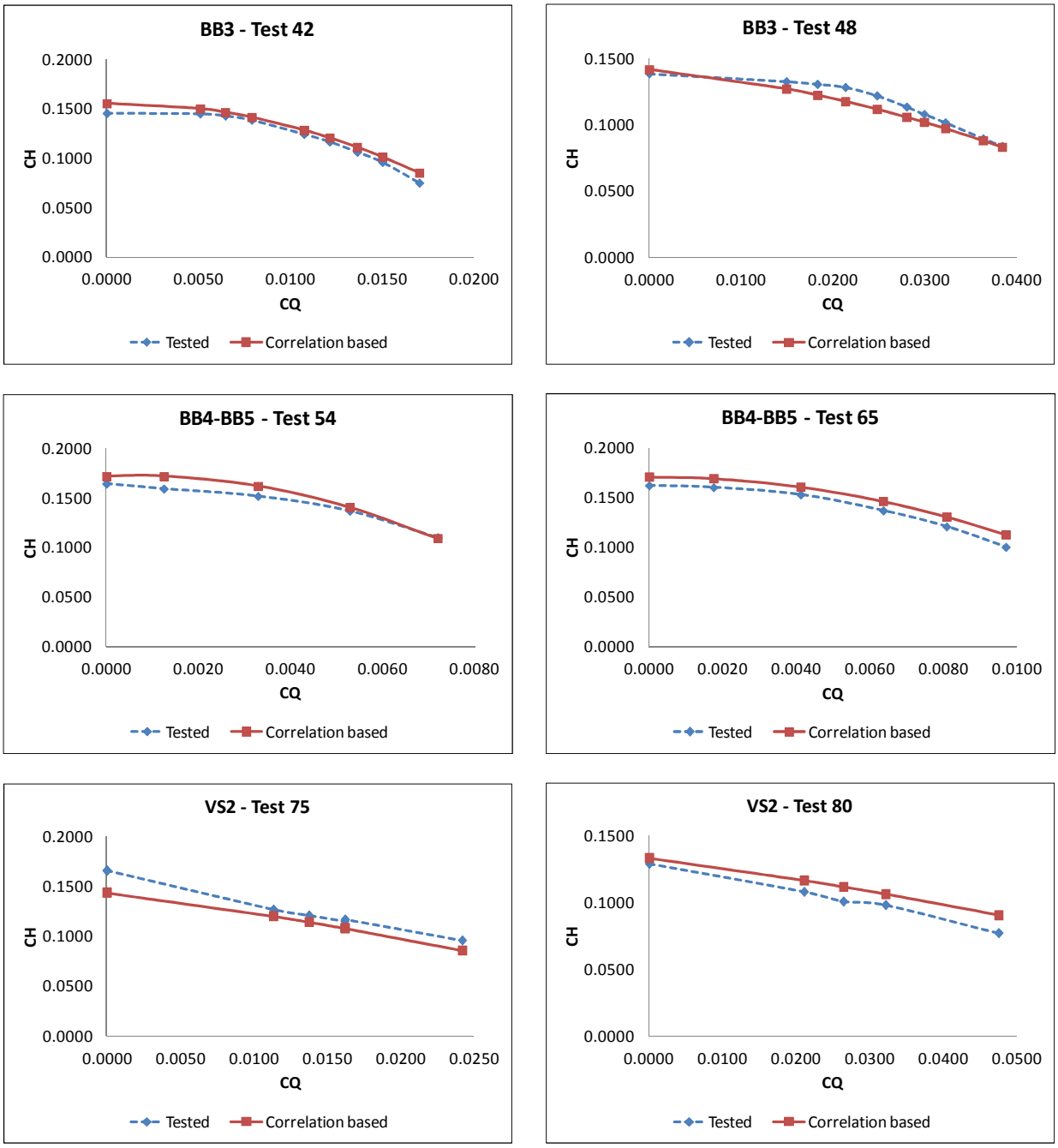

Figure 36 - Correlation based and tested curves (continued).

In order to compare the correlation based curves to the tested ones, the standard deviation was calculated. By analyzing all the comparisons, three different behaviors are observed.

In most cases (64 tests), the correlations (Table 2) were able to predict the tested curve with good accuracy. The standard deviation limit set to define good accuracy is 0.02. This behavior was observed in all the pump types.

In some cases (10 tests), the correlations (Table 2) were able to predict the shape of the tested curve, but an offset was observed due an error on the *shut-off* head prediction. This behavior was observed in few cases of all pump types.

In few cases (6 tests), the shape of the curve was not well predicted. This behavior was observed in 2 tests of BB1 pumps and 4 tests of BB3 pumps. It happened more critically with the tests of BB3 pumps, but it is important to note that the pump hydraulics was the same in these 4 tests.

As already mentioned, there are several proposed models to predict the hydraulic performance of centrifugal pumps in literature. However, even the best CFD simulations can't predict the pump performance accurately.

The correlations proposed between the equation coefficients and the basic information of the pumps represent the mean tendency among a huge amount of experimental data from several types of pumps. Therefore the provided values of the coefficients may not be so accurate in some cases.

Given all the assumptions and simplifications, the objective of this work is to present correlations applicable to several pump types that easily provide a prediction of the head curve with reasonable error. This error is natural and expected. Since pumps have numerous configurations and their hydraulics are very complex, it is not expected that their performance be accurately predicted with only a handful of parameters.

Therefore, considering the goal of this work and all the tested data used to validate it, it is possible to affirm that the proposed correlations (Table 2) are able to easily predict the head curve of pumps in several different configurations with reasonable error.

5.4.1 Previous work curves predicted based on the correlations

The three pumps tested by Biazussi (2014) are multistage pumps, with 3 stages and diffusers. Therefore they are considered BB4 pumps. They are called P23, P47 and P100, with

specific speeds of 28, 46 and 68, in SI units, respectively. Each one of these pumps was tested in three speeds. Therefore 9 tests are available.

For all the tests, the coefficients k_1, k_4, k_5 and k_6 were adjusted by the model presented by Biazussi (2014) and their values were plotted over the curve with the coefficients calculated for all the 80 tests presented in this work. This is shown in Figure 37.

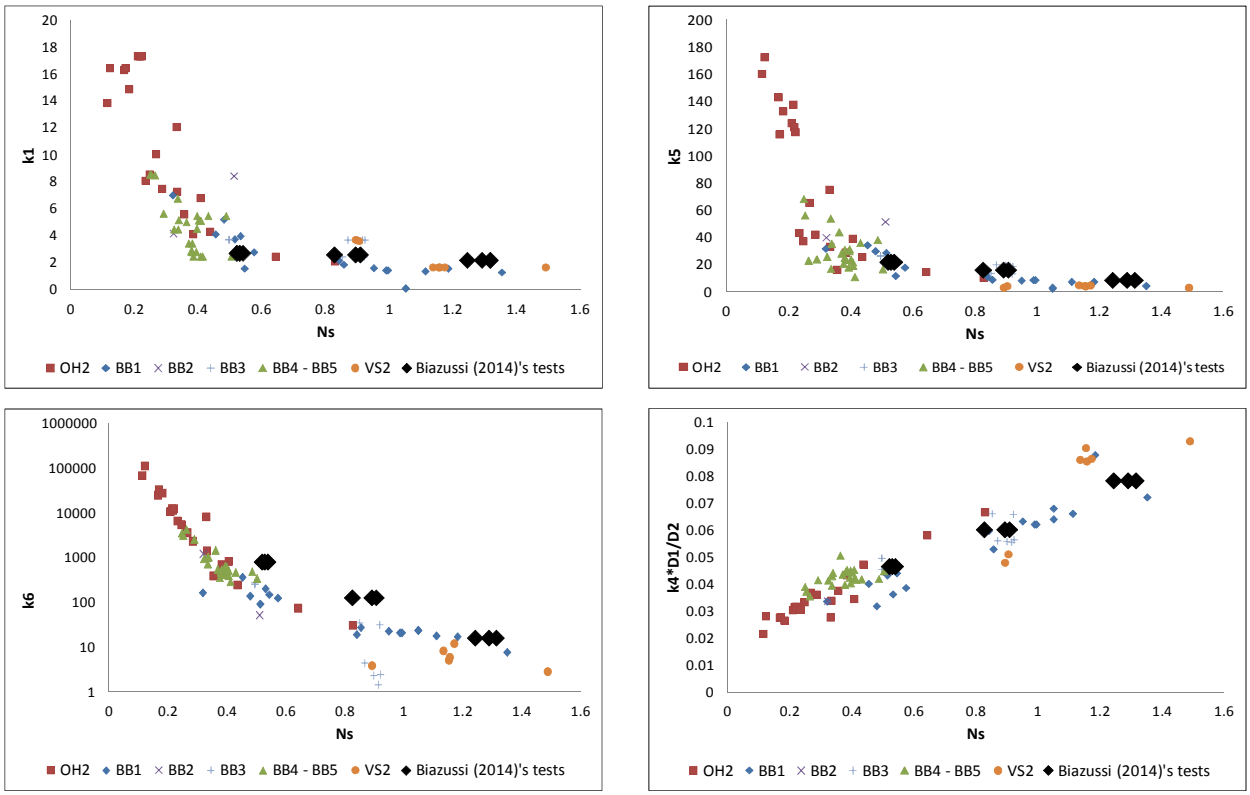

Figure 37 - Equation coefficients vs. specific speed for the 80 tests presented in this work and also the tests analyzed by Biazussi (2014).

For Biazussi (2014)'s tests, the values adjusted by the model for the coefficients k_1, k_4 and k_5 fit the correlations previously established between the coefficients of the 80 tests and the related specific speed. However the values adjusted for k_6 don't fit the tendency curves. Since k_6 multiplies C_Q^2 on the model curve, this deviation reflects on the head curve prediction based on the correlations (Table 2), as shown in Figure 38.

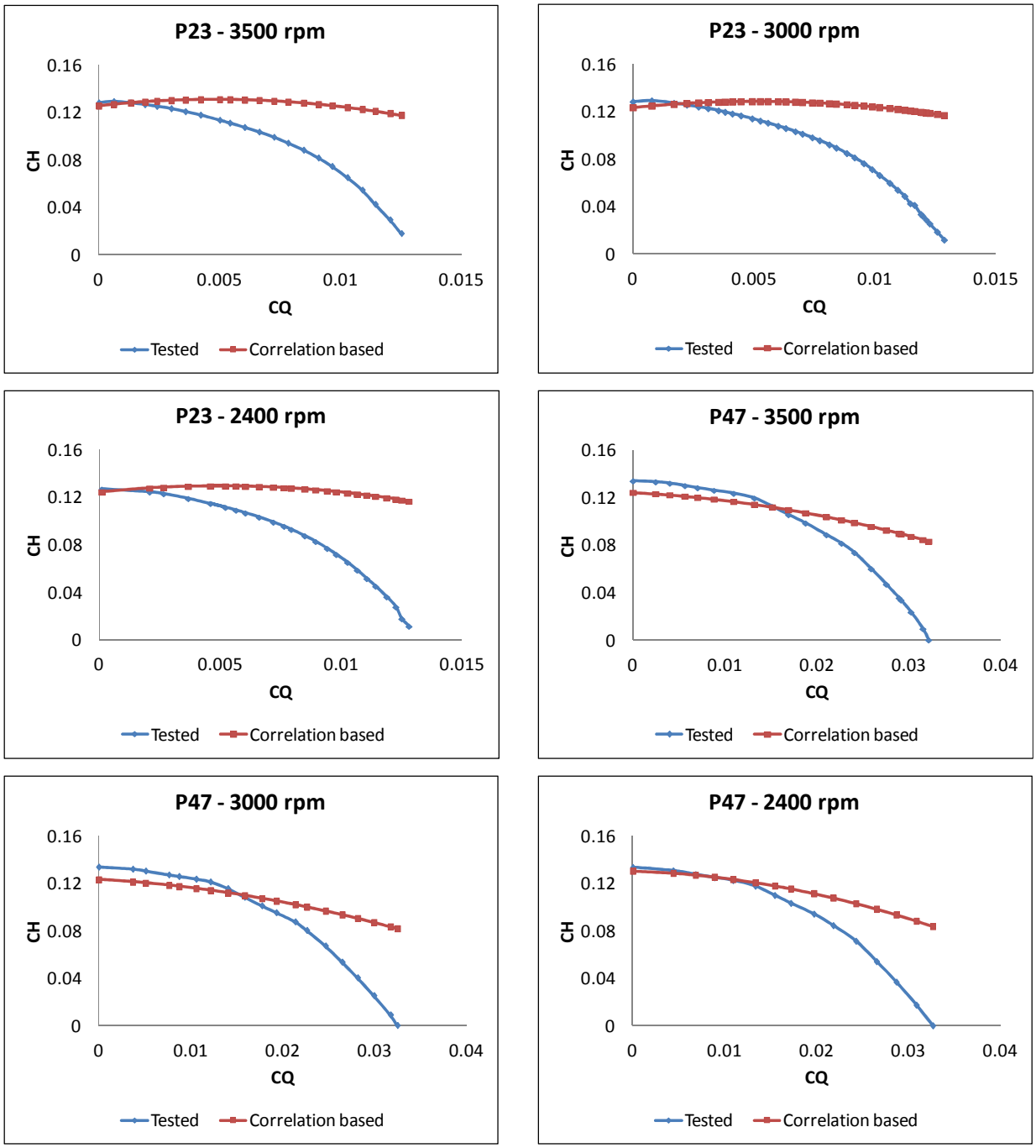

Figure 38 - Correlation based and tested curves analyzed by Biazussi (2014).

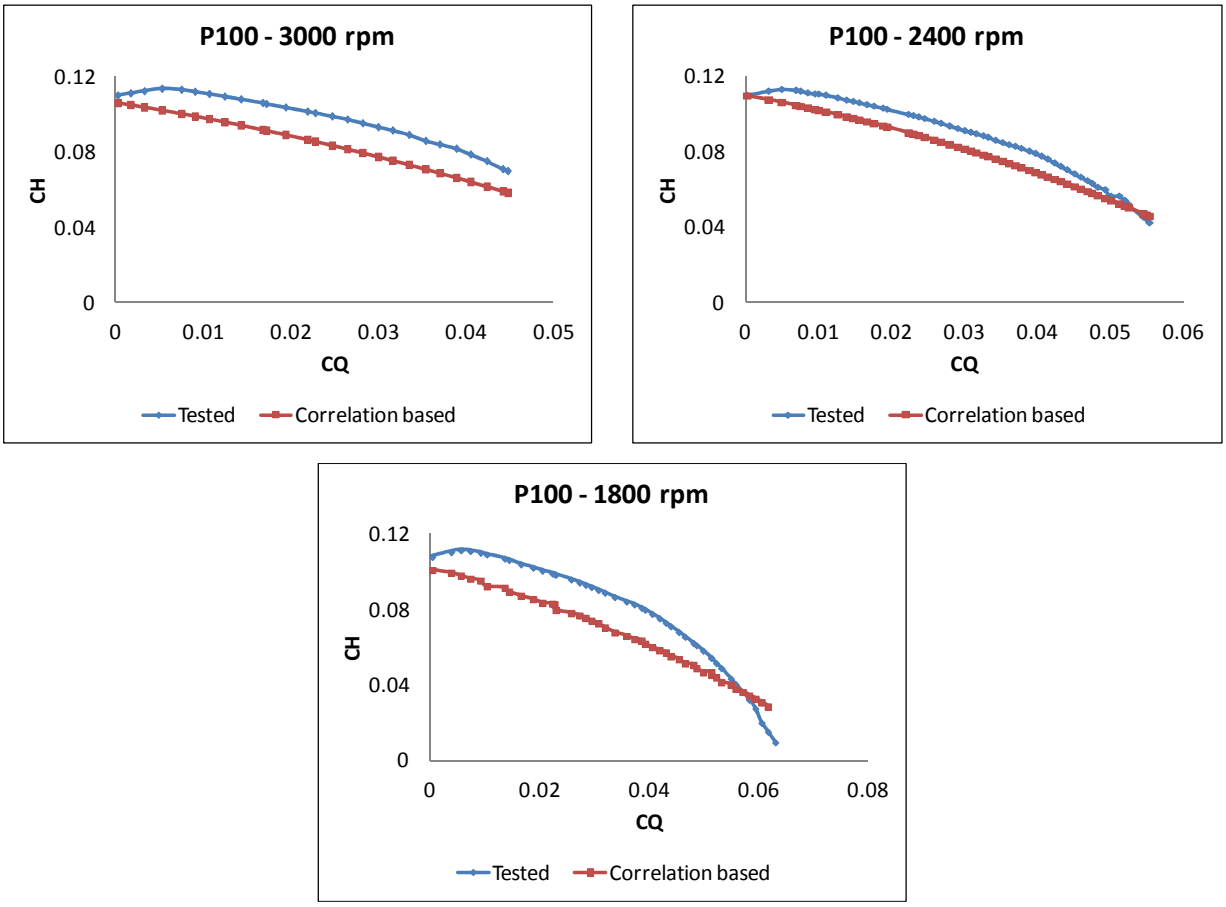

Figure 38 - Correlation based and tested curves analyzed by Biazussi (2014) (continued).

For the pumps P23 and P47, the pressure losses were underestimated and, as a consequence, the correlation based head curves are flatter than the tested ones. It is important to mention that, even with specific speeds in the same range of the ones of the 80 tests, these pumps are very small. Therefore, the pressure losses tend to be more relevant than the ones in big pumps.

Among these three pumps, it is possible to notice that the bigger the pump, the closer its predicted curve to the tested one. P100 is bigger than P23 and P47, which could explain why the losses were not underestimated. The deviation on the curve could be associated to the deviation observed on k_6.

5.5 Improvement on the *shut-off* head prediction

As mentioned previously, for many years, much of the pump community's focus has been on improving prediction methods for best efficiency point conditions. The design of machines has evolved to such an extent that their efficiencies now approach the theoretical values and their design points can be estimated to within a few percentage points. This cannot be said of the prediction methods available to estimate off-design performance. Investigations at partload operation are difficult. The flow is impulsive, unsteady and strongly influenced by the time dependent nature of the rotor/stator interactions. The area of off-design behavior that has received least attention is the prediction of the level of head a pump produces when its discharge valve is closed and the flow through the pump approaches zero, the *shut-off* condition.

Not surprisingly, the main source of error on the correlation based curves was the *shut-off* head prediction. The offset observed between the correlation based and the tested curves in some cases is related to the error on the *shut-off* head prediction.

For this reason, some of the *shut-off* prediction methods presented in Chapter 2 were analyzed and used to optimize the correlations proposed to predict the head curve (Table 2) by changing the equation coefficient k_4.

According to the Equation (61), at *shut-off* ($C_Q = 0$), the head coefficient $C_H = 1/4 - k_4$. Therefore, from the *shut-off* head estimated by the several *shut-off* prediction methods, it is possible to calculate the related k_4 to be used on the whole head curve prediction. The coefficients k_1, k_5 and k_6 remain the same ones based on the correlations (Table 2).

It is important to notice that the improved prediction of k_4 has also an influence on the shape of the curve, since this coefficient also multiplies C_Q and C_Q^2 .

For each test and each one of these methods, the *shut-off* head was calculated and used to estimate the value of k_4 and then the whole head curve was raised.

In this work, improved curves are the head versus flow curves predicted based on the correlations presented in Table 2 and improved by a *shut-off* head prediction method presented in Chapter 2.

The standard deviation of the improved curves was used to compare them to the tested curve and also among themselves. As a consequence, it was possible to identify the best prediction method for the whole head curve for each pump type.

Since the goal of this work is to predict the pump hydraulic performance only with few and accessible hydraulic dimensions, some methods were discarded because they considered several hydraulic dimensions that are not easily obtained. This was the case of the Thorne's, Stirling's and Frost and Nilsen's methods.

The methods analyzed are the ones proposed by Stepanoff (1957), Peck (1968), Patel (1981) and Gülich (2007). The first three methods present correction factors to the Euler's equation, based on the statistical analysis of several test results. The fourth method is also based on statistical data, but it presents a graph for the *shut-off* head prediction based on the specific speed of the pump. These methods are presented in detail in Chapter 2.

Table 3 presents the sum of the standard deviation (total standard deviation) of the improved curves, grouped by pump type, for each method.

Table 3 - Total standard deviation of the improved curves.

Methods	**Pump type**					
	OH2	**BB1**	**BB2**	**BB3**	**BB4-BB5**	**VS2**
Correlations (Table 2)	0.22	0.25	0.031	0.24	0.24	0.12
Stepanoff	0.14	0.24	0.04	0.21	0.38	0.11
Peck	0.15	0.25	0.027	0.21	0.32	0.11
Patel	0.17	0.33	0.04	0.29	0.39	0.14
Gülich	0.15	0.24	0.04	0.24	0.28	0.08

For the OH2 pumps, by using Stepanoff's method of *shut-off* head prediction to improve the head curve predicted based on the correlations (Table 2), the total standard deviation drops in 36%, from 0.22 to 0.14.

With regard to the BB1 pumps, besides Patel's, all the methods presented similar values of total standard deviation. The use of Stepanoff's or Gülich's method presents total standard deviation of 0.24, which is 4% smaller than the one calculated for the predicted curve based on the correlations.

Since there are just two tests of BB2 pumps available, the total standard deviation is smaller than the ones calculated for the other pump types. Even though, it is possible to evaluate the best method to predict the head curve. In this case, Peck's method presents the smallest total standard

deviation, 0.027, which is 13% smaller than the one calculated for the predicted curve based on the correlations.

Considering all the tests of BB3 pumps, Stepanoff's and Peck's methods present the smallest total standard deviation, 0.21. However, as mentioned previously, among the 9 tests of BB3 pumps, 4 of them had the same hydraulics and presented serious deviation on the prediction of the shape of the curve. This hydraulics is very peculiar and could not represent well the behavior of this type of pump. If these tests are ignored, the smallest total standard deviation is 0.013 with Stepanoff's method, against 0.017 based on the correlations and 0.022 with Peck's method.

The correlations (Table 2) predict the head curve of BB4-BB5 pumps better than all the other methods. In fact, the comparison of the correlation based curves with the tested ones shows the smallest total standard deviation, 0.24.

For VS2 pumps, Gülich's method presents the best head curve prediction, with total standard deviation of 0.08. Even being vertical and with high specific speed (semi axial pumps), it was possible to find a good method to predict the head curve of VS2 pumps.

Comparisons among tested, correlation based and improved curves are presented in Figure 39. The standard deviation among these correlation based, improved and tested curves are presented in Table 4. In all cases, besides test 75, the standard deviation of the improved curve is smaller than the one of the correlation based curve. Test 75 represents the exceptions, which means that the method chosen as the best one to predict the head curves of a certain pump type doesn't correspond to the best method to predict the head curve in this particular case.

Table 4 - Standard deviation of the correlation based and improved curves of the selected tests.

Standard deviation				
Test	**Pump type**	**Correlation based curve**	**Improved curve**	**Std. deviation reduction**
17	OH2	0.0090	0.0028	68.5%
20	OH2	0.0085	0.0010	88.7%
23	BB1	0.0110	0.0093	15.4%
26	BB1	0.0219	0.0061	72.4%
39	BB2	0.0202	0.0171	15.3%
40	BB2	0.0109	0.0099	9.1%
42	BB3	0.0059	0.0027	53.7%
48	BB3	0.0067	0.0049	26.7%
54	BB4-BB5	0.0081	-	-
65	BB4-BB5	0.0097	-	-
75	VS2	0.0136	0.0203	-48.9%
80	VS2	0.0095	0.0042	56.5%

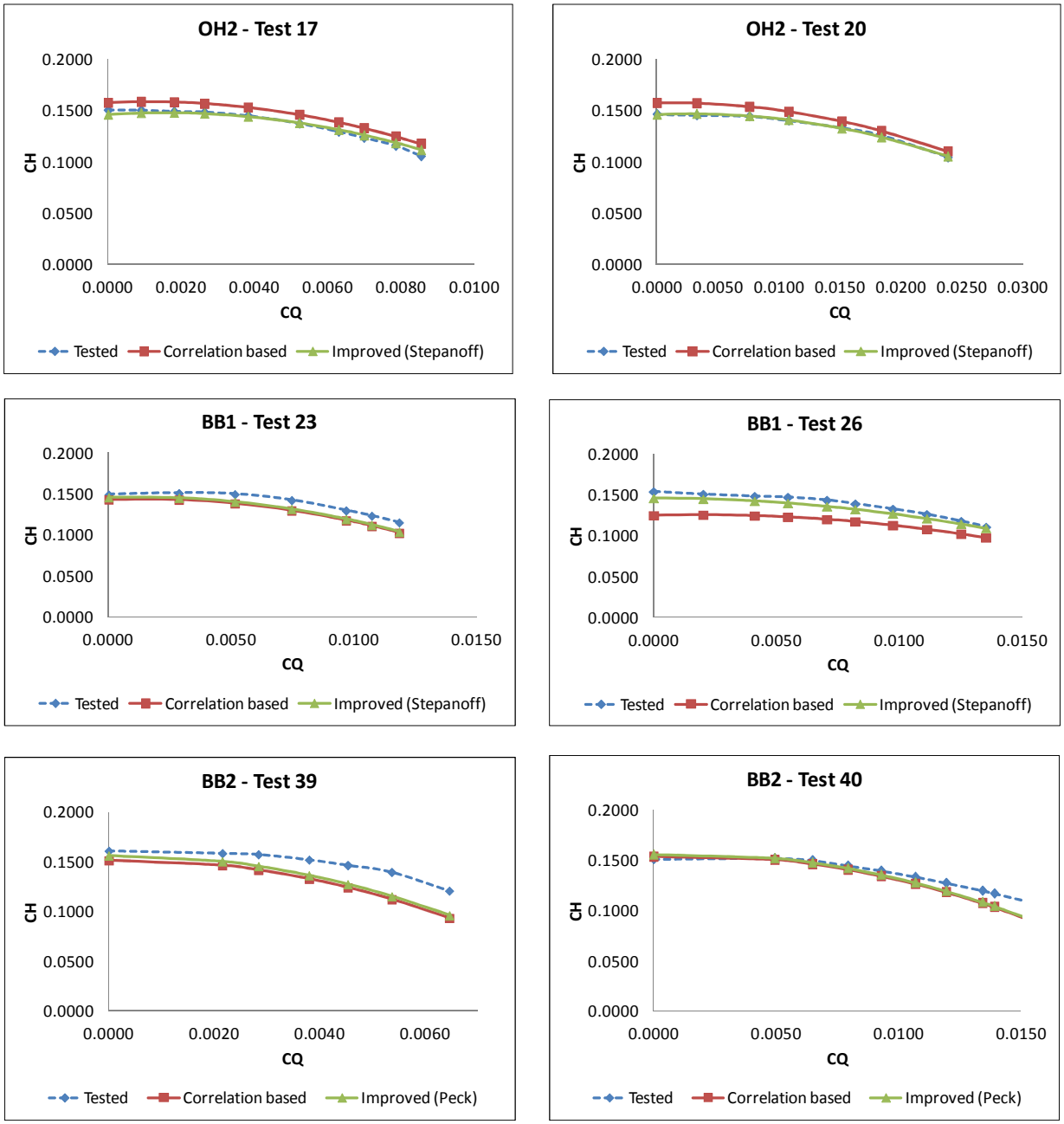

Figure 39 - Correlation based, improved and tested curves.

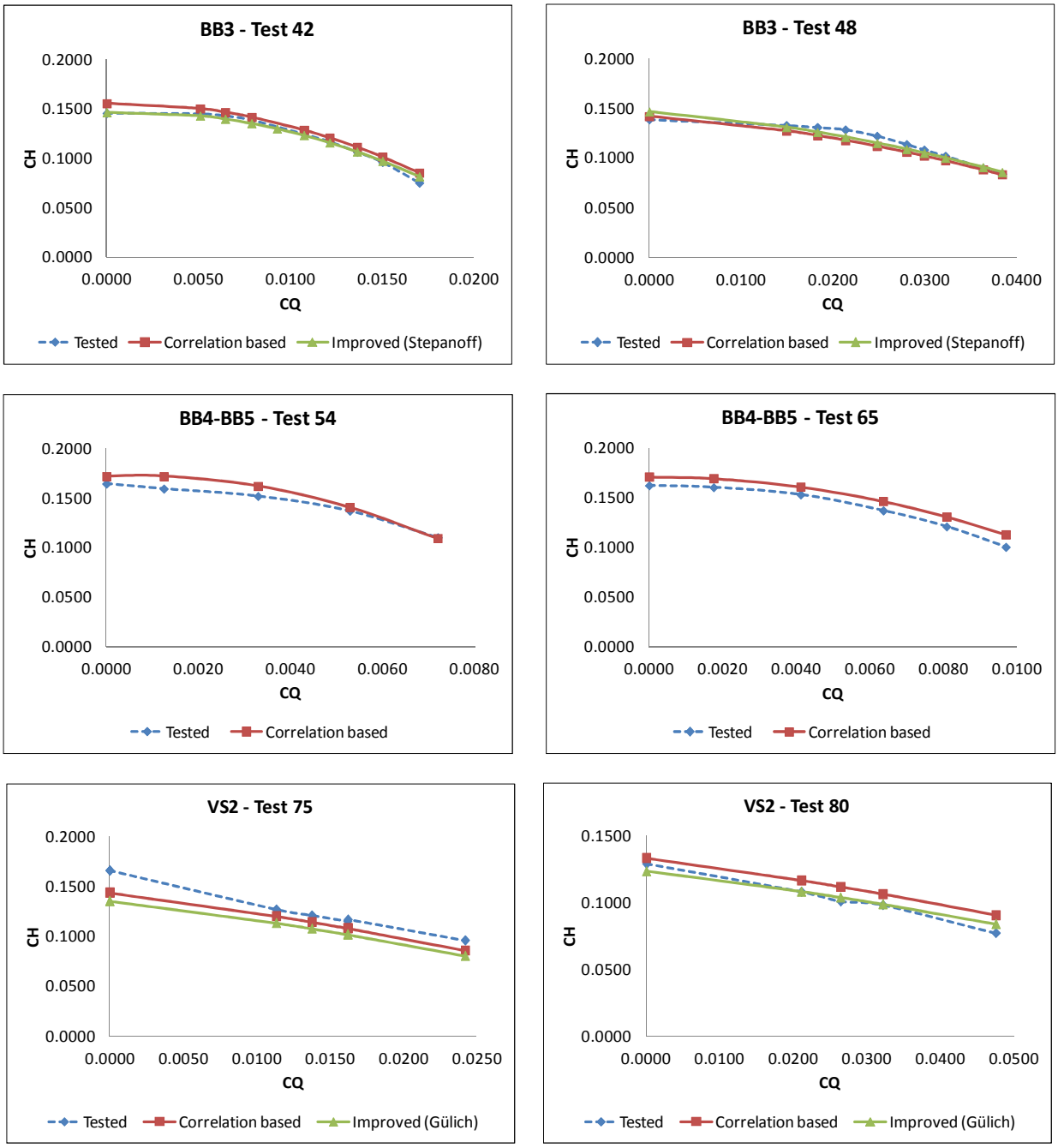

Figure 39 – Correlation based, improved and tested curves (continued).

6 CONCLUSIONS

In literature, there are several models that attempt to predict the hydraulic performance of centrifugal pumps. Some of them are based on fluid dynamic principles, but others are based on empirical data and there are also the modern ones based on numerical simulation. In order to decide the best one to be used, the available information about the pump has to be taken into account.

The current work proposes correlations for the head curve prediction based on few and accessible pump characteristics. The data of eighty tests of different pump types are used, covering a wide range of specific speeds. Even with simple input data, results with reasonable accuracy are obtained.

In addition, the use of simple *shut-off* head prediction methods increases the accuracy of the whole pump head curve predicted by the correlations (Table 2). This combination does predict the pump hydraulic performance with acceptable accuracy only with few and accessible hydraulic dimensions.

To summarize, the recommended methods to predict whole head curve for each pump type are the following ones:

- Correlations (Table 2) + Stepanoff's method for OH2, BB1 and BB3 pumps;
- Correlations (Table 2) + Peck's method for BB2 pumps;
- Correlations (Table 2) for BB4-BB5 pumps;
- Correlations (Table 2) + Gülich's method for VS2 pumps.

7 RECOMMENDATION FOR FUTURE PROJECTS

One of the assumptions considered on the theoretical model was that the effects of the recirculation losses, losses due to secondary flow and shock losses overlap themselves, which makes it difficult to separate them. Therefore, they were represented as just one type of loss, called distortion loss.

In fact, all of them depend on the flow rate, tend to a minimum value at the best efficiency point and are more critical at partload. However it would be important to know the contribution of each component.

The correlation found between the equation coefficient k_4 and the specific speed depends on D_1/D_2. It would be valuable if this ratio could be considered since the theoretical model definition.

Since the energy consumption has always been an issue, for sure the best complement for this work would be the analysis of the available data also with regard to the pump power, so that it would be possible to predict the power consumption of a centrifugal pump only with few and accessible hydraulic dimensions.

REFERENCES

ANSI/HI 1.4. *Rotodynamic (centrifugal) pumps for manuals describing installation, operation, and maintenance*. Parsippany: Hydraulic Institute, 2010.

ANSI/HI 14.6. *Rotodynamic pumps for hydraulic performance acceptance tests*. Parsippany: Hydraulic Institute, 2011.

API 610, 11th edition. *Centrifugal pumps for petroleum, petrochemical and natural gas industries*. Winterthur: ISO copyright office, 2009.

Asuaje, M., Bakir, F., Kouidri, S., Kenyery, F., Rey, R. "Numerical modelization of the flow in centrifugal pump: volute influence in velocity and pressure fields." *International Journal of Rotating Machinery* (2005).

Biazussi, J. L. "Modelo de deslizamento para escoamento gás-líquido em bomba centrífuga submersa operando com líquido de baixa viscosidade." *Ph.D. Thesis. Curso de Ciências e Engenharia de Petróleo, Departamento de Engenharia do Petróleo, Universidade Estadual de Campinas*. Campinas, 2014.

Biazussi, J. L., Verde, W. M., Varón, M. P., Bannwart, A. C. "Comparison of experimental curves of ESP with a simple single-phase approach." *22nd International Congress of Mechanical Engineering (COBEM 2013)*. Ribeirão Preto, 2013.

Cheah, K.W., Lee, T. S., Winoto, S. H., Zhao, Z. M. "Numerical flow simulation in a centrifugal pump at design and off-design conditions." *International Journal of Rotating Machinery* (2007).

Das, L. G., Sen, P. K., Saha, T. K., Chanda, A. "Performance prediction of vertical submersible centrifugal slurry pumps." *International Journal of Fluid Machinery and Systems* (2010).

Dyson, G. "A review of closed valve head prediction methods for centrifugal pumps." *David Brown Pumps* 2002.

El-Naggar, M. A. "A one-dimensional flow analysis for the prediction of centrifugal pump performance characteristics." *International Journal of Rotating Machinery* (2013).

Fraser, W. H. "Flow recirculation in centrifugal pumps." 1981.

Gülich, J. F. *Centrifugal pumps, 2nd edition*. Berlin: Springer, 2007.

Gülich, J. F. "Selection criteria for suction impellers of centrifugal pumps." *World Pumps*. 2001.

Jafarzadeh, B., Hajari, A., Alishahi, M. M., Akbari, M. H. "The flow simulation of a low-specific-speed high-speed centrifugal pump." *Elsevier* 2011.

Li, W. G., Su, F. Z., Xue, J. X., Xiao, C. "Experimental investigations into the performance of a commercial centrifugal oil pump." *World Pumps* (2002).

Lobanoff, V.S, Ross, R.R. *Centrifugal pumps: design & application, 2nd edition*. Houston: Gulf Publishing Company, 1985.

Newton, T. M. "Rotor-stator interaction in radial flow pumps and fans at shut-off condition." *Ph.D. Thesis. University of Newcastle upon Tyne*. 1998.

Patel, D. P., Srivastava, R. K. and Shah, C. S. "Performance prediction in complete range of centrifugal pumps." *17th Technical Conference of British Pump Manufacturers' Association* 1981.

Paternost, G. M. "Estudo experimental sobre bomba centrífuga operando com fluido viscoso e escoamento bifásico gás-líquido." *Dissertação de Mestrado. Curso de Ciências e Engenharia de Petróleo, Departamento de Engenharia do Petróleo, Universidade Estadual de Campinas*. Campinas, 2013.

Peck, J. F. "Design of centrifugal pumps with computer aid." *Proc. Instn Mech. Engrs* 1968: 321-352.

Shah, S. R., Jain, S. V., Patel, R. N., Lakhera, V. J. "CFD for centrifugal pumps: a review of the state-of-the-art." *Elsevier* 2013.

Stepanoff, A. J. *Centrifugal and axial flow pumps*. New York: John Wiley&Sons, 1957.

Sulzer Pumps Ltd. *Centrifugal pump handbook, 3rd edition*. Winterthur: Butterworth-Heinemann, 2010.

Sun, D., Prado, M. "Single-phase model for ESP's head performance." *SPE Production and Operations Symposium* 2003.

Sun, J., Tsukamoto, H. "Off-design performance prediction for diffuser pumps." (2001).

Thin, K. C., Khaing, M. M., Aye, K. M. "Design and performance analysis of centrifugal pumps." *World Academy of Science, Engineering and Technology* (2008).

Tomasini, Filippo. "Shut-off head prediction in single stage centrifugal pumps." École Polythecnique Fédérale de Lausanne, n.d.

APPENDIX A – Experimental data error analysis

The experimental data error represents the maximum deviation around the best estimated value of a parameter. This uncertainty is the result of a lack of information regarding the parameter being measured. In other words, infinite information would be necessary to define its exact value. Therefore, when experimental data is presented, its error needs to be informed.

The error is calculated according to normalized procedures. INMETRO presents general rules for the experimental error evaluation. Two types of errors are considered:

- Error type A: based on the statistical analysis of a series of measured data;
- Error type B: based on other examinations not based on statistical analysis.

Since the data acquisition was not part of the scope of this work, only one measure of each parameter was available. Therefore, the errors considered in this work are of type B, with the exception of the density error.

A.1 – Combined error

Combined error can be understood as the standard deviation of a variable z based on the standard deviation of its dependent variables, x and y, according to the equation below:

$$u_z^2 = \left(\frac{\partial z}{\partial x} u_x\right)^2 + \left(\frac{\partial z}{\partial y} u_y\right)^2 \quad \text{(A.1)}$$

where u_x and u_y are the errors associated to the variables x and y, and u_z is the error associated to variable z.

A.2 – Combined error of the differential pressure provided by the pump

The differential pressure provided by the pump is obtained based on the pressure measured at the suction and discharge of the pump, according to the equation below:

$$\Delta P = P_{discharge} - P_{suction} \quad \text{(A.2)}$$

where $P_{discharge}$ is the pressure measured at the discharge of the pump and $P_{suction}$ is the pressure measured at the suction of the pump.

The error associated with the differential pressure provided by the pump is calculated according to the following equation:

$$u_{\Delta P}^2 = \left(\frac{\partial \Delta P}{\partial P_{discharge}} u_{P_{discharge}}\right)^2 + \left(\frac{\partial \Delta P}{\partial P_{suction}} u_{P_{suction}}\right)^2 \quad \text{(A.3)}$$

where $u_{\Delta P}$ is the error of the differential pressure, $u_{P_{discharge}}$ is the error of the discharge pressure and $u_{P_{suction}}$ is the error of the suction pressure. Therefore,

$$u_{\Delta P} = \sqrt{u_{P_{discharge}}^2 + u_{P_{suction}}^2} \quad \text{(A.4)}$$

A.3 – Combined error of the head coefficient

According to Equation (6), the head coefficient is defined as:

$$C_H = \frac{\Delta P}{\rho \omega^2 {D_2}^2}$$

The error associated with the head coefficient is calculated according to the following equation:

$$u_{C_H}^2 = \left(\frac{\partial C_H}{\partial \Delta P} u_{\Delta P}\right)^2 + \left(\frac{\partial C_H}{\partial \rho} u_\rho\right)^2 + \left(\frac{\partial C_H}{\partial \omega} u_\omega\right)^2 + \left(\frac{\partial C_H}{\partial D_2} u_{D_2}\right)^2 \quad \text{(A.5)}$$

where u_{C_H} is the error of the head coefficient, u_ρ is the error of the density, u_ω is the error of the speed and u_{D_2} is the error of D_2. Therefore:

$$u_{C_H} = \sqrt{\frac{4\Delta P^2 u_{D_2}^2}{D_2^6 \rho^2 \omega^4} + \frac{\Delta P^2 u_\rho^2}{D_2^4 \rho^4 \omega^4} + \frac{4\Delta P^2 u_\omega^2}{D_2^4 \rho^2 \omega^6} + \frac{u_{\Delta P}^2}{D_2^4 \rho^2 \omega^4}} \quad \text{(A.6)}$$

A.4 – Combined error of the flow coefficient

According to the Equation (5), the flow coefficient is defined as:

$$C_Q = \frac{Q}{\omega {D_2}^3}$$

The error associated with the flow coefficient is calculated according to the following equation:

$$u_{C_Q}^2 = \left(\frac{\partial C_Q}{\partial Q} u_Q\right)^2 + \left(\frac{\partial C_Q}{\partial \omega} u_\omega\right)^2 + \left(\frac{\partial C_Q}{\partial D_2} u_{D_2}\right)^2 \quad \text{(A.7)}$$

where u_{C_Q} is the error of the flow coefficient, u_Q is the error of the flow. Therefore:

$$u_{C_Q} = \sqrt{\frac{9Q^2u_{D_2}^2}{D_2^8\omega^2} + \frac{u_Q^2}{D_2^6\omega^2} + \frac{Q^2u_\omega^2}{D_2^6\omega^4}} \quad \text{(A.8)}$$

A.5 – Calculation of the combined errors

According to the combined error definition, the errors associated with the flow and head coefficients, C_Q and C_H, calculated for test 17 and presented in Figure 22, are the following:

Table A.1 – Variables and errors

Variable	Error	Error type
ρ	± 0.4%	Error type A
P	± 0.5%	Error type B (Table 1)
ω	± 0.3%	Error type B (Table 1)
$D2$	± 0.015%	Error type B (Table 1)
Q	± 1.0%	Error type B (Table 1)
ΔP	± 0.7%	Combined error
C_H	± 1.4%	Combined error
C_Q	± 7.9%	Combined error

APPENDIX B – Experimental data

Test	1	2	3	4	5
Pump type	OH2	OH2	OH2	OH2	OH2
ρ (kg/m3)	1000	1000	1000	1000	1000
μ (cP)	1	1	1	1	1
B2 (mm)	9.84	8	11	8	11
D2 (mm)	409	324	409	324	458
D1 (mm)	90	87	111	87	111
$\beta 2$ (graus)	25.5	21.4	19.95	21.4	24
nq (1/s)	0.1130	0.1216	0.1660	0.1699	0.1812
ω (1/s)	373.3259	184.3068	371.7551	371.2315	184.8304
X	1.60E-08	5.17E-08	1.61E-08	2.57E-08	2.58E-08
Cqbep (-)	0.0006	0.0006	0.0012	0.0011	0.0012
Chbep (-)	0.1346	0.1166	0.1239	0.1133	0.1127
Cq1 (-)	0.00000	0.00000	0.00000	0.00000	0.00000
Cq2 (-)	0.00007	0.00007	0.00022	0.00013	0.00035
Cq3 (-)	0.00015	0.00013	0.00034	0.00026	0.00047
Cq4 (-)	0.00023	0.00024	0.00055	0.00040	0.00063
Cq5 (-)	0.00031	0.00033	0.00065	0.00053	0.00086
Cq6 (-)	0.00038	0.00037	0.00086	0.00066	0.00100
Cq7 (-)	0.00046	0.00045	0.00099	0.00079	0.00124
Cq8 (-)	0.00053	0.00052	0.00109	0.00093	0.00141
Cq9 (-)	0.00061	0.00060	0.00131	0.00110	
Cq10 (-)	0.00068	0.00062	0.00153	0.00132	
Ch1 (-)	0.1522	0.1452	0.1496	0.1460	0.1404
Ch2 (-)	0.1520	0.1457	0.1481	0.1463	0.1412
Ch3 (-)	0.1524	0.1457	0.1483	0.1452	0.1408
Ch4 (-)	0.1518	0.1431	0.1466	0.1436	0.1375
Ch5 (-)	0.1499	0.1388	0.1460	0.1407	0.1304
Ch6 (-)	0.1477	0.1370	0.1401	0.1359	0.1251
Ch7 (-)	0.1448	0.1308	0.1347	0.1303	0.1127
Ch8 (-)	0.1414	0.1237	0.1310	0.1227	0.1013
Ch9 (-)	0.1368	0.1179	0.1171	0.1133	
Ch10 (-)	0.1296	0.1107	0.1051	0.0958	
k1 model	13.8692	16.4477	16.3029	16.4477	14.8837
k4 model	0.0984	0.1049	0.1018	0.1041	0.1097
k5 model	160.55	172.94	143.43	116.11	133.09
k6 model	68970.31	112557.04	24937.37	33041.22	27711.48

Test	6	7	8	9	10
Pump type	OH2	OH2	OH2	OH2	OH2
ρ (kg/m3)	1000	1000	1000	1000	1000
μ (cP)	1	1	1	1	1
B2 (mm)	13	13	13	13	17.5
D2 (mm)	406	406	406	406	514
D1 (mm)	124	124	124	124	154
β2 (graus)	16	16	16	16	30
nq (1/s)	0.2086	0.2142	0.2173	0.2206	0.2330
ω (1/s)	185.8776	185.8776	185.8776	185.8776	186.4012
X	3.26E-08	3.26E-08	3.26E-08	3.26E-08	2.03E-08
Cqbep (-)	0.0018	0.0018	0.0018	0.0018	0.0022
Chbep (-)	0.1214	0.1173	0.1153	0.1124	0.1178
Cq1 (-)	0.00000	0.00000	0.00000	0.00000	0.00000
Cq2 (-)	0.00056	0.00055	0.00058	0.00058	0.00033
Cq3 (-)	0.00078	0.00078	0.00077	0.00078	0.00066
Cq4 (-)	0.00098	0.00099	0.00098	0.00098	0.00132
Cq5 (-)	0.00118	0.00119	0.00117	0.00118	0.00164
Cq6 (-)	0.00138	0.00139	0.00138	0.00138	0.00198
Cq7 (-)	0.00161	0.00163	0.00158	0.00161	0.00220
Cq8 (-)	0.00184	0.00184	0.00185	0.00183	0.00263
Cq9 (-)					0.00296
Cq10 (-)					0.00316
Ch1 (-)	0.1512	0.1466	0.1463	0.1461	0.1498
Ch2 (-)	0.1473	0.1480	0.1459	0.1460	0.1468
Ch3 (-)	0.1496	0.1469	0.1442	0.1431	0.1438
Ch4 (-)	0.1465	0.1433	0.1407	0.1401	0.1368
Ch5 (-)	0.1427	0.1386	0.1370	0.1350	0.1310
Ch6 (-)	0.1371	0.1342	0.1330	0.1286	0.1231
Ch7 (-)	0.1307	0.1269	0.1266	0.1208	0.1178
Ch8 (-)	0.1214	0.1173	0.1153	0.1124	0.1038
Ch9 (-)					0.0918
Ch10 (-)					0.0801
k1 model	17.3343	17.3343	17.3343	17.3343	8.0967
k4 model	0.0998	0.1035	0.1040	0.1037	0.1019
k5 model	124.32	137.97	121.39	117.65	43.59
k6 model	10778.43	12606.60	11542.90	12656.54	6641.83

Test	11	12	13	14	15
Pump type	OH2	OH2	OH2	OH2	OH2
ρ (kg/m3)	1000	1000	1000	1000	1000
μ (cP)	1	1	1	1	1
B2 (mm)	14	12.7	14	15	29
D2 (mm)	400	292	324	514	648
D1 (mm)	128	104.775	117	140	220
$\beta 2$ (graus)	28	20	26.2	24.28	26
nq (1/s)	0.2460	0.2661	0.2849	0.3302	0.3326
ω (1/s)	185.3540	373.8495	373.3259	185.3540	123.5693
X	3.37E-08	3.14E-08	2.55E-08	2.04E-08	1.93E-08
Cqbep (-)	0.0023	0.0030	0.0035	0.0020	0.0044
Chbep (-)	0.1144	0.1211	0.1226	0.0692	0.1170
Cq1 (-)	0.00000	0.00000	0.00000	0.00000	0.00000
Cq2 (-)	0.00082	0.00065	0.00050	0.00023	0.00055
Cq3 (-)	0.00141	0.00123	0.00088	0.00044	0.00115
Cq4 (-)	0.00196	0.00174	0.00145	0.00066	0.00220
Cq5 (-)	0.00258	0.00207	0.00192	0.00078	0.00277
Cq6 (-)	0.00304	0.00255	0.00219	0.00088	0.00331
Cq7 (-)		0.00299	0.00289	0.00114	0.00388
Cq8 (-)			0.00348	0.00155	0.00443
Cq9 (-)			0.00386	0.00177	0.00498
Cq10 (-)			0.00433	0.00199	0.00553
Ch1 (-)	0.1467	0.1470	0.1502	0.1486	0.1522
Ch2 (-)	0.1393	0.1477	0.1494	0.1479	0.1476
Ch3 (-)	0.1337	0.1454	0.1482	0.1479	0.1452
Ch4 (-)	0.1239	0.1406	0.1458	0.1465	0.1417
Ch5 (-)	0.1071	0.1366	0.1428	0.1453	0.1374
Ch6 (-)	0.0906	0.1293	0.1404	0.1443	0.1319
Ch7 (-)		0.1211	0.1316	0.1416	0.1246
Ch8 (-)			0.1226	0.1317	0.1170
Ch9 (-)			0.1163	0.1257	0.1090
Ch10 (-)			0.1071	0.1207	0.0992
k1 model	8.5522	10.0539	7.4855	12.0899	7.2915
k4 model	0.1042	0.1029	0.1002	0.1018	0.1000
k5 model	37.49	65.62	42.33	75.38	33.50
k6 model	5496.98	3642.13	2328.94	8183.54	1428.86

Test	16	17	18	19	20
Pump type	OH2	OH2	OH2	OH2	OH2
ρ (kg/m3)	1000	1000	1000	1000	1000
μ (cP)	1	1	1	1	1
B2 (mm)	37	20	40.8	48	48
D2 (mm)	648	324	680	648	409
D1 (mm)	255	140	250	297	228
$\beta 2$ (graus)	26.5	32	21.3	26.5	29
nq (1/s)	0.3545	0.3829	0.4059	0.4359	0.6417
ω (1/s)	187.2389	371.7551	187.4484	124.5118	186.9248
X	1.27E-08	2.56E-08	1.15E-08	1.91E-08	3.20E-08
Cqbep (-)	0.0056	0.0066	0.0066	0.0090	0.0184
Chbep (-)	0.1264	0.1264	0.1174	0.1311	0.1259
Cq1 (-)	0.00000	0.00000	0.00000	0.00000	0.00000
Cq2 (-)	0.00132	0.00090	0.00237	0.00205	0.00326
Cq3 (-)	0.00201	0.00180	0.00311	0.00360	0.00758
Cq4 (-)	0.00272	0.00263	0.00382	0.00512	0.01080
Cq5 (-)	0.00344	0.00382	0.00477	0.00665	0.01515
Cq6 (-)	0.00416	0.00522	0.00564	0.00820	0.01840
Cq7 (-)	0.00485	0.00629	0.00662	0.00969	0.02385
Cq8 (-)	0.00565	0.00699		0.01116	
Cq9 (-)		0.00785		0.01155	
Cq10 (-)		0.00854			
Ch1 (-)	0.1552	0.1505	0.1561	0.1488	0.1465
Ch2 (-)	0.1492	0.1504	0.1518	0.1453	0.1456
Ch3 (-)	0.1466	0.1491	0.1488	0.1433	0.1446
Ch4 (-)	0.1450	0.1485	0.1441	0.1418	0.1404
Ch5 (-)	0.1416	0.1449	0.1367	0.1439	0.1333
Ch6 (-)	0.1378	0.1375	0.1279	0.1346	0.1259
Ch7 (-)	0.1329	0.1295	0.1174	0.1271	0.1046
Ch8 (-)	0.1264	0.1235		0.1179	
Ch9 (-)		0.1158		0.1153	
Ch10 (-)		0.1057			
k1 model	5.5906	4.1262	6.8035	4.3094	2.4465
k4 model	0.0957	0.1003	0.0939	0.1035	0.1045
k5 model	16.48	29.21	39.25	25.81	14.80
k6 model	393.25	702.89	829.64	247.75	74.69

Test	21	22	23	24	25
Pump type	OH2	BB1	BB1	BB1	BB1
ρ (kg/m3)	1000	1000	1000	1000	1000
μ (cP)	1	1	1	1	1
B2 (mm)	75	65.2	63.02	67.6	67.6
D2 (mm)	514	850	794	730	525
D1 (mm)	320	340.8	321.38	249	249
$\beta 2$ (graus)	27.5	16.5	26	18.3	18.3
nq (1/s)	0.8276	0.3187	0.4532	0.4791	0.5135
ω (1/s)	123.5693	179.6991	89.5354	186.4012	186.4012
X	3.06E-08	7.70E-09	1.77E-08	1.01E-08	1.95E-08
Cqbep (-)	0.0273	0.0058	0.0097	0.0111	0.0145
Chbep (-)	0.1167	0.1481	0.1303	0.1330	0.1444
Cq1 (-)	0.00000	0.00000	0.00000	0.00000	0.00000
Cq2 (-)	0.00580	0.00100	0.00286	0.00498	0.00587
Cq3 (-)	0.00730	0.00177	0.00514	0.00604	0.00776
Cq4 (-)	0.01194	0.00254	0.00745	0.00713	0.00964
Cq5 (-)	0.01653	0.00326	0.00966	0.00785	0.01158
Cq6 (-)	0.02049	0.00430	0.01071	0.00860	0.01351
Cq7 (-)	0.02443	0.00528	0.01182	0.01006	0.01448
Cq8 (-)	0.02983	0.00579		0.01113	0.01609
Cq9 (-)	0.03341			0.01272	0.01776
Cq10 (-)	0.03644			0.01443	0.01862
Ch1 (-)	0.1458	0.1658	0.1495	0.1567	0.1580
Ch2 (-)	0.1397	0.1645	0.1513	0.1518	0.1620
Ch3 (-)	0.1392	0.1626	0.1502	0.1511	0.1613
Ch4 (-)	0.1383	0.1605	0.1428	0.1495	0.1581
Ch5 (-)	0.1348	0.1575	0.1303	0.1469	0.1536
Ch6 (-)	0.1293	0.1540	0.1237	0.1436	0.1477
Ch7 (-)	0.1232	0.1507	0.1156	0.1371	0.1444
Ch8 (-)	0.1100	0.1481		0.1330	0.1387
Ch9 (-)	0.0995			0.1261	0.1328
Ch10 (-)	0.0914			0.1162	0.1298
k1 model	2.0953	7.0047	4.1113	5.1968	3.7374
k4 model	0.1073	0.0839	0.0993	0.0934	0.0915
k5 model	10.59	31.85	34.46	30.06	28.78
k6 model	31.10	164.41	367.09	139.19	92.39

Test	26	27	28	29	30
Pump type	BB1	BB1	BB1	BB1	BB1
ρ (kg/m3)	1000	1000	1000	1000	1000
μ (cP)	1	1	1	1	1
B2 (mm)	40	100	47.64	66.4	145.6
D2 (mm)	509	450	405	382	707
D1 (mm)	190	207.14	178.65	217.8	395.9
$\beta 2$ (graus)	27	24.5	26	23	22.6
nq (1/s)	0.5317	0.5440	0.5735	0.8408	0.8554
ω (1/s)	185.3540	156.0324	185.3540	374.8967	156.0324
X	2.08E-08	3.16E-08	3.29E-08	1.83E-08	1.28E-08
Cqbep (-)	0.0119	0.0143	0.0158	0.0301	0.0302
Chbep (-)	0.1212	0.1328	0.1320	0.1218	0.1195
Cq1 (-)	0.00000	0.00000	0.00000	0.00000	0.00000
Cq2 (-)	0.00202	0.00196	0.00223	0.00668	0.00455
Cq3 (-)	0.00411	0.00396	0.00455	0.00990	0.00912
Cq4 (-)	0.00546	0.00625	0.00677	0.01303	0.01319
Cq5 (-)	0.00705	0.00820	0.00913	0.01674	0.01762
Cq6 (-)	0.00820	0.01024	0.01130	0.01990	0.02172
Cq7 (-)	0.00974	0.01214	0.01357	0.02342	0.02617
Cq8 (-)	0.01112	0.01433	0.01577	0.02663	0.03021
Cq9 (-)	0.01252	0.01599	0.01828	0.03005	0.03409
Cq10 (-)	0.01353	0.01762	0.02018	0.03320	0.04003
Ch1 (-)	0.1543	0.1567	0.1643	0.1459	0.1576
Ch2 (-)	0.1512	0.1538	0.1615	0.1439	0.1534
Ch3 (-)	0.1486	0.1517	0.1598	0.1435	0.1484
Ch4 (-)	0.1474	0.1504	0.1566	0.1407	0.1451
Ch5 (-)	0.1439	0.1488	0.1524	0.1378	0.1422
Ch6 (-)	0.1394	0.1456	0.1473	0.1360	0.1372
Ch7 (-)	0.1329	0.1393	0.1402	0.1330	0.1294
Ch8 (-)	0.1265	0.1328	0.1320	0.1285	0.1195
Ch9 (-)	0.1180	0.1234	0.1204	0.1218	0.1090
Ch10 (-)	0.1110	0.1135	0.1044	0.1136	0.0918
k1 model	3.9748	1.5716	2.7741	2.1571	1.8513
k4 model	0.0971	0.0959	0.0877	0.1050	0.0947
k5 model	22.36	11.76	18.03	11.12	9.08
k6 model	203.02	149.51	125.24	19.20	27.68

Test	31	32	33	34	35
Pump type	BB1	BB1	BB1	BB1	BB1
ρ (kg/m3)	1000	1000	1000	1000	1000
μ (cP)	1	1	1	1	1
B2 (mm)	158.6	140	140	277.8	277.8
D2 (mm)	660	630	630	1100	1100
D1 (mm)	400	382	382	693.8	693.8
$\beta 2$ (graus)	22.5	26.5	26.5	32.5	32.5
nq (1/s)	0.9496	0.9880	0.9940	1.0495	1.0495
ω (1/s)	124.0929	93.2006	93.2006	62.3083	62.3083
X	1.85E-08	2.70E-08	2.70E-08	1.33E-08	1.33E-08
Cqbep (-)	0.0350	0.0393	0.0395	0.0448	0.0448
Chbep (-)	0.1146	0.1174	0.1169	0.1183	0.1183
Cq1 (-)	0.00000	0.00000	0.00000	0.00000	0.00000
Cq2 (-)	0.00697	0.00298	0.00599	0.02013	0.00256
Cq3 (-)	0.01397	0.00600	0.01194	0.02683	0.00499
Cq4 (-)	0.02111	0.01190	0.02169	0.03371	0.00754
Cq5 (-)	0.02801	0.02183	0.02886	0.03938	0.01511
Cq6 (-)	0.03500	0.02879	0.03574	0.04483	0.02033
Cq7 (-)	0.03908	0.03564	0.03947		0.02683
Cq8 (-)	0.04336	0.03927	0.04265		0.03371
Cq9 (-)	0.04612	0.04098	0.04777		0.03938
Cq10 (-)		0.04277	0.05481		0.04483
Ch1 (-)	0.1462	0.1486	0.1474	0.1481	0.1438
Ch2 (-)	0.1442	0.1484	0.1465	0.1473	0.1436
Ch3 (-)	0.1415	0.1483	0.1461	0.1421	0.1433
Ch4 (-)	0.1350	0.1485	0.1427	0.1334	0.1432
Ch5 (-)	0.1264	0.1437	0.1326	0.1263	0.1444
Ch6 (-)	0.1146	0.1340	0.1228	0.1183	0.1444
Ch7 (-)	0.1058	0.1234	0.1169		0.1421
Ch8 (-)	0.0962	0.1174	0.1107		0.1334
Ch9 (-)	0.0873	0.1135	0.0994		0.1263
Ch10 (-)		0.1104	0.0802		0.1183
k1 model	1.5990	1.4365	1.4365	0.0989	0.0989
k4 model	0.1046	0.1027	0.1027	0.1017	0.1080
k5 model	8.41	8.81	8.81	2.51	3.22
k6 model	22.84	21.06	21.06	23.75	23.84

Test	36	37	38	39	40
Pump type	BB1	BB1	BB1	BB2	BB2
ρ (kg/m3)	1000	1000	1000	1000	1000
μ (cP)	1	1	1	1	1
B2 (mm)	157	77	94.8	24.2	46.4
D2 (mm)	570	390	315	381	381
D1 (mm)	358.8	261	206	143.3	173.2
$\beta 2$ (graus)	23	27.3	22.5	19.6	20.8
nq (1/s)	1.1114	1.1833	1.3512	0.3205	0.4666
ω (1/s)	123.5693	375.1062	185.3540	373.8495	374.2684
X	2.49E-08	1.75E-08	5.44E-08	1.84E-08	1.84E-08
Cqbep (-)	0.0437	0.0411	0.0549	0.0054	0.0107
Chbep (-)	0.1078	0.0951	0.0967	0.1397	0.1340
Cq1 (-)	0.00000	0.00000	0.00000	0.00000	0.00000
Cq2 (-)	0.01212	0.01508	0.00971	0.00215	0.00494
Cq3 (-)	0.01835	0.01873	0.01926	0.00284	0.00648
Cq4 (-)	0.02522	0.02248	0.02875	0.00380	0.00793
Cq5 (-)	0.03173	0.02696	0.03850	0.00453	0.00928
Cq6 (-)	0.04006	0.03160	0.04797	0.00537	0.01068
Cq7 (-)	0.04649	0.03488	0.05491	0.00646	0.01194
Cq8 (-)	0.05218	0.03877	0.06120		0.01342
Cq9 (-)	0.05769	0.04321	0.06726		0.01391
Cq10 (-)	0.06308	0.04733	0.07721		0.01530
Ch1 (-)	0.1442	0.1201	0.1433	0.1610	0.1516
Ch2 (-)	0.1444	0.1165	0.1336	0.1585	0.1526
Ch3 (-)	0.1419	0.1152	0.1266	0.1574	0.1505
Ch4 (-)	0.1338	0.1144	0.1201	0.1521	0.1451
Ch5 (-)	0.1276	0.1126	0.1131	0.1466	0.1401
Ch6 (-)	0.1150	0.1081	0.1044	0.1397	0.1340
Ch7 (-)	0.1020	0.1048	0.0967	0.1211	0.1279
Ch8 (-)	0.0905	0.0995	0.0863		0.1201
Ch9 (-)	0.0781	0.0905	0.0750		0.1173
Ch10 (-)	0.0632	0.0798	0.0543		0.1091
k1 model	1.3613	1.5618	1.2767	7.0368	3.4403
k4 model	0.1052	0.1316	0.1106	0.0898	0.0978
k5 model	7.46	7.48	4.44	56.23	24.15
k6 model	17.98	17.17	7.73	1085.25	215.55

Test	41	42	43	44	45
Pump type	BB3	BB3	BB3	BB3	BB3
ρ (kg/m3)	1000	1000	1000	1000	1000
μ (cP)	1	1	1	1	1
B2 (mm)	39.5	39.5	39.5	65.5	85.27
D2 (mm)	470	470	470	415	810
D1 (mm)	223	223	223	244.8	452.3
$\beta 2$ (graus)	27	27	27	22.5	22.3
nq (1/s)	0.4950	0.4950	0.4950	0.8508	0.8684
ω (1/s)	364.4247	374.3731	141.3717	375.2109	125.6637
X	0.0000	0.0000	0.0000	0.0000	0.0000
Cqbep (-)	0.0107	0.0107	0.0107	0.0280	0.0312
Chbep (-)	0.1243	0.1243	0.1243	0.1143	0.1196
Cq1 (-)	0.00000	0.00000	0.00000	0.00000	0.00000
Cq2 (-)	0.00508	0.00508	0.00508	0.01501	0.01254
Cq3 (-)	0.00645	0.00645	0.00645	0.02158	0.01664
Cq4 (-)	0.00789	0.00789	0.00789	0.02798	0.02542
Cq5 (-)	0.00927	0.01074	0.00927	0.03582	0.02927
Cq6 (-)	0.01074	0.01074	0.01074		0.03351
Cq7 (-)	0.01213	0.01213	0.01213		0.03628
Cq8 (-)	0.01363	0.01363	0.01363		0.03908
Cq9 (-)	0.01501	0.01500	0.01501		0.04068
Cq10 (-)	0.01701	0.01701	0.01701		0.04246
Ch1 (-)	0.1454	0.1454	0.1454	0.1383	0.1513
Ch2 (-)	0.1449	0.1449	0.1449	0.1324	0.1430
Ch3 (-)	0.1428	0.1428	0.1428	0.1271	0.1408
Ch4 (-)	0.1385	0.1385	0.1385	0.1143	0.1320
Ch5 (-)	0.1320	0.1243	0.1320	0.0880	0.1236
Ch6 (-)	0.1243	0.1243	0.1243		0.1116
Ch7 (-)	0.1167	0.1167	0.1167		0.1035
Ch8 (-)	0.1062	0.1062	0.1062		0.0945
Ch9 (-)	0.0959	0.0959	0.0959		0.0886
Ch10 (-)	0.0749	0.0749	0.0749		0.0818
k1 model	3.7167	3.7167	3.7167	2.4345	3.6863
k4 model	0.1048	0.0960	0.1048	0.1123	0.1007
k5 model	26.53	26.89	26.53	13.86	20.12
k6 model	273.72	254.89	273.77	35.13	4.46

Test	46	47	48	49	50
Pump type	BB3	BB3	BB3	BB3	BB4-BB5
ρ (kg/m3)	1000	1000	1000	1000	1000
μ (cP)	1	1	1	1	1
B2 (mm)	85.27	85.27	65.5	85.27	13.7
D2 (mm)	810	810	415	810	275
D1 (mm)	452.3	452.3	244.8	452.3	120.5
$\beta 2$ (graus)	22.3	22.3	22.5	22.3	20.5
nq (1/s)	0.8988	0.9138	0.9189	0.9214	0.2479
ω (1/s)	125.6637	125.6637	375.2109	125.6637	374.8967
X	0.0000	0.0000	0.0000	0.0000	3.53E-08
Cqbep (-)	0.0322	0.0327	0.0299	0.0327	0.0029
Chbep (-)	0.1168	0.1152	0.1079	0.1139	0.1301
Cq1 (-)	0.00000	0.00000	0.00000	0.00000	0.00000
Cq2 (-)	0.01264	0.00827	0.01493	0.00370	0.00110
Cq3 (-)	0.01658	0.01533	0.01831	0.00831	0.00155
Cq4 (-)	0.02097	0.02566	0.02136	0.01662	0.00235
Cq5 (-)	0.02541	0.03361	0.02480	0.02536	0.00293
Cq6 (-)	0.02910	0.04219	0.02802	0.03351	0.00357
Cq7 (-)	0.03235		0.02994	0.03820	0.00402
Cq8 (-)	0.03370		0.03224	0.03921	0.00450
Cq9 (-)	0.03782		0.03634	0.04080	0.00477
Cq10 (-)	0.04185		0.03843	0.04245	
Ch1 (-)	0.1520	0.1525	0.1385	0.1508	0.1623
Ch2 (-)	0.1431	0.1461	0.1326	0.1478	0.1581
Ch3 (-)	0.1390	0.1399	0.1306	0.1456	0.1553
Ch4 (-)	0.1370	0.1321	0.1283	0.1372	0.1479
Ch5 (-)	0.1323	0.1122	0.1219	0.1306	0.1380
Ch6 (-)	0.1243	0.0865	0.1134	0.1116	0.1237
Ch7 (-)	0.1165		0.1079	0.0972	0.1133
Ch8 (-)	0.1126		0.1016	0.0945	0.0976
Ch9 (-)	0.0999		0.0895	0.0904	0.0850
Ch10 (-)	0.0860		0.0837	0.0838	
k1 model	3.6863	3.6863	2.4345	3.6863	8.5447
k4 model	0.1001	0.0996	0.1119	0.1013	0.0892
k5 model	19.57	18.97	13.38	18.85	68.48
k6 model	2.34	1.46	31.68	2.45	3563.47

Test	51	52	53	54	55
Pump type	BB4-BB5	BB4-BB5	BB4-BB5	BB4-BB5	BB4-BB5
ρ (kg/m3)	1000	1000	1000	1000	1000
μ (cP)	1	1	1	1	1
B2 (mm)	13.7	13.7	13	16	19.1
D2 (mm)	274	273	225	260	328
D1 (mm)	120.5	120.5	104	124	156.7
$\beta 2$ (graus)	20.5	20.5	26	30	22
nq (1/s)	0.2524	0.2630	0.2897	0.3228	0.3344
ω (1/s)	374.0590	374.1637	373.8495	373.4306	418.8790
X	3.56E-08	3.59E-08	5.28E-08	3.96E-08	2.22E-08
Cqbep (-)	0.0031	0.0029	0.0035	0.0053	0.0058
Chbep (-)	0.1345	0.1198	0.1205	0.1371	0.1386
Cq1 (-)	0.00000	0.00000	0.00000	0.00000	0.00000
Cq2 (-)	0.00000	0.00040	0.00060	0.00125	0.00154
Cq3 (-)	0.00144	0.00075	0.00118	0.00329	0.00248
Cq4 (-)	0.00144	0.00109	0.00177	0.00529	0.00350
Cq5 (-)	0.00250	0.00151	0.00235	0.00720	0.00455
Cq6 (-)	0.00251	0.00185	0.00294		0.00515
Cq7 (-)	0.00357	0.00221	0.00351		0.00549
Cq8 (-)	0.00357	0.00244	0.00412		0.00604
Cq9 (-)	0.00441	0.00287	0.00471		0.00655
Cq10 (-)	0.00442	0.00334	0.00529		0.00718
Ch1 (-)	0.1653	0.1684	0.1589	0.1645	0.1683
Ch2 (-)	0.1647	0.1665	0.1583	0.1594	0.1656
Ch3 (-)	0.1596	0.1644	0.1565	0.1519	0.1641
Ch4 (-)	0.1607	0.1609	0.1505	0.1371	0.1607
Ch5 (-)	0.1463	0.1529	0.1427	0.1101	0.1517
Ch6 (-)	0.1474	0.1457	0.1327		0.1462
Ch7 (-)	0.1251	0.1374	0.1205		0.1424
Ch8 (-)	0.1245	0.1306	0.1099		0.1351
Ch9 (-)	0.1043	0.1198	0.0962		0.1278
Ch10 (-)	0.1045	0.1072	0.0795		0.1185
k1 model	8.5136	8.4825	5.6478	4.4796	6.7647
k4 model	0.0848	0.0806	0.0900	0.0869	0.0829
k5 model	56.40	23.08	24.03	25.91	54.07
k6 model	3115.75	4237.50	2581.28	948.06	999.23

Test	56	57	58	59	60
Pump type	BB4-BB5	BB4-BB5	BB4-BB5	BB4-BB5	BB4-BB5
ρ (kg/m3)	1000	1000	1000	1000	1000
μ (cP)	1	1	1	1	1
B2 (mm)	16	16	12	21	27
D2 (mm)	260	270	220	300	360
D1 (mm)	124	126	108	152	190
$\beta 2$ (graus)	30	27.5	30.2	33.5	36.7
nq (1/s)	0.3354	0.3376	0.3619	0.3692	0.3763
ω (1/s)	375.4203	371.7551	362.3304	374.8967	123.0457
X	3.94E-08	3.69E-08	5.70E-08	2.96E-08	6.27E-08
Cqbep (-)	0.0054	0.0054	0.0055	0.0074	0.0082
Chbep (-)	0.1322	0.1308	0.1204	0.1435	0.1500
Cq1 (-)	0.00000	0.00000	0.00000	0.00000	0.00000
Cq2 (-)	0.00000	0.00152	0.00103	0.00191	0.00195
Cq3 (-)	0.00116	0.00343	0.00206	0.00415	0.00570
Cq4 (-)	0.00118	0.00539	0.00308	0.00632	0.00964
Cq5 (-)	0.00330	0.00646	0.00410	0.00956	0.01196
Cq6 (-)	0.00331		0.00515		
Cq7 (-)	0.00540		0.00617		
Cq8 (-)	0.00541		0.00717		
Cq9 (-)	0.00683				
Cq10 (-)	0.00699				
Ch1 (-)	0.1609	0.1551	0.1475	0.1645	0.1727
Ch2 (-)	0.1618	0.1547	0.1481	0.1635	0.1762
Ch3 (-)	0.1547	0.1464	0.1481	0.1582	0.1635
Ch4 (-)	0.1542	0.1308	0.1430	0.1499	0.1378
Ch5 (-)	0.1473	0.1166	0.1350	0.1208	0.1232
Ch6 (-)	0.1467		0.1243		
Ch7 (-)	0.1323		0.1094		
Ch8 (-)	0.1320		0.0892		
Ch9 (-)	0.1136				
Ch10 (-)	0.1123				
k1 model	4.4796	5.1593	5.0134	3.4351	2.8470
k4 model	0.0903	0.0950	0.1033	0.0862	0.0755
k5 model	17.03	35.57	43.97	28.30	20.56
k6 model	725.65	1038.20	1468.49	547.77	359.63

Test	61	62	63	64	65
Pump type	BB4-BB5	BB4-BB5	BB4-BB5	BB4-BB5	BB4-BB5
ρ (kg/m3)	1000	1000	1000	1000	1000
μ (cP)	1	1	1	1	1
B2 (mm)	27	21	21	27	18
D2 (mm)	354	300	300	354	278
D1 (mm)	190	152	152	190	142
$\beta 2$ (graus)	36.7	33.5	32	36.7	28.5
nq (1/s)	0.3795	0.3799	0.3831	0.3923	0.3945
ω (1/s)	375.3156	371.7551	185.8776	375.3156	374.2684
X	2.13E-08	2.99E-08	5.98E-08	2.13E-08	3.46E-08
Cqbep (-)	0.0078	0.0078	0.0077	0.0082	0.0072
Chbep (-)	0.1437	0.1435	0.1401	0.1413	0.1291
Cq1 (-)	0.00000	0.00000	0.00000	0.00000	0.00000
Cq2 (-)	0.00346	0.00162	0.00138	0.00347	0.00175
Cq3 (-)	0.00595	0.00424	0.00284	0.00598	0.00411
Cq4 (-)	0.00784	0.00650	0.00417	0.00844	0.00636
Cq5 (-)	0.00850	0.00784	0.00551	0.01151	0.00808
Cq6 (-)	0.01104		0.00690		0.00969
Cq7 (-)			0.00850		
Cq8 (-)			0.00979		
Cq9 (-)			0.01112		
Cq10 (-)			0.01246		
Ch1 (-)	0.1711	0.1621	0.1619	0.1669	0.1620
Ch2 (-)	0.1648	0.1623	0.1616	0.1654	0.1601
Ch3 (-)	0.1553	0.1606	0.1592	0.1562	0.1528
Ch4 (-)	0.1437	0.1528	0.1561	0.1392	0.1367
Ch5 (-)	0.1391	0.1435	0.1518	0.1109	0.1206
Ch6 (-)	0.1161		0.1462		0.1000
Ch7 (-)			0.1341		
Ch8 (-)			0.1218		
Ch9 (-)			0.1079		
Ch10 (-)			0.0895		
k1 model	2.7995	3.4351	2.4649	2.7995	4.5272
k4 model	0.0830	0.0885	0.0895	0.0792	0.0884
k5 model	25.20	31.09	23.76	18.01	30.14
k6 model	492.51	460.61	540.85	425.31	654.82

Test	66	67	68	69	70
Pump type	BB4-BB5	BB4-BB5	BB4-BB5	BB4-BB5	BB4-BB5
ρ (kg/m3)	1000	1000	1000	1000	1000
μ (cP)	1	1	1	1	1
B2 (mm)	25	16	21	16	21
D2 (mm)	365	269	300	268	300
D1 (mm)	184	126	152	126	152
$\beta 2$ (graus)	23	27.5	32	27.5	32
nq (1/s)	0.3951	0.3999	0.4060	0.4064	0.4124
ω (1/s)	314.1593	373.8495	374.4778	374.5826	373.8495
X	2.39E-08	3.70E-08	2.97E-08	3.72E-08	2.97E-08
Cqbep (-)	0.0078	0.0067	0.0087	0.0070	0.0089
Chbep (-)	0.1360	0.1204	0.1402	0.1217	0.1404
Cq1 (-)	0.00000	0.00000	0.00000	0.00000	0.00000
Cq2 (-)	0.00144	0.00000	0.00331	0.00249	0.00158
Cq3 (-)	0.00372	0.00154	0.00596	0.00411	0.00480
Cq4 (-)	0.00609	0.00160	0.00866	0.00586	0.00771
Cq5 (-)	0.00783	0.00358	0.01063	0.00759	0.01097
Cq6 (-)	0.00966	0.00368			
Cq7 (-)		0.00568			
Cq8 (-)		0.00572			
Cq9 (-)		0.00764			
Cq10 (-)		0.00781			
Ch1 (-)	0.1699	0.1562	0.1607	0.1610	0.1681
Ch2 (-)	0.1682	0.1557	0.1598	0.1509	0.1658
Ch3 (-)	0.1608	0.1510	0.1533	0.1450	0.1560
Ch4 (-)	0.1493	0.1513	0.1402	0.1334	0.1465
Ch5 (-)	0.1360	0.1441	0.1253	0.1155	0.1236
Ch6 (-)	0.1193	0.1446			
Ch7 (-)		0.1305			
Ch8 (-)		0.1311			
Ch9 (-)		0.1115			
Ch10 (-)		0.1087			
k1 model	5.4742	5.1402	2.4649	5.1210	2.4649
k4 model	0.0802	0.0948	0.0896	0.0896	0.0823
k5 model	31.53	23.83	21.92	19.27	10.92
k6 model	417.77	613.28	399.72	510.68	290.75

Test	71	72	73	74	75
Pump type	BB4-BB5	BB4-BB5	BB4-BB5	VS2	VS2
ρ (kg/m3)	1000	1000	1000	1000	1000
μ (cP)	1	1	1	1	1
B2 (mm)	25	25	21	65.14	60.8
D2 (mm)	365	365	300	628	571.8
D1 (mm)	184	184	152	378.8	340.8
$\beta 2$ (graus)	23	23	32	22.5	22.5
nq (1/s)	0.4302	0.4861	0.5025	0.8925	0.9031
ω (1/s)	314.1593	314.1593	373.8495	124.9307	124.4071
X	2.39E-08	2.39E-08	2.97E-08	2.03E-08	2.46E-08
Cqbep (-)	0.0085	0.0096	0.0109	0.02361	0.02421
Chbep (-)	0.1287	0.1186	0.1229	0.09578	0.09586
Cq1 (-)	0.00000	0.00000	0.00000	0.00000	0.00000
Cq2 (-)	0.00145	0.00142	0.00165	0.01131	0.00000
Cq3 (-)	0.00365	0.00369	0.00470	0.01753	0.01135
Cq4 (-)	0.00600	0.00600	0.00771	0.02361	0.01377
Cq5 (-)	0.00964	0.00965	0.01088	0.02892	0.01620
Cq6 (-)					0.01623
Cq7 (-)					0.02421
Cq8 (-)					
Cq9 (-)					
Cq10 (-)					
Ch1 (-)	0.1661	0.1656	0.1615	0.1711	0.1661
Ch2 (-)	0.1681	0.1683	0.1612	0.1311	0.1658
Ch3 (-)	0.1602	0.1613	0.1554	0.1134	0.1269
Ch4 (-)	0.1494	0.1494	0.1436	0.0958	0.1209
Ch5 (-)	0.1185	0.1186	0.1229	0.0722	0.1153
Ch6 (-)					0.1169
Ch7 (-)					0.0959
Ch8 (-)					
Ch9 (-)					
Ch10 (-)					
k1 model	5.4742	5.4742	2.4649	3.7043	3.6136
k4 model	0.0831	0.0834	0.0886	0.0797	0.0859
k5 model	36.11	38.29	16.78	3.24	4.31
k6 model	467.88	491.20	345.55	3.88	0.00

Test	76	77	78	79	80
Pump type	VS2	VS2	VS2	VS2	VS2
ρ (kg/m3)	1000	1000	1000	1000	1000
μ (cP)	1	1	1	1	1
B2 (mm)	83.1	83.1	83.1	83.1	83.1
D2 (mm)	489.6	489.6	489.6	489.6	489.6
D1 (mm)	375.8	375.8	375.8	375.8	375.8
$\beta 2$ (graus)	29.5	29.5	29.5	29.5	29.5
nq (1/s)	1.1350	1.1534	1.1563	1.1718	1.4888
ω (1/s)	160.2212	167.5516	157.0796	160.2212	167.5516
X	2.60E-08	2.49E-08	2.66E-08	2.60E-08	2.49E-08
Cqbep (-)	0.04083	0.04047	0.04146	0.04037	0.04747
Chbep (-)	0.10015	0.09745	0.09870	0.09525	0.07712
Cq1 (-)	0.00000	0.00000	0.00000	0.00000	0.00000
Cq2 (-)	0.03438	0.01552	0.02103	0.02089	0.02104
Cq3 (-)	0.04083	0.03173	0.02854	0.02787	0.02637
Cq4 (-)	0.04682	0.04047	0.03485	0.03418	0.03211
Cq5 (-)	0.05218	0.04644	0.04146	0.04037	0.04747
Cq6 (-)		0.04923	0.05022	0.04578	
Cq7 (-)				0.05151	
Cq8 (-)					
Cq9 (-)					
Cq10 (-)					
Ch1 (-)	0.1378	0.1315	0.1386	0.1379	0.1289
Ch2 (-)	0.1032	0.1222	0.1204	0.1178	0.1080
Ch3 (-)	0.1001	0.1015	0.1092	0.1064	0.1007
Ch4 (-)	0.0882	0.0975	0.1035	0.1031	0.0981
Ch5 (-)	0.0778	0.0889	0.0987	0.0953	0.0771
Ch6 (-)		0.0818	0.0808	0.0810	
Ch7 (-)				0.0672	
Ch8 (-)					
Ch9 (-)					
Ch10 (-)					
k1 model	1.6574	1.6574	1.6574	1.6574	1.6574
k4 model	0.1124	0.1181	0.1116	0.1129	0.1214
k5 model	4.96	4.42	4.23	4.90	3.19
k6 model	8.35	5.13	5.98	12.07	2.87